Unraveling chitin signaling in fungi: Insights into Lipo-chitooligosaccharides, LysM Effectors, and Regulatory Networks in *Aspergillus fumigatus*

By

Cristobal X. Carrera Carriel

A dissertation in partial fulfillment of the requirements for a degree of

Doctor of Philosophy
(Genetics)

at the
University of Wisconsin-Madison
2024

Date of final oral examination: July 11, 2024

The dissertation is approved by the following members of the Final Oral Committee:
Jean-Michel Ané, Professor, Bacteriology and Plant and Agroecosystem Sciences
Nancy P. Keller, Professor, Medical Microbiology and Immunology and Plant Pathology
Jae-Hyuk Yu, Professor, Bacteriology and Food Research Institute
Patrick Masson, Professor, Genetics
Nicole Perna, Professor, Genetics

Abstract

In 2019, researchers revealed that most fungi secrete chitin-based signaling molecules called lipo-chitooligosaccharides (LCOs). This finding upended the long-held belief that symbiotic microbes exclusively secreted LCOs to initiate symbiotic associations with plants. Furthermore, they observed that treating fungi with LCOs leads to significant changes in growth and development, as seen in the mold *Aspergillus fumigatus* and the mushroom *Laccaria bicolor*. This discovery sparked the hypothesis that fungi employ LCOs as signals to regulate growth and development through autocrine (acting on the same cell) or paracrine (acting on nearby cells) mechanisms. We sought to answer the fundamental question: what are the genetic drivers underlying a fungus' response to chitin-based signaling molecules?

To uncover gene regulators involved in LCO response, we used the MERLIN+P+TFA algorithm to infer a comprehensive gene regulatory network in *A. fumigatus* based on publicly available expression datasets. Our network revealed the role of the transcription factor, *Af*AtfA, as a critical regulator of LCO responses. Experimental assays validated this prediction by showing that deleting the gene coding for *Af*AtfA disrupts the ability to respond to LCOs. Furthermore, we implemented our network into a free online resource called GRAsp (**G**ene **R**egulation of ***Asp****ergillus fumigatus*), allowing users to explore their genes and pathways of interest and develop new hypotheses.

Our research also explored how fungi physically detect LCOs. In plants, LysM domains on cell-membrane receptors physically bind chitin-derived molecules, including LCOs. Proteins containing LysM domains are conserved throughout fungi, especially within

secreted proteins with no catalytic domains called effectors. We found that LysM effector *AfldpA* from *A. fumigatus* is essential for the fungal responses to LCOs, and we hypothesize that these effectors act as LCO receptors. Binding assays between these heterologously expressed proteins and LCOs are being conducted to confirm our hypothesis.

Our discoveries significantly advance our knowledge of chitin signaling in fungi; continuing to dissect this LCO response pathway, especially with the aid of GRAsp, will help us link the activity of LysM effectors to the regulatory activity of *Af*AtfA. Furthermore, the ability to engineer fungi that are non-responsive to LCOs will help us understand the importance of these molecules in microbial interactions and possibly manipulate fungal beneficial or detrimental behaviors.

Acknowledgments

I consider myself truly fortunate to have the support and encouragement of many remarkable individuals. I am deeply grateful to each of you.

First and foremost, I owe a profound thank you to my mom, Tanya. My accomplishments are hers just as much as they are mine. We came to this country with very little, but her determination and work ethic allowed us to thrive. Her unwavering belief in me has been my greatest source of strength and motivation. She has been my steadfast supporter through every challenge and triumph, and I am endlessly thankful for her love and sacrifice. Te quiero mucho, Patty!

I am incredibly grateful to my two graduate mentors, Dr. Jean-Michel Ané and Dr. Nancy P. Keller. Their guidance, unwavering support, and passion for science shaped me into the scientist I am today. I'm forever thankful for all the opportunities they provided me. I also wish to extend my gratitude to my graduate advisory committee members: Dr. Patrick Masson, Dr. Jae-Hyuk Yu, and Dr. Nicole Perna. Their guidance and perspectives propelled my research to where it is today.

My journey has also been enriched by the support of my lab mates, both past and present. Their camaraderie has been a highlight of my academic journey. Special thanks to Dr. Dianiris Luciano-Rosario, Dr. Christina Arther, Dante Calise, Aidan Schmidt, Dr. Jin Woo Bok, Dr. Hye-Won Seo, Dr. Sung Chul Park, and Dr. Mira Syahfriena Amir Rawa.

I also want to thank the rest of my family and the friends I've made outside the lab. Katherine Hubert, James Sebold, and Ryan Ward made my time in Madison fun and exciting. The love and support from my dads, Cristobal Carrera Sr. and Victor Londono, and my siblings have been invaluable. Thank you all for sticking by me.

Finally, I want to pay tribute to my late sister, Nathaly. She was a remarkable artist building a promising career in interior design. Her resilience, humor, and boundless optimism were a beacon of hope for everyone who knew her. This work is dedicated to her memory, and I strive to honor her in everything I do.

Table of Contents

Chapter 1: Introduction

1.1 Lipo-chitooligosaccharides and its role in plant-microbe symbioses.

Lipo-chitooligosaccharides (LCOs) are signaling molecules in fungi and nitrogen-fixing bacteria (1–3). These molecules are derivatives of chitin, the second-most naturally abundant polysaccharide, following cellulose, and are made up of *N*-acetyl-D-glucosamine monomers **(Figure 1A)** (4, 5). Specifically, LCOs are fragments of 3-5 *N*-acetyl-D-glucosamine residues, a fatty acid attached to the chitin backbone's non-reducing end, with various possible functional groups **(Figure 1B, C)** (6). The study of LCOs was initially rooted in plant-microbe symbiosis. In particular, legumes have symbiotic relationships with nitrogen-fixing bacteria, collectively referred to as rhizobia, and these relationships are, in part, enabled by an exchange of signaling cues that involve LCOs (7).

Rhizobia produce LCOs in response to flavonoids secreted from the roots of legumes. The plant host further recognizes the secreted LCO molecules via receptor-like kinases (8). This recognition activates the Common Symbiosis Pathway (CSP), a conserved signaling cascade found across many plant species. It facilitates the successful establishment and maintenance of symbiotic relationships with their bacterial or fungal partners (8, 9).

In rhizobia, activating the Common Symbiosis Pathway in legume species is required for intracellular infection and developing root nodules, specialized structures that house rhizobia (10). This symbiotic association facilitates atmospheric nitrogen conversion into ammonium, allowing for an exchange of resources between the host and

the microbe. The host receives access to a usable form of nitrogen to carry out processes that support growth and development, while the microbe receives sources of carbon from the plant host (10). For LCO's role in plant symbioses, these molecules are also called Nodulation, or Nod, factors.

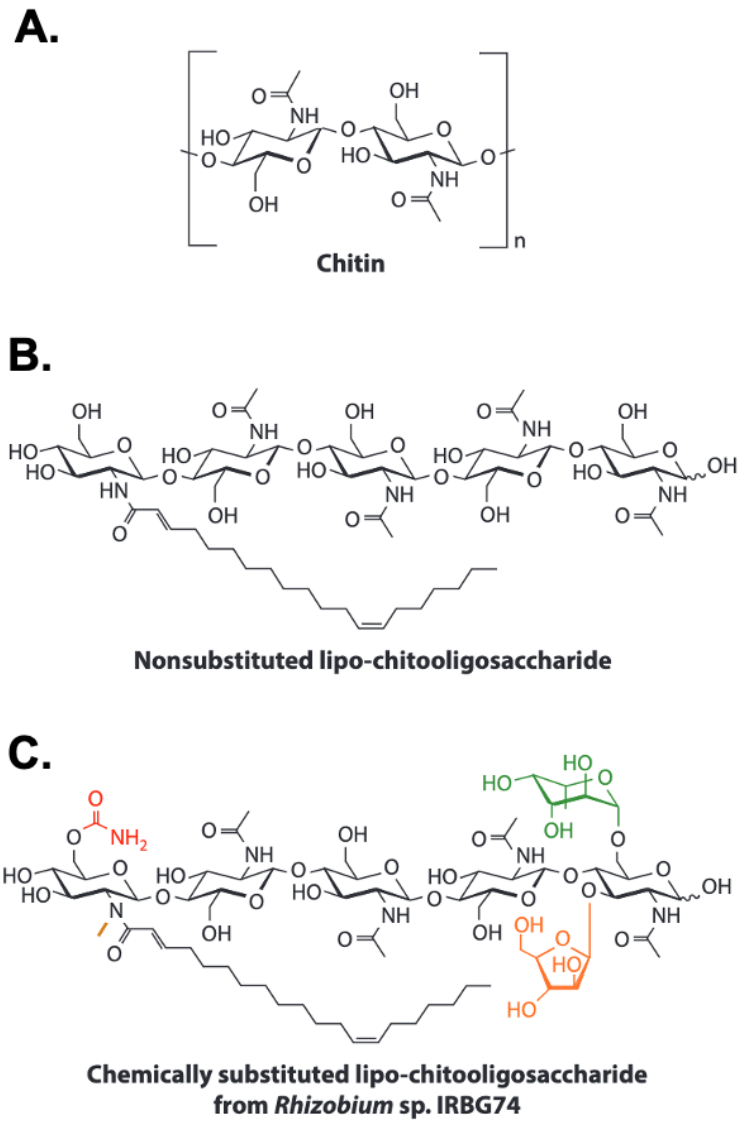

Figure 1. Chemical structures of chitin molecules. A) Chitin. (B) Non-Substituted LCO. (C) Chemically substituted LCO from *Rhizobium* sp. IRBG74.

Carbamoyl groups are red, fucosyl green, arabinosyl orange, and methyl brown. Modified from Khokhani *et al.* 2021 (3).

The plant host's ability to detect LCOs depends on LysM-containing receptor-like kinases (3). These receptors can discriminate between rhizobial symbionts by recognizing variations in the degree of chitin polymerization, lipid structure, or the type of functional group (3, 11). For example, the legume *Vicia Sativa* responds to non-sulfated LCOs, while another legume, *Medicago truncatula,* responds to sulfated LCOs (3, 12, 13). The specificity of LCOs and their receptors ensures that the plant forms symbiotic associations only with compatible rhizobia (14). It was not long, however, before LCO signaling was discovered in other symbiotic associations (15, 16).

The role of LCOs expanded with the discovery that these molecules were also crucial for associations between plants and fungi, not just rhizobia (16). Arbuscular mycorrhizal fungi are soil fungi that establish mutually beneficial associations with roughly 90% of land plants (17). Similar to associations with bacteria, the fungus receives carbon from the plant, and, in return, the plant gets access to sources of minerals like phosphorus, increased water uptake, and improved resistance to abiotic stressors like drought (3, 18).

This symbiotic relationship begins with a chemical dialogue between the arbuscular mycorrhizal fungus and the plant host (18). When near plant signals, the fungus secretes LCOs that the plant host recognizes via receptor kinases that contain LysM domains. This recognition triggers a signaling cascade that activates the Common Symbiosis Pathway and pathways that suppress innate immune responses to fungi (3,

18). A successful dialogue allows the fungus to colonize the roots. Specifically, the fungus can form branched structures, called arbuscules, inside plant root cells, which will, in turn, facilitate the exchange of resources (3). To distinguish LCOs from those from rhizobia, LCOs from mycorrhizal fungi were colloquially called Myc-LCOs (19).

While LCOs are essential for microbial cross-talk with plants, derivatives of chitin, referred to as chitin oligomers (COs), are also involved in plant-fungal interactions (3, 20). The main difference between the two molecules is that COs do not contain the lipid moiety. While chitin is known for its structural role in the fungus' cell wall, smaller chitin oligomers have signaling roles in mutualistic and pathogenic plant interactions (20).

COs are generally categorized by their degree of polymerization, separating molecules into either short-chain COs (polymerization of 4-5 N-acetyl-glucosamine residues) and long-chain COs (polymerization of 8 or more N-acetyl-glucosamine residues) (20). Early evidence suggested that short-chain COs produced by mycorrhizal fungi were involved in activating the Common Symbiosis Pathway. In contrast, long-chain COs produced by fungal plant pathogens elicited an immune reaction by the plant (3). These views are challenged by work that suggests that COs are not limited to eliciting specific symbiotic or defense responses from the plant; long-chain COs, for example, can trigger the early stages of symbiotic signaling (3, 20, 21). While short-chain and long-chain COs are essential in a plant's interaction with a fungus, the ambiguity of their roles speaks to a more complex chitin signaling system (3).

The discovery that LCOs were also crucial in ectomycorrhizal associations foreshadowed that LCO molecules are found throughout the fungal kingdom (1, 15). Ectomycorrhizal fungi form symbiotic relationships with their plant host, allowing resource

transfer (3, 22). Like in arbuscular mycorrhizal fungi, the fungus receives carbon sources from the plant while the plant gets increased access to minerals. Unlike arbuscular mycorrhizal associations, colonization by ectomycorrhizal fungi occurs by forming a sheath around the plant root and penetrating the intercellular space (3). Molecular research into these associations commonly uses the ectomycorrhizal mushroom, *Laccaria bicolor*, as a model organism (23).

In 2019, Cope *et al.* discovered that *L. bicolor* secretes a range of LCOs and that these molecules facilitated ectomycorrhizal symbiosis (15). Specifically, treating poplar plants with LCOs from *L. bicolor* activated calcium spiking, a critical step of the signaling cascade that activates the Common Symbiosis Pathway (3, 15).

L. bicolor produces two primary forms of LCOs, one that is sulfated and one that is non-sulfated. Interestingly, both molecules have different roles in signaling. Sulfated LCOs generally increased the efficiency of the fungus' ability to colonize the plant roots, while non-sulfated LCOs increased lateral root formation (15).

1.2 LCOs are signaling molecules found throughout the fungal kingdom.

It was not until 2019 that Dr. Tomas Rush *et al.* discovered that LCOs are produced by most fungi, irrespective of their ability to develop symbiotic associations with plants (1). Researchers tested the exudates of 59 species spanning the fungal kingdom and several oomycete species for the presence of LCOs. They found that 53 fungi had detectable levels of LCOs (**Figure 2**). Chemical analyses further revealed that LCO structures were similar across fungi, with LCOs containing three to five N-acetyl-glucosamine residues and sulfated, fucosyl, and methylfucosyl functional groups. The

standard lab yeast, *Saccharomyces cerevisiae*, and oomycetes (filamentous microbes that grossly resemble and sometimes are mistaken for fungi) did not have detectable LCOs (1, 3).

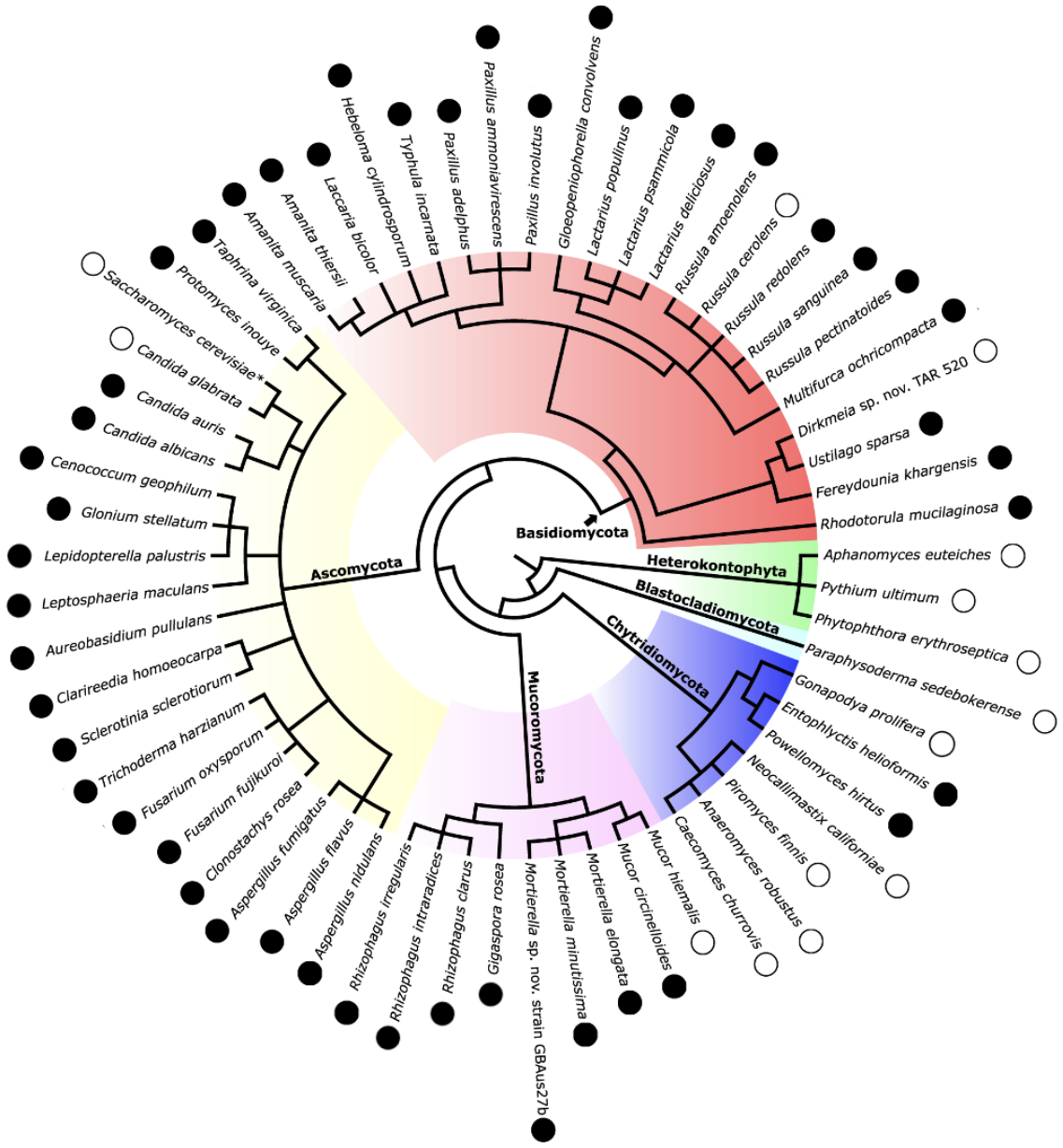

Figure 2. Fifty-nine fungi representing five of the eight phyla (indicated by colors) and three species of oomycetes (Heterokontophyta, green) were tested for the presence of (LCO)s in their culture supernatants. Modified from Rush *et al.* 2020.

Another groundbreaking revelation was that LCO treatment altered the growth and development of fungi. The filamentous mold *Aspergillus fumigatus* was treated with various LCO, CO, and lipid structures to determine if it affected germination and lateral branch formation. Sulfated LCOs with palmitic acid lipid moiety (C16:0 sLCO) reduced lateral, or secondary, branches coming off the primary hypha, even at concentrations as low as 10^{-8} M. C16:0 sLCO also increased germination of asexual spores, termed conidia; this however was not specific to LCO as oleic acid (C18:1) also elicited a similar phenotype. Treatment with C16:0 sLCO altered the transcriptional activity of *A. fumigatus* after 30 minutes and two hours. In the yeast *Candida glabrata*, all tested LCOs, CO, and lipids induced pseudohyphae formation but were most strongly observed in treatments C16:0 sLCO in treatments as low as 10^{-13} M (1, 3).

In a follow-up study, treatment of *A. fumigatus* with LCOs, even those that did not elicit germination or secondary branching changes, altered the metabolites produced by *A. fumigatus* (24). The metabolites secreted by LCO-treated *A. fumigatus* further altered the growth of various plant-associated bacteria, supporting the idea that LCOs in non-symbiotic fungi have roles in inter-kingdom signaling (24).

Treatments of *L. bicolor* with LCOs and COs further elicited changes in symbiotic fungi. Specifically, treatment with C16:0 nsLCOs, C18:1 sLCOs, C18:1 nsLCOs, and CO4 reduced radical growth and hyphal branching in *L. bicolor* (25). Rush *et al.* also examined how LCOs and COs affect clamp connections (25). Clamp connections are structures found in fungi from the Basidiomycota division and resemble hooks or loops that protrude

from the fungal septum, the wall separating two cells, and play a role in cell division (26). Treatment with C16:0 sLCOs, C16:0 nsLCOs, or C18:1 sLCOs elicited increased clamp connections (25).

Proteomic analysis of *L. bicolor* reveals that sLCO and nsLCOs purified from rhizobia, along with CO4 and CO8, reduced protein abundance and induced distinct proteomic profiles in the fungus. Gene Ontology (GO) enrichment analyses of these proteins revealed that these molecules generally affected processes involved in the development and response to environmental triggers (e.g., cellular component assembly, the establishment of cell polarity) (25).

These discoveries altered our understanding of chitin signaling and supported the idea that the role of LCOs goes further than established symbiotic associations; LCOs are regulatory signal molecules in fungi and are potentially involved in cross-kingdom interactions (25).

1.3 LysM domains and binding of chitin oligomers

As previously mentioned, plants have a system to recognize and respond to LCOs and COs; these molecules are recognized by Lysin motif receptor-like kinases (LysM-RLKs) found on the cell membrane (3).

LCO recognition occurs through direct binding by two LysM domains, one LysM domain from LysM-RLKs proteins with an inactive kinase domain (LYR) and another LysM domain from a LysM-RLKs with an active kinase domain, called LYK (3, 27). LCO binding creates a protein complex between the LysM-RLKs and other components, such as a leucine-rich repeat (LRR)-type receptor kinase, that will transduce the signal into the cell (3, 28). In the legume *M. truncatula,* for example, the binding of LCOs occurs through

*Mt*Lyk3, which has the LYK domain, and *Mt*NFP, which has the LYR domain. Along with MtDMI2, a leucine-rich repeat (LRR)-type receptor kinase, these receptors form a complex to activate the plant Common Symbiosis Pathway (3, 11, 29).

The binding of COs is similar to that of LCOs. For example, binding the eight residue chitin oligomer, CO8, by *M. truncatula* occurs through the receptor complex formed by *Mt*LYR4, a LysM-RLK with an inactive kinase domain, and MtCERK1, a LysM-RLK with an active kinase domain (30). Whether LCOs or COs, it is clear that LysM domains are essential for binding chitin molecules in plant species. Fungi could also employ LysM-containing proteins to bind and respond to LCOs and COs (3).

LysM (Lysin Motif) domains are protein sequences conserved throughout bacteria, bacteriophages, archaea, and eukaryotes (31, 32). This sequence usually consists of 40-50 amino acids, translating into a beta-alpha-alpha-beta secondary structure to create anti-parallel domains that form a binding groove for carbohydrates containing N-acetylglucosamine residues (32). There also appear to be two major groups of LysM motifs based on phylogenetics: bacterial/fungal and fungal-specific. One of the major distinctions between the domains is that the bacterial/fungal has 0-1 cysteine residues within the motifs, while the fungal-specific group, on the other hand, has 3-4 cysteine residues (31, 33). Various proteins, such as secreted proteins, receptors, and cell wall-localized proteins, contain these domains (31). While LysM domains can bind chitin oligomers, these domains can also bind peptidoglycan. Enzymes in bacteria, such as peptidoglycan hydrolases, can contain LysM domains and participate in cell wall remodeling (34). As mentioned, plants employ LysM-containing proteins to detect LCOs and COs and respond accordingly (32).

In fungi, LysM domains generally belong to two types of proteins: catalytic or effector proteins. Catalytic proteins contain one or more LysM domains and a catalytic activity domain. Chitinases often possess LysM domains (35). LysM effectors are proteins with no catalytic domain, one or more LysM, and signal peptides that mark the protein for secretion (31).

LysM effectors are conserved throughout the fungal kingdom. While present in non-pathogenic fungi, research into LysM effectors has primarily occurred in the context of plant-fungi interactions.

Early research implicated the LysM effectors of plant pathogenic fungi in three primary activities: 1) binding chitin molecules, 2) the suppression of the plant immune response, generally by sequestering immunogenic chitin, and 3) protection of the fungus from plant chitinases, potentially by physically blocking chitinases thought the polymerization of LysM effector; These activities facilitate the successful colonization of the fungus' plant host (36–41). LysM effectors of mycoparasite *Clonostachys rosea*, insect pathogen *Beauveria bassiana*, plant-beneficial fungus *Trichoderma atrovirde*, and plant symbiont *Rhizophagus irregularis* have similar roles (42–45). Two LysM effectors, ClLysM1 and ClLysM2, from *Clonostachys rosea* exhibited roles in fungal development, such as germination and mycelial growth (42).

Similar to LysM-receptors in plants, chitin-binding occurs through LysM domain dimerization. However, there are two strategies by which LysM domain-containing proteins bind chitin: either through 1) intramolecular dimerization, where LysM domains on the same protein bind chitin, and 2) intermolecular dimerization, whereby LysM domains from two different proteins bind chitin **(Figure 3)** (46).

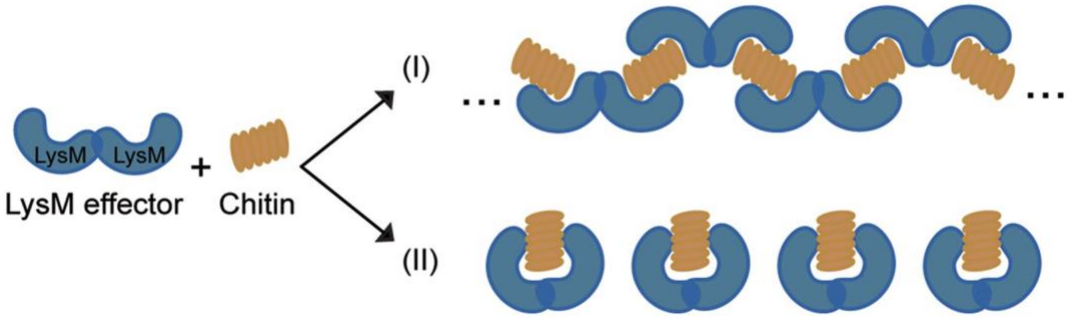

Figure 3. Two proposed strategies for LysM domain-mediated chitin binding. (I) Intermolecular dimerization between two LysM domains from separate proteins. II) intramolecular dimerization between LysM domains located on the same protein. Modified Tian *et al.* 2022 (46).

While most research on LysM effectors focused on plant-associated fungi, there is research on at least one human pathogen. In 2019, characterization of the two LysM effectors, *Af*LdpA and *Af*LdpB, in the human pathogen *A. fumigatus* revealed that deletion gene mutants of these effectors had no observable effect on cell wall integrity, chitin content and had not affect survival in immunosuppressed mice model (47).

However, tagging with GFP (Green Fluorescent Protein) revealed that *Af*LdpA localizes to the cell wall while *Af*LdpB is present mainly in the cell cross-walls, called septa. Both LysM effectors are also present in the extracellular matrix, potentially signifying that the proteins play a role in biofilm formation. Like bacteria, biofilms are a fungal community within an extracellular matrix that allows surface adherence and enhanced antibiotic resistance (47).

LysM effectors can also bind chitin, chitosan, and chitin oligomers. One effector, Blys5 from the insect pathogen *Beauveria bassiana*, could bind cellulose (43). The LysM effector, RiSLM, from the symbiotic fungus, *Rhizophagus irregularis*, could bind sulfated and non-sulfated LCOs. This observation allows us to hypothesize that LysM effectors, especially cell-localizing proteins like *Af*LdpA from *A. fumigatus*, could have a role as both an LCO and CO receptor (45).

1.4 Significance and Objectives.

LCOs are widespread in fungi, and these molecules alter a fungus' growth and development (1). Current hypotheses suggest that LCOs serve as signaling molecules throughout the fungal kingdom, as autocrine and paracrine signaling. Furthermore, the discovery that LCOs alter the metabolic profiles of *A. fumigatus*, which affects the growth of neighboring bacteria, suggests that LCOs could also be involved in cross-kingdom signaling (1, 3).

The role of LCOs in fungi, especially pathogens, has implications for both the agricultural and healthcare industries. For example, sellers of fertilizers and plant-growth-promoting products containing LCOs must now consider how these products could affect the fungal community surrounding the plant. Considering that LCOs alter the growth and development of pathogenic fungi like *A. fumigatus*, research into LCO signaling opens up new avenues for understanding drivers of virulence (3).

Fundamental questions arise from these discoveries, with one asking: what are the genetic mechanisms that allow fungi to respond to LCOs? Answering this question would help future work in dissecting chitin-signaling among fungi.

To expand our understanding of chitin-signaling in fungi, I have focused my Ph.D dissertation on unraveling the genetics underlying a fungus's response to LCOs and COs. Most of my work used the ascomycete mold *A. fumigatus* as a model for studying LCO signaling. **Chapter 2** of my thesis will discuss how we used regulatory gene networks to uncover a fungus's first known regulator of LCO response. **Chapter 3** will focus on our discovery that LysM effectors are important for LCO response in *A. fumigatus.* **Chapter 4** will summarize our findings and further discuss how this knowledge impacts the future of the field.

References

1. Rush,T.A., Puech-Pagès,V., Bascaules,A., Jargeat,P., Maillet,F., Haouy,A., Maës,A.Q., Carriel,C.C., Khokhani,D., Keller-Pearson,M., *et al.* (2020) Lipo-chitooligosaccharides as regulatory signals of fungal growth and development. *Nat. Commun.*, **11**, 3897.

2. Jaiswal,S.K., Mohammed,M., Ibny,F.Y.I. and Dakora,F.D. (2021) Rhizobia as a Source of Plant Growth-Promoting Molecules: Potential Applications and Possible Operational Mechanisms. *Front. Sustain. Food Syst.*, **4**, 619676.

3. Khokhani,D., Carrera Carriel,C., Vayla,S., Irving,T.B., Stonoha-Arther,C., Keller,N.P. and Ané,J.-M. (2021) Deciphering the Chitin Code in Plant Symbiosis, Defense, and Microbial Networks. *Annu. Rev. Microbiol.*, **75**, 583–607.

4. Tharanathan,R.N. and Kittur,F.S. (2003) Chitin--the undisputed biomolecule of great potential. *Crit. Rev. Food Sci. Nutr.*, **43**, 61–87.

5. Elieh-Ali-Komi,D. and Hamblin,M.R. (2016) Chitin and Chitosan: Production and Application of Versatile Biomedical Nanomaterials. *Int J Adv Res (Indore)*, **4**, 411–427.

6. Poinsot,V., Crook,M.B., Erdn,S., Maillet,F., Bascaules,A. and Ané,J.-M. (2016) New insights into Nod factor biosynthesis: Analyses of chitooligomers and lipo-chitooligomers of Rhizobium sp. IRBG74 mutants. *Carbohydr. Res.*, **434**, 83–93.

7. Gough,C. and Cullimore,J. (2011) Lipo-chitooligosaccharide signaling in endosymbiotic plant-microbe interactions. *Mol. Plant. Microbe. Interact.*, **24**, 867–878.

8. Dong,W. and Song,Y. (2020) The Significance of Flavonoids in the Process of Biological Nitrogen Fixation. *Int. J. Mol. Sci.*, **21**.

9. MacLean,A.M., Bravo,A. and Harrison,M.J. (2017) Plant Signaling and Metabolic Pathways Enabling Arbuscular Mycorrhizal Symbiosis. *Plant Cell*, **29**, 2319–2335.

10. Mus,F., Crook,M.B., Garcia,K., Garcia Costas,A., Geddes,B.A., Kouri,E.D., Paramasivan,P., Ryu,M.-H., Oldroyd,G.E.D., Poole,P.S., *et al.* (2016) Symbiotic Nitrogen Fixation and the Challenges to Its Extension to Nonlegumes. *Appl. Environ. Microbiol.*, **82**, 3698–3710.

11. Cope,K.R., Prates,E.T., Miller,J.I., Demerdash,O.N.A., Shah,M., Kainer,D., Cliff,A., Sullivan,K.A., Cashman,M., Lane,M., *et al.* (2023) Exploring the role of plant lysin motif receptor-like kinases in regulating plant-microbe interactions in the bioenergy crop Populus. *Comput. Struct. Biotechnol. J.*, **21**, 1122–1139.

12. de Ruijter,N.C.A., Bisseling,T. and Emons,A.M.C. (1999) Rhizobium Nod Factors Induce an Increase in Sub-apical Fine Bundles of Actin Filaments in Vicia sativa Root Hairs within Minutes. *Mol. Plant. Microbe. Interact.*, **12**, 829–832.

13. Oldroyd,G.E., Engstrom,E.M. and Long,S.R. (2001) Ethylene inhibits the Nod factor signal transduction pathway of Medicago truncatula. *Plant Cell*, **13**, 1835–1849.

14. Krönauer,C. and Radutoiu,S. (2021) Understanding Nod factor signalling paves the way for targeted engineering in legumes and non-legumes. *Curr. Opin. Plant Biol.*, **62**, 102026.

15. Cope,K.R., Bascaules,A., Irving,T.B., Venkateshwaran,M., Maeda,J., Garcia,K., Rush,T.A., Ma,C., Labbé,J., Jawdy,S., *et al.* (2019) The Ectomycorrhizal Fungus Laccaria bicolor Produces Lipochitooligosaccharides and Uses the Common Symbiosis Pathway to Colonize Populus Roots. *Plant Cell*, **31**, 2386–2410.

16. Vierheilig,H. and Piché,Y. (2002) Signalling in arbuscular mycorrhiza: facts and hypotheses. *Adv. Exp. Med. Biol.*, **505**, 23–39.

17. Wilkes,T.I. (2021) Arbuscular Mycorrhizal Fungi in Agriculture. *Encyclopedia*, **1**, 1132–1154.

18. Wahab,A., Muhammad,M., Munir,A., Abdi,G., Zaman,W., Ayaz,A., Khizar,C. and Reddy,S.P.P. (2023) Role of Arbuscular Mycorrhizal Fungi in Regulating Growth, Enhancing Productivity, and Potentially Influencing Ecosystems under Abiotic and Biotic Stresses. *Plants*, **12**.

19. Camps,C., Jardinaud,M.-F., Rengel,D., Carrère,S., Hervé,C., Debellé,F., Gamas,P., Bensmihen,S. and Gough,C. (2015) Combined genetic and transcriptomic analysis reveals three major signalling pathways activated by Myc-LCOs in Medicago truncatula. *New Phytol.*, **208**, 224–240.

20. Giovannetti,M., Binci,F., Navazio,L. and Genre,A. (2024) Nonbinary fungal signals and calcium-mediated transduction in plant immunity and symbiosis. *New Phytol.*, **241**, 1393–1400.

21. Giovannetti,M. and Genre,A. (2024) Plant-fungus symbiosis: One receptor to switch on the green light. *Curr. Biol.*, **34**, R507–R509.

22. Garcia,K., Delaux,P.-M., Cope,K.R. and Ané,J.-M. (2015) Molecular signals required for the establishment and maintenance of ectomycorrhizal symbioses. *New Phytol.*, **208**, 79–87.

23. Martin,F., Aerts,A., Ahrén,D., Brun,A., Danchin,E.G.J., Duchaussoy,F., Gibon,J., Kohler,A., Lindquist,E., Pereda,V., *et al.* (2008) The genome of Laccaria bicolor provides insights into mycorrhizal symbiosis. *Nature*, **452**, 88–92.

24. Rush,T.A., Tannous,J., Lane,M.J., Gopalakrishnan Meena,M., Carrell,A.A., Golan,J.J., Drott,M.T., Cottaz,S., Fort,S., Ané,J.-M., *et al.* (2022) Lipo-Chitooligosaccharides Induce Specialized Fungal Metabolite Profiles That Modulate Bacterial Growth. *mSystems*, **7**, e0105222.

25. Villalobos Solis,M.I., Engle,N.L., Spangler,M.K., Cottaz,S., Fort,S., Maeda,J., Ané,J.-M., Tschaplinski,T.J., Labbé,J.L., Hettich,R.L., *et al.* (2022) Expanding the Biological Role of Lipo-Chitooligosaccharides and Chitooligosaccharides in Laccaria bicolor Growth and Development. *Front Fungal Biol*, **3**, 808578.

26. Gladfelter,A. and Berman,J. (2009) Dancing genomes: fungal nuclear positioning. *Nat. Rev. Microbiol.*, **7**, 875–886.

27. Buendia,L., Girardin,A., Wang,T., Cottret,L. and Lefebvre,B. (2018) LysM Receptor-Like Kinase and LysM Receptor-Like Protein Families: An Update on Phylogeny and Functional Characterization. *Front. Plant Sci.*, **9**, 1531.

28. Liu,J., Deng,J., Zhu,F., Li,Y., Lu,Z., Qin,P., Wang,T. and Dong,J. (2018) The MtDMI2-MtPUB2 Negative Feedback Loop Plays a Role in Nodulation Homeostasis. *Plant Physiol.*, **176**, 3003–3026.

29. Malkov,N., Fliegmann,J., Rosenberg,C., Gasciolli,V., Timmers,A.C.J., Nurisso,A., Cullimore,J. and Bono,J.-J. (2016) Molecular basis of lipo-chitooligosaccharide recognition by the lysin motif receptor-like kinase LYR3 in legumes. *Biochem. J*, **473**, 1369–1378.

30. Feng,F., Sun,J., Radhakrishnan,G.V., Lee,T., Bozsóki,Z., Fort,S., Gavrin,A., Gysel,K., Thygesen,M.B., Andersen,K.R., *et al.* (2019) A combination of chitooligosaccharide and lipochitooligosaccharide recognition promotes arbuscular mycorrhizal associations in Medicago truncatula. *Nat. Commun.*, **10**, 5047.

31. Oguiza,J.A. (2022) LysM proteins in mammalian fungal pathogens. *Fungal Biol. Rev.*, **40**, 114–122.

32. Buist,G., Steen,A., Kok,J. and Kuipers,O.P. (2008) LysM, a widely distributed protein motif for binding to (peptido)glycans. *Mol. Microbiol.*, **68**, 838–847.

33. Suarez-Fernandez,M., Aragon-Perez,A., Lopez-Llorca,L.V. and Lopez-Moya,F. (2021) Putative LysM Effectors Contribute to Fungal Lifestyle. *Int. J. Mol. Sci.*, **22**, 3147.

34. Steen,A., Buist,G., Leenhouts,K.J., Khattabi,M.E., Grijpstra,F., Zomer,A.L., Venema,G., Kuipers,O.P. and Kok,J. (2003) Cell Wall Attachment of a Widely Distributed Peptidoglycan Binding Domain Is Hindered by Cell Wall Constituents*. *J. Biol. Chem.*, **278**, 23874–23881.

35. Langner,T., Öztürk,M., Hartmann,S., Cord-Landwehr,S., Moerschbacher,B.,

Walton,J.D. and Göhre,V. (2015) Chitinases Are Essential for Cell Separation in Ustilago maydis. *Eukaryot. Cell*, **14**, 846–857.

36. Sánchez-Vallet,A., Saleem-Batcha,R., Kombrink,A., Hansen,G., Valkenburg,D.-J., Thomma,B.P.H.J. and Mesters,J.R. (2013) Fungal effector Ecp6 outcompetes host immune receptor for chitin binding through intrachain LysM dimerization. *Elife*, **2**, e00790.

37. Sánchez-Vallet,A., Tian,H., Rodriguez-Moreno,L., Valkenburg,D.-J., Saleem-Batcha,R., Wawra,S., Kombrink,A., Verhage,L., de Jonge,R., van Esse,H.P., *et al.* (2020) A secreted LysM effector protects fungal hyphae through chitin-dependent homodimer polymerization. *PLoS Pathog.*, **16**, e1008652.

38. Tian,H., MacKenzie,C.I., Rodriguez-Moreno,L., van den Berg,G.C.M., Chen,H., Rudd,J.J., Mesters,J.R. and Thomma,B.P.H.J. (2021) Three LysM effectors of Zymoseptoria tritici collectively disarm chitin-triggered plant immunity. *Mol. Plant Pathol.*, **22**, 683–693.

39. Mentlak,T.A., Kombrink,A., Shinya,T., Ryder,L.S., Otomo,I., Saitoh,H., Terauchi,R., Nishizawa,Y., Shibuya,N., Thomma,B.P.H.J., *et al.* (2012) Effector-mediated suppression of chitin-triggered immunity by magnaporthe oryzae is necessary for rice blast disease. *Plant Cell*, **24**, 322–335.

40. Kombrink,A., Rovenich,H., Shi-Kunne,X., Rojas-Padilla,E., van den Berg,G.C.M., Domazakis,E., de Jonge,R., Valkenburg,D.-J., Sánchez-Vallet,A., Seidl,M.F., *et al.* (2017) Verticillium dahliae LysM effectors differentially contribute to virulence on plant hosts. *Mol. Plant Pathol.*, **18**, 596–608.

41. Dölfors,F., Holmquist,L., Dixelius,C. and Tzelepis,G. (2019) A LysM effector protein from the basidiomycete Rhizoctonia solani contributes to virulence through suppression of chitin-triggered immunity. *Mol. Genet. Genomics*, **294**, 1211–1218.

42. Dubey,M., Vélëz,H., Broberg,M., Jensen,D.F. and Karlsson,M. (2020) LysM Proteins Regulate Fungal Development and Contribute to Hyphal Protection and Biocontrol Traits in Clonostachys rosea. *Front. Microbiol.*, **11**, 679.

43. Cen,K., Li,B., Lu,Y., Zhang,S. and Wang,C. (2017) Divergent LysM effectors contribute to the virulence of Beauveria bassiana by evasion of insect immune defenses. *PLoS Pathog.*, **13**, e1006604.

44. Romero-Contreras,Y.J., Ramírez-Valdespino,C.A., Guzmán-Guzmán,P., Macías-Segoviano,J.I., Villagómez-Castro,J.C. and Olmedo-Monfil,V. (2019) Tal6 From Trichoderma atroviride Is a LysM Effector Involved in Mycoparasitism and Plant Association. *Front. Microbiol.*, **10**, 2231.

45. Zeng,T., Rodriguez-Moreno,L., Mansurkhodzaev,A., Wang,P., van den Berg,W., Gasciolli,V., Cottaz,S., Fort,S., Thomma,B.P.H.J., Bono,J.-J., *et al.* (2020)

A lysin motif effector subverts chitin-triggered immunity to facilitate arbuscular mycorrhizal symbiosis. *New Phytol.*, **225**, 448–460.

46. Tian,H., Fiorin,G.L., Kombrink,A., Mesters,J.R. and Thomma,B.P.H.J. (2022) Fungal dual-domain LysM effectors undergo chitin-induced intermolecular, and not intramolecular, dimerization. *Plant Physiol.*, **190**, 2033–2044.

47. Muraosa,Y., Toyotome,T., Yahiro,M. and Kamei,K. (2019) Characterisation of novel-cell-wall LysM-domain proteins LdpA and LdpB from the human pathogenic fungus Aspergillus fumigatus. *Sci. Rep.*, **9**, 3345.

Chapter 2

A network-based model of *Aspergillus fumigatus* elucidates regulators of development and defensive natural products of an opportunistic pathogen

Cristobal Carrera Carriel[1], Saptarshi Pyne[2], Spencer A. Halberg-Spencer[2,7], Sung Chul Park[5], Hye-won Seo[5], Aidan Schmidt[5], Dante G. Calise[5], Jean-Michel Ané[3,4], Nancy P. Keller[5, 6*], Sushmita Roy[2,7*]

[1] Department of Genetics
[2] Wisconsin Institute for Discovery
[3] Departments of Bacteriology
[4] Department of Agronomy
[5] Department of Medical Microbiology and Immunology
[6] Department of Plant Pathology
[7] Department of Biostatistics and Medical Informatics

University of Wisconsin-Madison, Madison, Wisconsin, USA 53715

* To whom correspondence should be addressed. Tel: +1 608 316 4453; Email: sroy@biostat.wisc.edu. Correspondence may also be addressed to npkeller@wisc.edu
The authors wish it to be known that, in their opinion, the first three authors should be regarded as joint First Authors.

Cristobal Carrera Carriel's Contribution to Chapter 2

CCC curated publicly available expression datasets and regulators of *A. fumigatus*. SAHS and SP normalized datasets and ran MERLIN. CCC assessed GRAsp's ability to recapitulate known pathways (presented in Figures 3 and 4). CCC also performed physiological assays of *AfatfA* mutants. CCC wrote the Introduction (with edits from SAHS), Methods for *AfatfA* work, and Conclusion. SAHS wrote computational methods pertaining to network inference. Results were also written by CCC, except for the first two sections (pages 41-42), which written by SAHS. CCC and SAHS both developed the GRAsp online resource. J.-M.A, N.P.K, and S.R. provided input on writing.

ABSTRACT

Aspergillus fumigatus is a notorious pathogenic fungus responsible for various harmful, sometimes lethal, diseases known as aspergilloses. Understanding the gene regulatory networks that specify the expression programs underlying this fungus' diverse phenotypes can shed mechanistic insight into its growth, development, and pathogenicity determinants. We constructed a comprehensive gene regulatory network resource, we used eighteen RNA-seq datasets (seventeen publicly available and one previously unpublished) of *Aspergillus fumigatus*. Our resource, named GRAsp (**G**ene **R**egulation of ***Asp****ergillus fumigatus*), was able to recapitulate known regulatory pathways such as response to hypoxia, iron and zinc homeostasis, and secondary metabolite synthesis. Further, GRAsp was experimentally validated in two cases: one in which GRAsp accurately identified an uncharacterized transcription factor negatively regulating the production of the virulence factor gliotoxin and another where GRAsp revealed the bZip protein, *Af*AtfA, as required for fungal responses to microbial signals known as lipo-chitooligosaccharides. Our work showcases the strength of using network-based approaches to generate new hypotheses about regulatory relationships in *Aspergillus fumigatus*. We also unveil an online, user-friendly GRAsp version that is available to the *Aspergillus* research community.

INTRODUCTION

Aspergillus fumigatus is an environmentally and medically relevant filamentous fungus found worldwide. While it is considered a soil-dwelling mold, living as a saprotroph and taking part in nutrient cycling, the airborne conidia's small size and abundance lend to

its notorious reputation as a lethal opportunistic pathogen (1–3). If the fungus can bypass a person's immune system, such as in immunocompromised individuals, it can cause various respiratory and invasive diseases. Invasive aspergillosis is the most serious of these diseases (4, 5) and has a high mortality rate (2, 6, 7). The fungus also causes a secondary infection of COVID-19, known as CAPA (COVID-19-associated pulmonary aspergillosis), that leads to an estimated mortality rate of ca. 50% (8).

The global success of *A. fumigatus* in diverse environments, from decaying organic matter to immunologically compromised patients, is reflected in significant shifts in programmed gene expression. Identifying gene regulatory networks (GRNs) that define regulatory relationships between regulatory proteins and target genes and drive these expression patterns holds promise in elucidating key genes and pathways required for virulence or interactions in different environments. At least seven studies in *Aspergillus fumigatus* have examined different sets of regulatory relationships involved in specific biological processes (9–16). For instance, Guthke et al. studied the regulatory mechanism(s) that allows *A. fumigatus* to adapt to a dramatic temperature shift during the infection process; in their study, they used an inferred GRN to hypothesize that *erg11,* a gene necessary for ergosterol synthesis, modulates the expression of genes encoding heat shock proteins and the allergen RPL3 in response to a temperature shift of 30 °C to 48 °C (9). In another instance, Linde et al. inferred and experimentally validated the role of the transcriptional regulator SrbA in iron homeostasis (16). While these studies have demonstrated how GRNs can capture regulatory mechanisms, they have focused on several regulators using small datasets. Uncovering genome-scale GRNs within a eukaryotic organism is a significant experimental challenge due to the

sheer magnitude of experiments required to comprehensively identify and verify regulatory relationships (17, 18). Computational methods for inferring GRNs, which leverage large-scale gene expression data (i.e., mRNA transcriptomic profiles) to reverse engineer GRN structure, offer a popular and cost-effective technique to provide an initial view of the GRN that can be experimentally verified. For example, Acerbi *et al.* applied a computational method using the transcriptome of several *A. fumigatus* genes to infer the regulatory connections involved in tryptophan synthesis (11). Although these studies have shed light on GRNs in *A. fumigatus,* the datasets have been limited to specific environmental conditions (e.g., tryptophan, temperature). Our goal in this study was to construct a comprehensive genome-wide GRN of *A. fumigatus* and provide a user-friendly interface to query this GRN, enabling the generation of testable hypotheses of *A. fumigatus* molecular responses to diverse environmental conditions. To address this goal, we applied a computational GRN inference algorithm called MERLIN-P-TFA (Siahpirani *et al.* in preparation, 2023, https://github.com/Roy-lab/MERLIN-P-TFA) on a curated set of publicly available and in-house RNA-seq profiles of *A. fumigatus*. Leveraging transcriptomic data of Aspergillus spp. to infer networks was successfully shown in 2019, when Schäpe *et al*. inferred and validated a comprehensive co-expression network in *Aspergillus niger (*19). MERLIN-P-TFA, specifically, uses a probabilistic graphical modeling approach (20) to infer a GRN (18). Moreover, MERLIN-P-TFA groups genes into modules where genes belonging to the same module have similar regulatory programs. MERLIN modules reflect small regulatory programs and provide insight into regulators driving these pathways.

The MERLIN-P-TFA inferred network successfully recapitulated known regulatory relationships for multiple processes, including ergosterol biosynthesis, iron homeostasis, and secondary metabolite regulation. Further, using the network predictions of MERLIN-P-TFA, we successfully identified one transcription factor involved in mediating *A. fumigatus* response to microbial signals called lipo-chitooligosaccharides (LCOs) and one transcription factor regulating the synthesis of the bioactive toxin gliotoxin. We have created a user-friendly online resource named GRAsp (**G**ene **R**egulation of ***Asp****ergillus fumigatus,* grasp.wid.wisc.edu) that allows for visualization and exploration of *A. fumigatus'* predicted GRN.

MATERIAL AND METHODS

Data acquisition and preprocessing

We obtained raw fastq reads from 17 previously published datasets and a newly generated bulk RNA-seq one (**Table S1**) (7, 15, 21–35). The adapter sequences were clipped with Trimmomatic (version 0.32, settings 2:30:10:2:keepBothReads LEADING:5 TRAILING:5 MINLEN:36) (36). The transcripts were counted with RSEM (37) using *A. fumigatus* strain Af293's reference transcriptome ASM265v1.49 (ftp://ftp.ensemblgenomes.org/pub/fungi/release-49/gff3/aspergillus_fumigatus/Aspergillus_fumigatus.ASM265v1.49.gff3.gz). RSEM produced transcripts per million (TPM) matrix for each dataset. In each TPM matrix, the rows represent the genes, and the columns represent the samples in that dataset. Finally, we log-transformed and quantile-normalized each TPM matrix. These initial matrices were given as input to the batch effect correction step.

Batch correction

Each TPM matrix was zero-mean transformed, i.e., the mean of each gene's expression was subtracted from its expression value in each sample. As a result, each gene had a mean expression of zero in every TPM matrix after the transformation. Subsequently, we performed principal component analysis (PCA) on the transformed matrices. We generated PCA plots using the combined matrix before and after zero-mean transformation (**Figures S5, S6, and S7**). PCA components after zero-mean transformation demonstrated that the variation between datasets was less prevalent than between experimental conditions. We generated correlation and gene expression heatmaps to verify further that batch correction was sufficient to remove variation between datasets. We identified one dataset, namely PRJEB2987, which was observed to have seven outlier samples: samples S1-S4, and samples from the third replicate (rep3), with unexpected correlation structure and expression (**Figure S8 and S9)**. We removed these seven samples from our dataset. The final expression matrix contained the values of 9,859 genes across 294 samples.

Inference of the gene regulatory network

To infer a GRN from the expression matrix, we applied a network inference method named MERLIN-P-TFA (Siahpirani et al., 2023, https://github.com/Roy-lab/MERLIN-P-TFA). This method extends our previous method, MERLIN-P, by estimating hidden TF activity levels from a noisy input prior network (38). This algorithm takes three inputs: (a) an expression matrix, (b) a list of regulators, and (c) a prior network. Only the genes mentioned on the input list of regulators are allowed to have outgoing edges in the inferred network.

Preparation of the list of regulators

We curated five lists of regulators and combined them to produce the final list of regulators. The lists are: (a) the predicted TFs for A. *fumigatus* strain Af293 in the JGI MycoCosm database, (b) the predicted TFs in Furukawa et al. (2020), (c) the signaling genes that are annotated for GO terms "G-protein coupled receptor protein signaling pathway" (GO:0007186) and “Calcium-mediated signaling” (GO:0019722) in the JGI MycoCosm database, (d) the list of G-protein coupled receptors (GPCRs) found in (39–41), and (e) the genes annotated for “Signal transduction” (GO:0007165) in the AspGD gene ontology database (39–42). The combined list comprises 820 distinct regulators (**Figure S1** (41)). In Furukawa et al., the TF names correspond to A. *fumigatus* strain A1160; hence, we used OrthoFinder to find the orthologous gene names for strain Af293 (40, 43, 44). See Supplementary File **S1_regulators.xlsx** for a detailed description of each sublist.

Construction of the prior network

MERLIN-P-TFA utilizes a prior network to guide its network inference task by incorporating prior knowledge on an edge when available. We utilized putative TF binding site sequence motifs to construct the prior network. We downloaded 628 (DNA-sequence) motifs corresponding to 99 TFs in *A. fumigatus* from the CIS-BP database (45). Additionally, we used four previously characterized *A. fumigatus* motifs corresponding to two TFs (46, 47); for brief descriptions, see **Supplementary Method S1** (46, 47). We scanned the A. *fumigatus* reference genome (ASM265v1 release 49) for each motif to determine using *pwmmatch.exact.*r (from the PIQ pipeline), to generate

the genome-wide coordinates of the motif instances on the genome (48). Each motif instance set of coordinates was then mapped to a gene if the coordinates overlapped a region 10 Kbp upstream and 1 Kbp downstream of the gene transcription start site (TSS). Our specified distance surrounding the TSS was motivated by experimental validation of regulator interactions at least 10kb upstream of the TSS (49, 50). Suppose motif M has two sets of coordinates mapped to genes A and B, respectively, and TF X can bind to motif M. In that case, two edges were included in the prior network, one from X to A, and another from X to B (**Figure S2**) (48). We designate each gene-motif instance pair as an edge in our prior network and assign each edge an edge weight corresponding to the log-likelihood of observing the motif-specific precision-weighted matrix. Moreover, we assigned each edge a PIQ score representing the likelihood of the motif appearing on the binding site of the target gene (48). The scores were calculated with the R package “Biostrings” (51, 52). We sorted the candidate binding sites by their scores for each motif and retained only the top 100,000 sites. We retained all the motifs with less than 100,000 candidate binding sites. The resultant prior network was extremely dense (containing 936,557 edges). Hence, we restricted its density to be 20% of the total number of possible edges (0.2 x Number of TFs in the prior network, i.e., 96 Number of target genes, i.e., 9,859), which corresponded to 189,292 edges. Finally, we converted all edge scores to a range of scores between 0 and 1 by applying percentile ranking to them. The highest score was 1, and the lowest was 0.000101688 (Supplementary File **S2_prior_network.xlsx**).

Network inference with MERLIN-P-TFA

MERLIN-P-TFA performs the network inference in two steps: First, it estimates the

transcription factor-level activities (TFA) of the regulators present in the prior network. Second, it infers the edges between the regulators and the target genes by regressing the estimated TFA profiles of the regulators present in the prior network and the gene expression profiles of all the regulators to the gene expression profiles of the candidate target genes (**Figure 1**).

In the first step, MERLIN-P-TFA estimates the TFA matrix. The TFA matrix is a regulators-by-samples matrix where the (i, j)th entry denotes the estimated TF-level activity (53–55) of the regulators (that are present in the prior network) across all the samples (in the expression matrix). To estimate the TFA matrix, P, MERLIN-P-TFA solves the minimization problem $\min(||Enxs - AnmPms||22 + ||Anm(Wnm)T||)$ where E is the given expression matrix, n is the number of target genes, s is the number of samples, A (called the "connectivity matrix" which is derived from the given "prior network") is the prior knowledge on the regulatory edges between the regulators and target genes, m is the number of regulators, and W is the prior edge-penalty matrix; W(i, j) represents the prior penalty on the edge from the j^{th} regulator to the i^{th} target gene calculated as (1 - the confidence of the edge in the prior network). The regularization term $||Anm(Wnm)T||$ is important for handling noise in the connectivity matrix (Siahpirani et al. in preparation, 2023, https://github.com/Roy-lab/MERLIN-P-TFA). The level of regularization depends upon ; the higher the value of , the higher the regularization level. In this work, we used $=0.1$.

Once the TFA is estimated, MERLIN-P-TFA uses the original MERLIN-P method to infer a GRN. Briefly, MERLIN-P represents the relationships between regulators and target

genes as a probabilistic graphical model (PGM) known as a “dependency network.” Given a dataset D, MERLIN-P infers a network G by solving regression problems. Additionally, MERLIN-P groups genes into modules with similar regulatory programs assigned to the same module.

MERLIN-P-TFA infers two items for each gene: (a) a set of directed edges from its predicted regulators to the gene itself and (b) a module assignment. We ran the TFA estimation step 50 times by randomly initiating the connectivity matrix “A” every time. This resulted in 50 estimated TFA matrices. We combined these matrices into a single TFA matrix by taking their mean. Subsequently, we produced a large matrix by appending the estimated TFA matrix to the gene expression matrix. This large matrix contained the expressions of 9,859 genes and the estimated TFAs of 30 regulators across all 294 samples. Then we generated 100 random subsamples of the large matrix through random sampling without replacement. Each subsample matrix contained 147 samples, i.e., half the number of samples in the large matrix. We ran MERLIN-P-TFA separately on each of these 100 subsample matrices. This results in 100 distinct GRNs, each having a unique module assignment (i.e., gene to module map). We combined these 100 GRNs into a single GRN by taking the union of their edges, and each edge was assigned a confidence score that reflected how many times the edge had appeared in the previous 100 GRNs. For downstream analyses, we only considered the edges having a confidence score of 80% or above. We also inferred a consensus module assignment requiring genes to be in the same module in at least 30 out of 100 module assignments.

Interpretation of MERLIN-P-TFA network and modules

We developed three strategies based on module enrichment and graph-theoretic analyses to interpret the results of MERLIN-P-TFA and the generation of new hypotheses. All three methods accept input gene lists representing known gene sets, such as from a Gene Ontology (GO) database or a gene list from an independent differential expression analysis experiment.

Interpretation of MERLIN modules based on enrichment analyses

MERLIN-P-TFA infers a per-gene module-constrained network. MERLIN-P-TFA modules are sets of genes with similar expression profiles and regulatory programs that are similar, although not identical. To interpret the MERLIN-P-TFA modules, we tested them for enrichment of GO terms using a hypergeometric test with FDR correction for multiple hypotheses (56). A module was labeled with a GO term if a significant number of genes in this module were enriched for that GO term (FDR<0.05). In addition to the GO enrichment analysis, we tested the modules for enrichment of gene sets identified from targeted experiments in *Aspergillus*, e.g., differentially expressed genes from a gene perturbation experiment. A similar FDR-corrected p-value threshold was used to test for the enrichment of such gene sets in the modules. Modules were also helpful in determining important regulators of specific gene programs. Since MERLIN-P-TFA does not require all genes in the same module to have the same set of regulators, we further use enrichment tests to determine the critical regulators of a module using a similar hypergeometric test with FDR correction (FDR<0.05).

Approximate Steiner Tree Construction for Identification of Related Regulatory Mechanisms

While modules capture part of a regulatory program indicated by the gene expression pattern, an entire regulatory program likely spans multiple modules and individual genes that may not be co-expressed with many other genes but are still part of the GRN. Thus, we developed a second method to identify critical pathways that connect a list of genes within a program to a set of modules and additional genes. To accomplish this task, we implemented a Steiner tree-based method to find approximately minimal trees connecting any user-provided set of genes. Briefly, the Steiner tree problem on unweighted, undirected graphs is defined as given a graph $G=(V,E)$, where V denotes the set of vertices and E denotes the set of edges and a set of terminals T, finds a subgraph $G = V, E$ that spans T such that the cardinality of E is minimized. Unfortunately, the Steiner tree problem for more than two terminals is computationally intractable; thus, an approximation of such a tree is generated (57). Based on the shortest path, the closest two genes from the list are connected to create the approximation and form an undirected subgraph. The next closest gene is then iteratively added to the new subgraph until all terminal genes in T are added. In our application of the Steiner tree approach, the terminal nodes come from an input gene list generated from differential expression or similar analyses. To guarantee algorithm convergence, genes from the gene list are only considered if they are contained within the largest connected component of the predicted regulatory network. Although the approximate Steiner tree is not unique, the tree can identify hub genes that are important for the regulation of multiple different components of the gene regulatory programs.

Ranking of Gene Importance via Laplacian Kernel Node Diffusion

Our third method of determining the relationship between a specific gene pathway and the predicted regulatory network is based on a gene prioritization scheme based on diffusion on a graph (58). This strategy has been used to predict new genes for pathways and examine the impact of genetic mutations in one gene on other genes connected via a protein-protein interaction network (58). In this approach, a graph kernel defines global similarity between nodes in the input set to all other nodes in the graph. In our case, we used the Laplacian graph kernel defined as $\mathrm{K}=(1+\lambda \mathrm{L})\text{-}1$, where is a hyper-parameter specifying the bandwidth of the kernel function and L is the graph Laplacian matrix defined as $\mathrm{L} = \mathrm{D}$ - A, where D is the diagonal matrix representation of each node degree and A is the symmetric graph adjacency matrix. Diffused scores for all genes are defined by $\mathrm{V} = \mathrm{K}\ \mathrm{S}$, where S are the initial scores specified by the user. In our setup, the input gene set corresponds to genes from a pathway of interest or differentially expressed genes, and the graph is the MERLIN-P-TFA inferred GRN. The input gene set is initialized with uniform scores of 1 or based on additional data, such as the change in expression in two conditions of interest. Diffused scores are then used to prioritize genes based on their connectivity to the input gene set, which can indicate particular gene pathways of interest.

Fungal strains and culture conditions

Aspergillus fumigatus strains used in this study are listed in **Table S2** (59–63)**.** All strains were grown at 25 °C for 9 days in the dark on solid glucose minimal medium in sterile 100 x 15 mm Petri dishes (64). Ten thousand spores were used for the initial inoculum. Conidia were collected in sterile 0.01% Tween 80, filtered through a 40 µm

nylon cell strainer, then quantified using a hemocytometer. For long-term storage, conidia were maintained as glycerol stocks at −80 °C.

Generating *rogA* mutant strains

To create the *rogA* (AFUA_3G11990) deletion strain (TSCP2), its 1.4 kb 5' flanking region and 1.0 kb 3' flanking region were amplified by PCR from the genomic DNA from *A. fumigatus* strain AF293. The *A. parasiticus pyrG* gene was used as a selective marker and was amplified by PCR from the pJW24 plasmid (65). To make the *rogA* overexpression strain (THWS25), 1.0 kb of the gene's 5' flanking region and the entire 1 kb *rogA* region, starting with ATG were amplified from Af293 genomic DNA. The *pyrG* linked with the *A. nidulans gpdA* promoter was amplified from the pJMP9 plasmid (66). These fragments were fused by double-joint PCR, respectively (67). About 25 µL of Sephadex® G-50 purified third-round PCR product was used to transform TFYL80.1 for both the deletion and overexpression mutants. All fungal transformations were done using the polyethylene glycol (PEG)-based method previously described (67). Both the deletion and overexpression mutants were confirmed by PCR and Southern blot (**Figure S3**). Primer sequences are listed in **Table S3.**

Metabolite Extraction

GMM cultures of WT, Δ*rogA,* and OE::*rogA* strains were grown (culture conditions described above) and lyophilized for 3 days in quadruplicate. The dehydrated agar and biomass were then crushed to powder. Each sample was extracted with 25 mL of 100% methanol and passed through filter paper. Extracts were reduced by air drying, weighed, and resuspended in 100% methanol at a final concentration of 1 mg/mL. Two authors performed these experiments independently.

UHPLC–HRMS and UHPLC–MS/MS analyses

UHPLC–HRMS was performed on a Thermo Scientific Vanquish UHPLC system connected to a Thermo Scientific Q Exactive Hybrid Quadrupole-Orbitrap mass spectrometer operated in positive ionization mode. A Waters Acquity UPLC BEH-C18 column (2.1 × 100 mm, 1.7 µm) was used with acetonitrile (0.1% formic acid) and water (0.1% formic acid) at a flow rate of 0.2 mL/min. A screening gradient method was implemented as follows: Starting at 10% organic for 5 min, followed by a linear increase to 90% organic over 20 min, another linear increase to 98% organic for 2 min, holding at 98% organic for 5 min, decreasing back to 10% organic for 3 min, and holding at 10% organic for the final 2 min, for a total of 37 min. Ten µL of each sample was injected into the system for the analysis. Gliotoxin was identified by comparison with a standard purchased from Cayman Chemical (Ann Arbor, MI, USA). An analog of gliotoxin, BMgliotoxin, was predicted by the analysis of UHPLC–MS/MS data through SIRIUS ver.5.5.7. The relative quantification of two compounds was calculated based on intensities obtained from UHPLC–MS/MS.

Analysis of secondary branching and germination in *A. fumigatus*

To look at the number of secondary branches in *A. fumigatus*, $1x10^{6}$ conidia per mL of *A. fumigatus* strains was inoculated in GMM broth treated with either 10^{-8} M sulfated C16:0 LCO (CERMAV) or the negative control, 0.005% ethanol (64). 100 µL of inoculated and treated broth was dispensed into a well in a 96-well flat bottom plate in triplicate. The plate was incubated at 37 °C for 11 hours, followed by imaging every 15 minutes over 3 hours using a Nikon TI inverted microscope with a 40X objective. Each frame captures the growth of one hypha, and ten frames were taken per well. The

number of secondary branches per apical hyphae was counted using NIS-Elements AR Analysis Version 4.30.

To quantify the germination of conidia, $1x10^5$ spores per mL of *A. fumigatus* strains were inoculated in GMM broth treated with either 10^{-8} M sulfated LCOs (LCO-IV (C:16,S)) or 0.005% ethanol (negative control). 1 mL of inoculated and treated broth was dispensed into a well in 24-well flat-bottom plates and incubated at 37°C for 3 hours. After 3 hours, 10 different areas in the well were captured as frames using a 40X objective. Each frame contained 20-30 conidia and was photographed every hour for 12 hours. Germination of conidia was counted using NIS-Elements AR Analysis Version 4.30.

RNAseq extraction from *A. fumigatus zfpA* mutants

For mycelial RNA, *A. fumigatus* wild type, Δ*zfpA*, and OE::*zfpA* conidia were inoculated at 10^6 spores per mL in liquid glucose minimal media and incubated at 37˚C shaking at 250 RPM overnight (63). The total tissue was combined from two 50mL cultures flash frozen and lyophilized for each sample. Total RNA was extracted using QIAzol Lysis Reagent (Qiagen) according to the manufacturer's instructions with an additional phenol:chloroform:isoamyl alcohol (24:1:1) extraction step before RNA precipitation. For conidial RNA, 10^6 WT, Δ*zfpA*, or OE::*zfpA* conidia were inoculated into 8mL of molten GMM top agar (0.75% agar) and overlaid onto cooled GMM plates containing 15mL bottom media (1.5% agar). Plates were incubated at 37˚C for 3 days before harvesting in 0.01% Tween 80 solution. Spore suspensions were filtered twice through two layers of sterile miracloth and once through 40µm cell strainers (Falcon) to remove hyphal fragments. Filtered conidia were pelleted at 1000 x g for 10 minutes and resuspended in

200µL 0.01% Tween 80. Concentrated conidia were lysed by bead beating for 5 minutes with 0.5mm zirconia/silica beads after adding QIAzol Lysis Reagent and chloroform. Total RNA extraction was completed per the manufacturer's instructions with an additional phenol:chloroform:isoamyl alcohol (24:1:1) extraction step before RNA precipitation. Total RNA from both mycelial and conidial samples was cleaned using RNeasy Mini Kit with on-column DNase digestion (Qiagen) per manufacturer's protocol. RNA integrity was tested via nanodrop, gel electrophoresis, and the Agilent 2100 Bioanalyzer. Library preparation and RNA sequencing were performed by Novogene, Inc. using the TruSeq Stranded mRNA Library Prep Kit and Illumina Novaseq 6000 Platform.

Statistical Analysis

Gliotoxin Mass-spectrometry

Relative abundance of BMgliotoxin and gliotoxin were measured by two authors in independent experiments. Normalization was performed for each author independently by dividing all relative abundance measurements by the mean of the WT condition. After normalization, data was pooled between authors (total *n*=8 per strain). Statistical analyses between the wild type and the genetically modified strains were performed using an Unpaired t-test (Graphpad Prism v9.4.1).

Network Diffusion utilizing differentially expressed genes of LCO-treated samples

For diffusion analysis, we used a list of differentially expressed genes (DEGs), published in Rush et al. 2020, of *A. fumigatus* 30 minutes after treatment with LCOs (**Table S1**, Serial number 16) (34). Diffusion was performed using Laplacian kernel

diffusion with hyperparameter, =10, and the absolute log fold change of the DEGs. Regulators with at least 5 targets were sorted to determine importance for the LCO-treated condition.

AfatfA mutant phenotype quantification in LCO-treated samples

Secondary branching and percent germination were quantified as described above. Germination studies had a *n*=16 total for WT; △*AfatfA, n*=19, OE::*AfatfA, n*=17. Branching studies had a *n*=60 total for WT; △*AfatfA, n*=59, OE::*AfatfA, n*=57. Statistical analyses comparing the phenotypic traits in *AfatfA* relative wildtype after treatment with LCO were performed using an Unpaired t-test utilizing Graphpad Prism (v9.4.1).

RESULTS

Genome-scale Gene Regulatory Network of *A. fumigatus* identified by MERLIN-P-TFA

MERLIN-P-TFA generated a genome-wide gene regulatory network (GRN) based on eighteen RNA-seq datasets of multiple *A. fumigatus* strains in various conditions **(Table S1, Figure 1**). Our network, which consists of 80% confident edges, contains 7,422 regulatory edges. Each regulatory edge connects one of 669 regulators to one of the 5274 target genes. Our regulator set includes 12 signaling proteins (**Figure S1**) and 30 regulators with motifs. MERLIN-P-TFA estimated the TFA of these 30 regulators. The gene encoding the mating type protein MAT1-2 and the stress response protein *Af*AtfA (incorporated based on TFA) are the top two regulators of the network, regulating 216 and 155 target genes, respectively (**Figure 2B**). Furthermore, MERLIN-P-TFA identified

164 modules with at least five genes. Jointly, they contain 3,381 genes. We performed a GO enrichment analysis to interpret these modules' biological relevance. Among the 164 modules, 74 were enriched with at least one GO term (Supplementary file **S3_module_details.xlsx**).

GRAsp: a visualization framework for interpretation and hypotheses generation of the *Aspergillus* GRN

Genome-wide regulatory networks are difficult to interpret due to the many predicted interactions between regulators and target genes. To aid in interpreting and analyzing our MERLIN-P-TFA inferred network, we have developed a network visualization framework called GRAsp (**G**ene **R**egulation of ***Asp****ergillus fumigatus*) that incorporates different graph theoretic tools to examine sets of genes related to a specific process of interest. GRAsp allows users to input a list of genes or gene ontology terms and then actively generates interactive network diagrams that can be used to determine regulators of interest. The networks visualized in the GRAsp display window can be extended to include all genes in associated MERLIN modules or the neighborhood of the list of selected genes, providing additional information about regulatory mechanisms of interest. GRAsp also incorporates a Steiner tree estimation method to connect sets across MERLIN modules. Given a list of genes of interest, the Steiner tree method connects all genes with an approximate spanning tree (**Methods**). The final approach in GRAsp allows the user to incorporate additional data into the network using node diffusion (58). For example, this feature allows users to use differential expression p-values or fold change information to prioritize regulators. The nodal gene values are

assigned to each node and diffused via a Laplacian kernel (58). GRAsp then displays the top regulators related to the pathway. The network visualization panel can be customized and saved as publication-quality figures. The GRAsp network tool is publicly accessible at grasp.wid.wisc.edu.

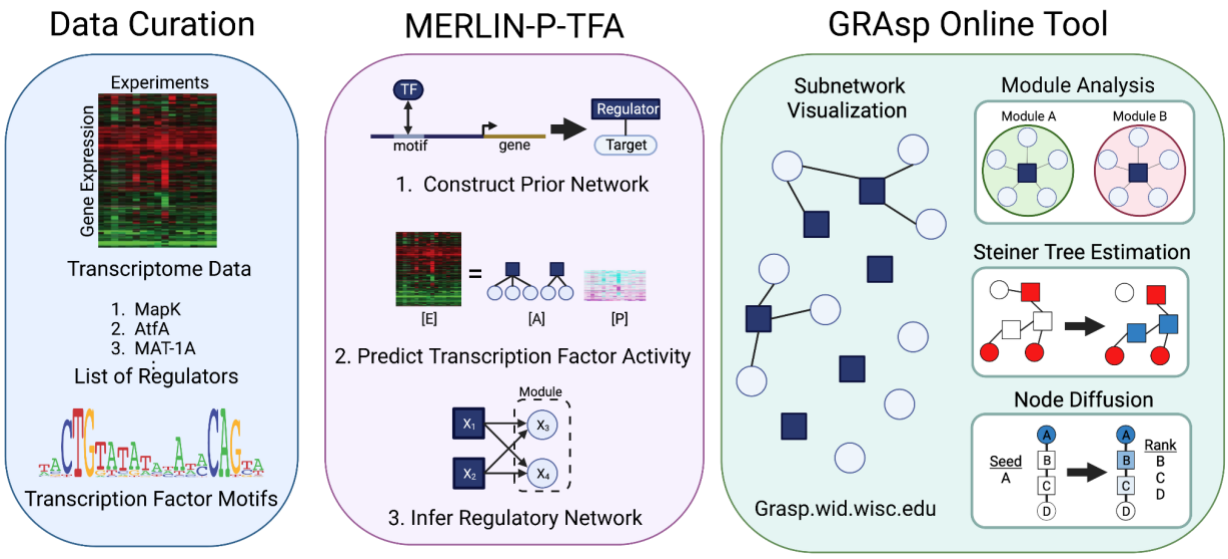

Figure 1. The Network-based Modeling and Analysis Workflow. ***Data Curation:*** We curated 18 *A. fumigatus* bulk RNA-seq profiles and combined them to produce a batch-corrected transcriptome data matrix of 9,859 genes across 294 experiments. We also prepared a list of 820 putative regulator genes and 632 TF binding site sequence motifs. ***MERLIN-P-TFA:*** We used our MERLIN-P-TFA method to infer a gene regulatory network from the curated expression data. MERLIN-P-TFA takes a prior network constructed based on the TF motif information as additional input. Given the prior network, the list of regulators, and the transcriptome data matrix, MERLIN-P-TFA first estimated a transcription factor activity (TFA) matrix. This matrix represents the

estimated TF-level activity of the regulators (present in the prior network) across all the experiments. Subsequently, MERLIN-P-TFA combined the TFA matrix with the transcriptome data matrix to infer the gene regulatory network. ***GRAsp Online Tool:*** GRAsp is an online visualization framework for interacting with the inferred regulatory network. GRAsp offers various network analysis techniques, such as gene module analysis, Steiner tree estimation, and node diffusion, to recapitulate known pathways and hypothesize novel gene regulatory activities (some of which were further experimentally validated). Created with Biorender.com.

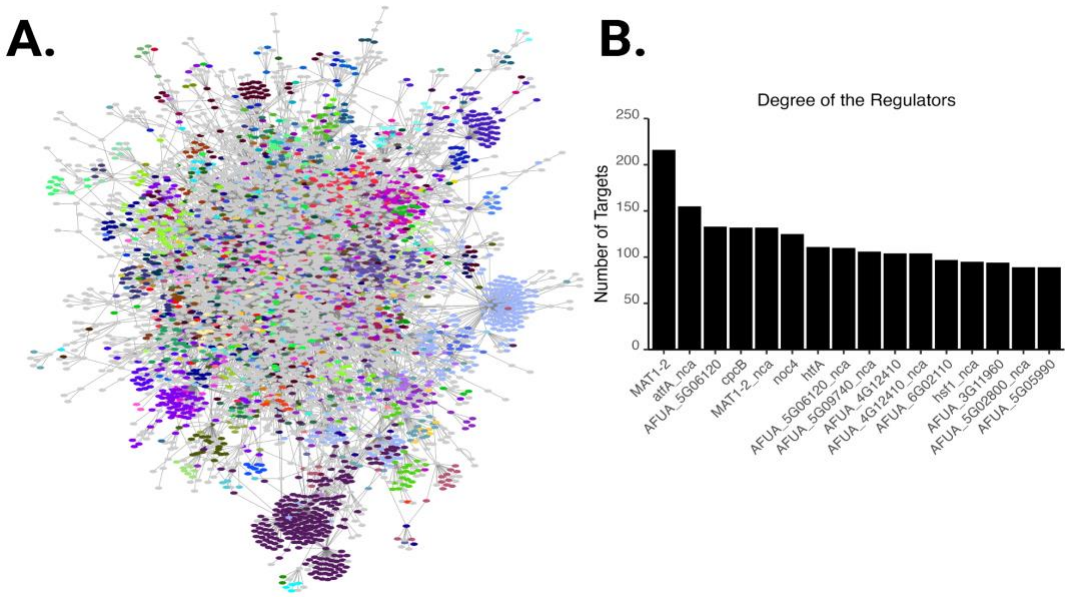

Figure 2*. A. fumigatus* gene regulatory network predicted by MERLIN-P-TFA. A) Force-directed layout of the inferred network where genes belonging to the same module are depicted with the same color. The network was visualized using Cytoscape (v.3.8.2) (68). B) Predicted major regulators ordered by their number of targets. The regulators having the "_nca" suffix indicates that the estimated TFA of the regulator was

included in the network based on its TFA. For example, “atfA_nca” represents that *AfatfA* was selected as a regulator based on its TFA. The “_nca” suffix refers to the regularized “network component analysis” technique used by MERLIN-P-TFA for estimating the TFA profiles of the regulators. (Siahpirani et al., 2023, https://github.com/Roy-lab/MERLIN-P-TFA). Figure prepared with Biorender.com

Diverse biological processes of *Aspergillus* are captured in GRAsp

We first evaluated GRAsp for its ability to recapitulate known regulatory pathways in *A. fumigatus*. Specifically, we looked at four previously characterized transcription factors and their roles in regulating different pathways: SrbA and its role in regulating hypoxia and various stress responses, ZafA and its response to zinc starvation, HapX and its response to iron starvation, and FapR’s regulation of secondary metabolites.

SrbA and hypoxia The ability of *Aspergillus fumigatus* to respond to hypoxia, low iron availability, and antifungals contributes to the fungus’ pathogenicity. The response to these conditions is partly mediated by the sterol regulatory element binding transcription factors SrbA and SrbB (16, 69). Chung et al., 2014 employed ChIP-seq technology to uncover the downstream targets of these two transcription factors. Under hypoxic conditions, SrbA and SrbB regulate each other while also regulating target genes involved in adaptation to hypoxia, such as ergosterol biosynthesis (*erg1, erg11A, erg25A, erg3B, erg5*), nitrate assimilation (*niaD*, *niiA*), nitric oxygen (NO)-detoxifying flavohemoprotein gene (*fhpA*), heme biosynthesis (*hem13*), and ethanol fermentation (*alcC*) (70). The module containing *srbA*, module 5395, recapitulated many known regulatory relationships (**Figure 3A, B)**. Additionally, many genes, such as *erG3A* or

niaD, which are not predicted to be directly regulated by either *srbA* or *srbB,* are still present in the MERLIN module. Only the regulatory relationship between *srbB* and *alcA* was missed entirely. Most importantly, GRAsp inferred new genes with additional functions in these processes, such as sterol biosynthesis (*cyp51A*) and heme biosynthesis (*hem14*), as well as genes of currently unknown function (in black in **Figure 3B**).

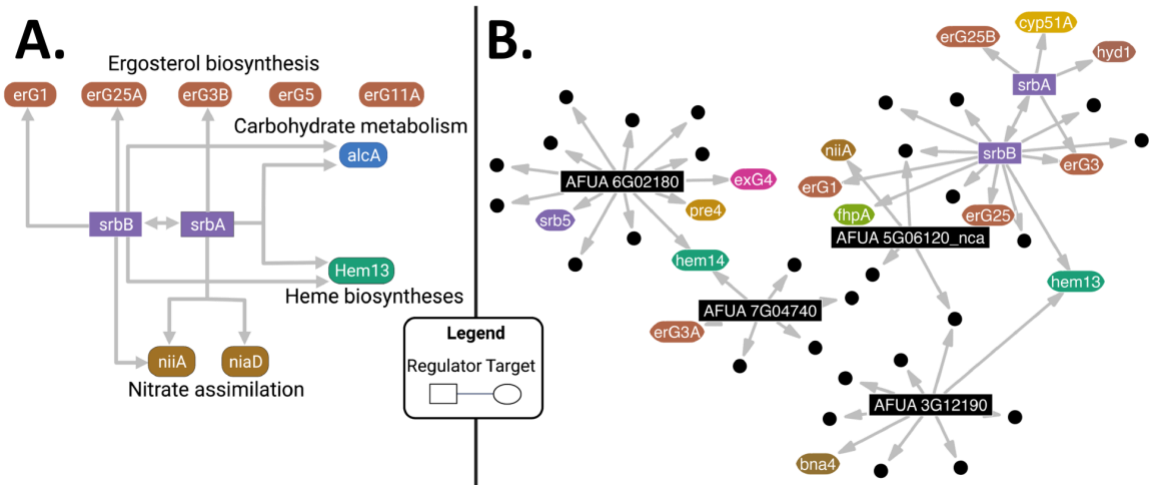

Figure 3. Recapitulation of SrbA targets. A) SrbA pathway inferred through ChIP-seq, reproduced from Chung *et al.* 2014 (Published under a Creative Commons attribution license). Genes in rectangles represent regulators; gene targets are contained in ovals. Gene colors represent each pathway. Created with Biorender.com. B) Module 5395 includes the transcription factors *srbA* and *srbB* visualized with GRAsp. Black circular nodes represent gene targets without a gene symbol in the fungiDB database. 22 genes within the module that are not part of the known *srbA* and *srbB* regulatory system and are not regulated by any module regulators have been removed to simplify the figure. Figure prepared with Biorender.com

ZafA and zinc homeostasis Zinc is important for proper growth and development in *A. fumigatus (71).* In circumstances where the fungus encounters low zinc environments, such as within host tissue, the acquisition of zinc ions is essential. To maintain zinc homeostasis, the transcription factor ZafA regulates *zrfA*, *zrfB*, and *zrfC* expression, which encode transporters involved in zinc uptake (71, 72). Module 5027, which is regulated by ZafA, contains *zrfA.* Additionally, *zrfB* and *zrfC* outside of this module are still predicted targets of *ZafA* (**Figure 4A**). The resulting subnetwork displays ZafA as the primary regulator of 15 target genes, including *zrfA*, *zrfB*, and *zrfC*. The subnetwork also reveals uncharacterized targets of ZafA, which could also be involved in zinc homeostasis. For example, AFUA_5G02010 has orthologs related to metalloendopeptidase activity, and AFUA_1G14700 is related to transmembrane transport.

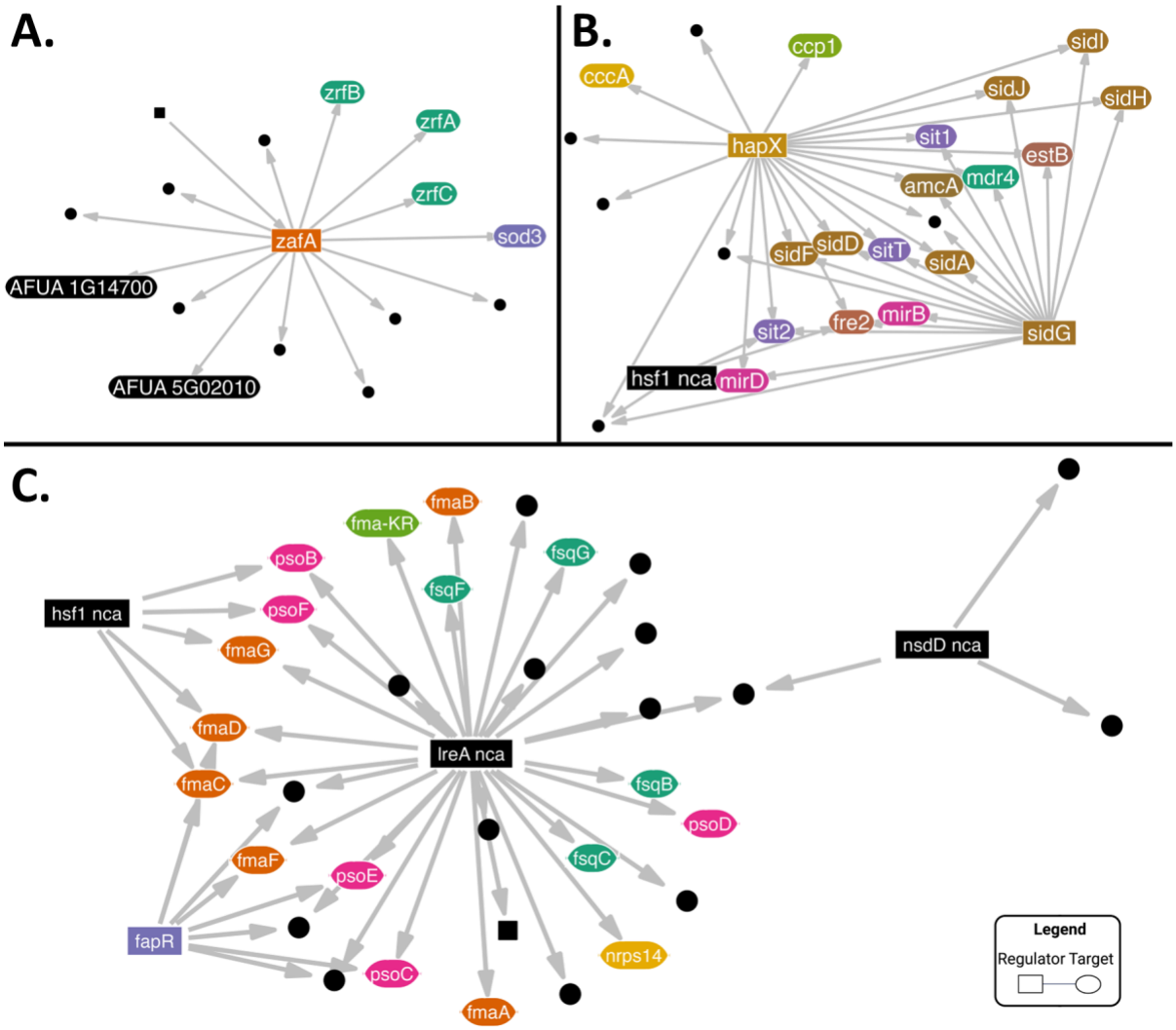

Figure 4. Recapitulation of known genetic pathways in GRAsp. Network representations of known genetic pathways are visualized with GRAsp. In all figures, node colors correspond to similar common name prefixes, i.e., fma, fsq, zrf, and sid. Black nodes represent gene targets without a gene symbol in the fungiDB database. Regulators are represented as rectangles and squares. Targets are represented as circles and ovals. A) The regulatory targets of *ZafA* were generated by selecting its neighbors. B) Modules 4901 and 5283 contain the *hapX* gene. C) Module 5396 which contains the *fapR* gene. Orange target genes represent fumagilin biosynthesis genes

(fma prefix), pink targets represent pseurotin genes (pso prefix), and green targets represent fumisoquin genes (fsq prefix). Figure prepared with Biorender.com.

HapX and iron starvation Similar to zinc, iron is a critical cofactor metal in *A. fumigatus,* and processes to acquire iron under iron-limiting conditions are partially regulated by the transcription factor HapX (73). Specifically, HapX plays an essential role in activating genes involved in the synthesis of specialized iron-acquiring metabolites called siderophores (*sid* genes and *estB* encoding a siderophore triacetylfusarinine C esterase), putative siderophore transporters (*sit* genes and *mirB* and *mirD*), and the metalloreductase important during iron starvation (*fre2* gene). The inferred MERLIN-P-TFA regulatory network contained modules 4901 and 5283 regulated by HapX (**Figure 4B**). These modules contain all of the known targets of HapX.

FapR and secondary metabolites *A. fumigatus* is renowned for its arsenal of secondary metabolites (SMs) that play critical roles in various ecological settings, from pathogenesis to encounters with other microbes (74). The genes required to synthesize an SM are usually grouped on the genome in what is known as a biosynthetic gene cluster, BGC (75). A prime example is the metabolite fumagillin. This compound, a virulence factor in invasive aspergillosis, targets methionine aminopeptidase, which removes the amino-terminal methionine residue from newly synthesized proteins (76). This functionality has led to various fumagillin applications, such as microsporicidal activity in treating honeybee hive infections (77). Interestingly, *A. fumigatus* is resistant to fumagillin, presumably due to extra copies of methionine aminopeptidase genes in its genome (78).

The fumagillin BGC is unique because its biosynthetic genes are intertwined with genes of another SM, pseurotin, known for its antibacterial properties (78, 79). The gene encoding the transcription factor FapR is embedded in the intertwined cluster, and FapR regulates the biosynthesis of both pseurotin *(psoF, psoG, psoB, psoA, psoC, psoD,* and *psoE)* and fumagillin (*fmaB, fmaC, fmaD, fmaG,* and *fmaA*). Querying GRAsp with *fapR* as an input gene found a MERLIN-P-TFA module containing many *fma* and *pso* biosynthetic genes (**Figure 4C**). Interestingly MERLIN-P-TFA suggested a relationship between fumagillin/pseurotin production and another secondary metabolite, fumisoquin (*fsq* genes) (80). At present, the ecological role of fumisoquin is still unknown.

MERLIN-P-TFA successfully predicts a novel regulator of gliotoxin

Considering the accurate recapitulation of known regulatory pathways by MERLIN-P-TFA, we next asked if we could successfully identify new regulatory connections using our resource. We were interested in querying the regulation of the SM gliotoxin, a virulence factor in murine models of invasive aspergillosis and a potent antifungal (81, 82). The gliotoxin BGC (*gli* BGC) is regulated by an in-cluster transcription factor GliZ (**Figure 5A**); however, how *gliZ* is regulated is largely unknown (83). Using *gliZ* as the query gene, GRAsp revealed a module enriched in most *gli* genes (**Figure 5B**). The module was predicted to be regulated by an uncharacterized gene, *AFUA_3G11990,* encoding for a GAL4 type C6 transcription factor. We deleted and overexpressed *AFUA_3G11990* to see how it affected the production of gliotoxin and its derivative bis(methylthio)gliotoxin (**Figure 5C**), both of which can be detected in human serum and are potential diagnostic indicators of *Aspergillus* infections (84). In the two

AFUA_3G11990 deletion mutant siblings, Δ*rogA.1 and* Δ*rogA.2*, we observed a significant increase in gliotoxin and no change to bis(methylthio)gliotoxin. Furthermore, we observed a significant decrease in both gliotoxin production and bis(methylthio)gliotoxin in the two *AFUA_3G11990* overexpression mutant siblings, OE::*rogA.1 and* OE::*rogA.2*, suggesting that AFUA_3G11990 is a negative regulator of the *gli* BGC, possibly through regulation of *gliZ* expression. Thus, we named AFUA_3G11990 as *rogA* for the **r**egulator **o**f **g**liotoxin. The normalized gene expression matrix also observed the repressive regulatory relationship between AFUA_3G11990 (**Figure S4**).

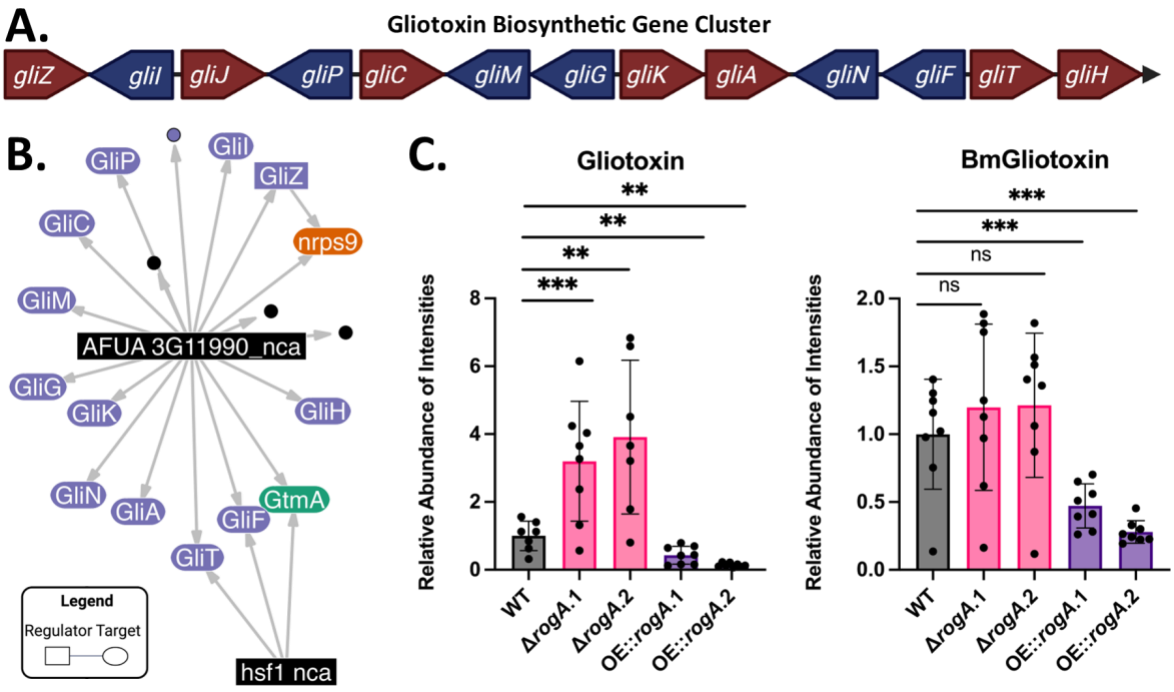

Figure 5. **Validation of a novel predicted regulator from MERLIN-P-TFA and GRAsp in Gliotoxin regulation.** A) Canonical gliotoxin biosynthetic gene cluster;

colored by direction. B) MERLIN-P-TFA module 5349, visualized by GRAsp; nodes are colored by gene family with black nodes representing genes without common name in fungiDB. C) Production of Gliotoxin and bis(methylthio)gliotoxin in two independent *rogA* transformants of Δ*rogA* and OE::*rogA*. Relative abundance of gliotoxin and bis(methylthio)gliotoxin (BMgliotoxin) was measured by intensities of UHPLC-HRMS spectra. Results are the average relative abundance of eight replicates ± standard deviation. Statistical analysis was performed using an unpaired two-sided t-test when comparing quantities to the relative abundance of the WT strain (* $p<0.1$, ** $p<0.05$, *** $p<0.01$). Samples were normalized to the wild type values of each author. Figure prepared with Biorender.com.

MERLIN-P-TFA and GRAsp identify the *Af*AtfA transcription factor as a critical component of the LCO signaling pathway in *A. fumigatus*

Fungi use diverse signals to interact with their environment (85). Lipo-chitooligosaccharides (LCOs) are small signaling molecules consisting of a chitin backbone, an attached long-chain fatty acyl group, and various functional groups, such as sulfated and fucose groups (86–88). For decades, the scientific community thought LCOs were solely produced by plant symbiotic microbes, including nitrogen-fixing rhizobia and mycorrhizal fungi, as LCOs are critical for recognition by host plants. However, we have recently shown that LCOs are synthesized throughout the fungal kingdom and that many fungi respond to LCOs in a dose-dependent manner (34). In particular, *A. fumigatus* treatment with a specific endogenous LCO (LCO-IV = C:16, S)

led to a significant reduction in hyphal branching (hypobranching) and an increased germination rate of conidia (34, 89).

To identify LCO signaling pathways leading to these phenotypes, Rush et al. performed RNA-seq analysis of LCO-IV (C:16, S) treated *A. fumigatus* cultures. However, the large number of differentially expressed genes (DEGs) made it challenging to identify key regulators to target with perturbation experiments. We used the node diffusion method in GRAsp to incorporate data from the differential expression analysis and prioritize regulators involved in LCO signaling. For each node, we associated it with an initial score based on the absolute value of the log fold change between *A. fumigatus* 30 minutes after treatment with LCOs or with negative control, then applied laplacian kernel diffusion ($= 10$) (34). After diffusion, we selected the top 10 regulators with at least 5 targets based on diffusion score (**Figure 6A**). The most connected of these regulators was the g ene *AfatfA*. *Af*AtfA is a well-known bZIP transcription factor essential for stress tolerance of conidia and reactive oxygen intermediate resistance during invasive aspergillosis (60, 90). To test if *AfatfA* plays a role in fungal response to LCOs, we examined the branching and germination rates of *A. fumigatus* treated or not with LCO-IV (C:16, S). **Figure 6B** shows that both △*AfatfA* and OE::*AfatfA* strains were unresponsive to LCO-IV compared to the wild-type. Furthermore, regardless of LCO treatment, the deletion of *AfatfA* led to increased hyphal branching (hyperbranching, top) and slow germination phenotypes (bottom). Reciprocally, the overexpression of *AfatfA* led to an extreme hypobranching phenotype even lower than the wild-type strain treated with LCO-IV. These results placed *AfatfA* as an essential component of the LCO signaling pathway and revealed its function in hyphal branching in *A. fumigatus*. *AfatfA*

loss has been implicated in a germination reduction in *A. oryzae*, matching our observations with *A. fumigatus (91)*.

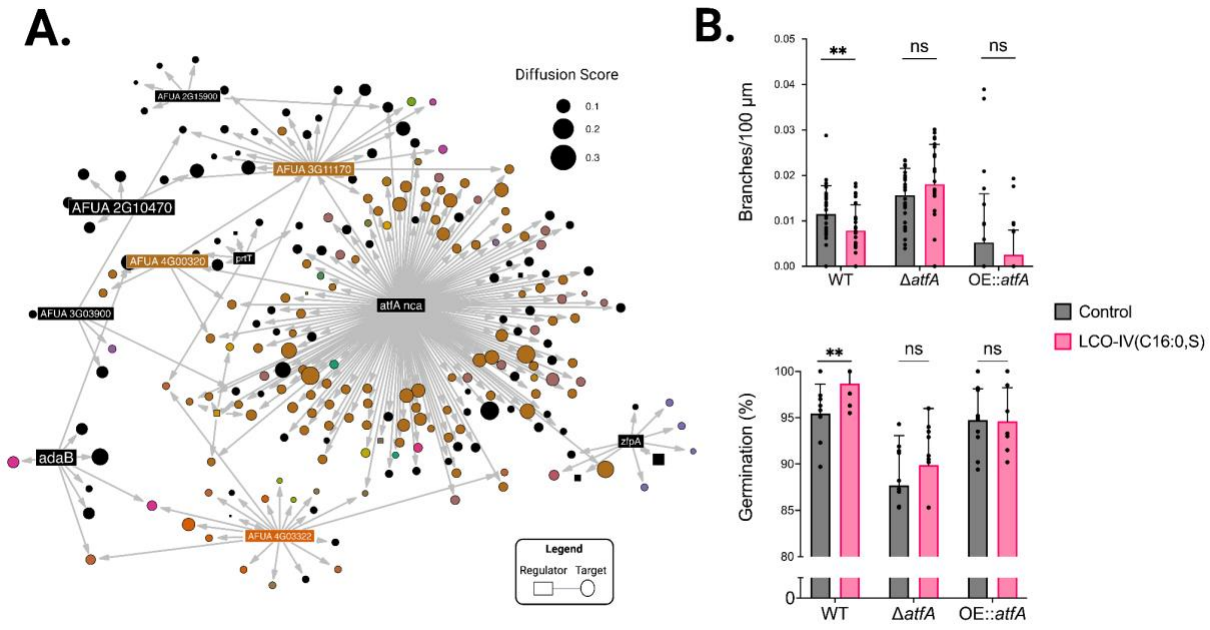

Figure 6. ***AfatfA* is necessary for branching and germination responses to LCO-IV.** A) Differentially expressed genes integrated with MERLIN-P-TFA network using network diffusion within GRAsp. Labeled regulators (rectangles) represent the top 10 regulators with at least 5 targets after diffusion of the absolute log fold change signal. Node size represents the score after diffusion. *AfatfA* (referred to as *atfA*) is a key regulator with many differentially expressed targets (large node size). Genes are colored by module identity, and black nodes represent genes not assigned to a module. B) Secondary branching *of AfatfA* mutant hyphae 12 hours after treatment with LCO-IV (C:16, S) or negative control, 0.005% EtOH. C) Percent germination *of AfatfA* mutant conidia 10 hours after treatment with LCO-IV (C:16, S) or negative control, 0.005% EtOH. Statistical analysis was performed using an unpaired two-sided t-test (* p<0.1, **

p<0.05, *** p<0.01, NS, not significant). Germination and branching experiments were performed in triplicates. Figure prepared with Biorender.com.

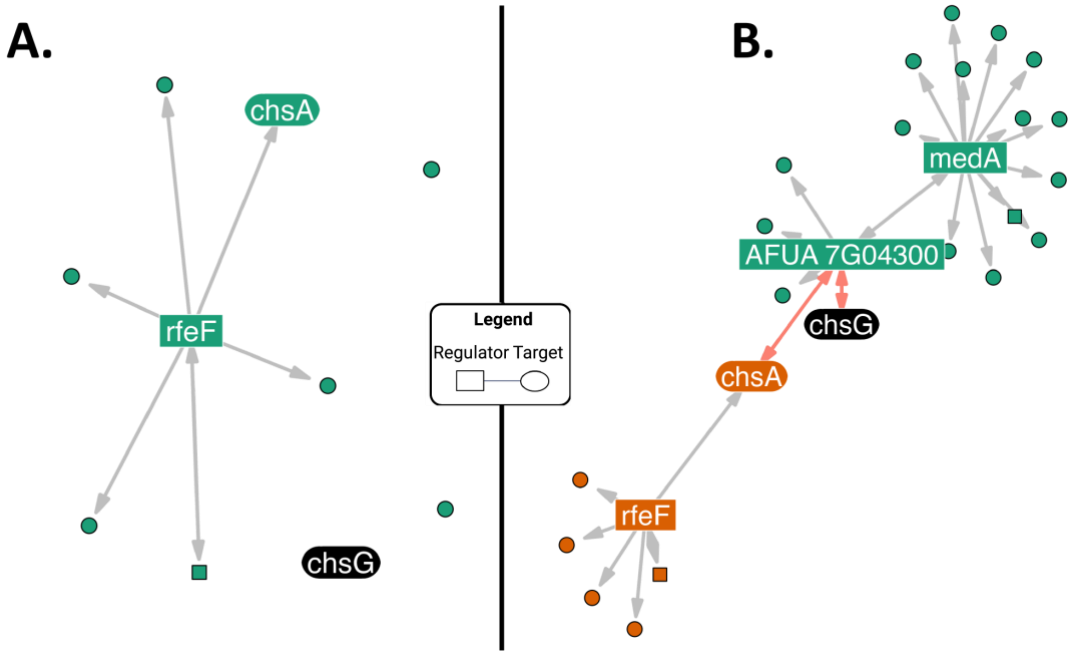

Figure 7. Predicted regulatory relationship of *chsA* and *chsG*. A) Network representation after searching for modules associated with *chsA* and *chsG*. B**)** An estimated Steiner tree generated to connect *chsA* and *chsB*. Red edges correspond to the Steiner tree, while the remaining edges represent the genes in the associated modules. Ovals represent gene targets, while rectangles represent regulators. Genes are colored by module identity, and black nodes represent genes not assigned to a module. The Steiner tree approximation shows a previously uncharacterized relationship between *chsA* and *chsG*. Figure prepared with Biorender.com.

The final feature of GRAsp we demonstrate in this work is an application of the Steiner tree approximation algorithm, which attempts to find connections between any set of genes regardless of whether they belong to the same module. As LCO biosynthesis is dependent on chitin availability and chitin is a critical component of the cell wall (92, 93), we set out to identify regulators targeting chitin synthase genes. In this example, we compare the networks that are generated by (i) modules that incorporate two genes encoding family one chitin synthases, *chsA,* and *chsG (94)* (**Figure 7A**), and (ii) the Steiner tree generated to connect these two nodes (**Figure 7B**). Figure prepared with Biorender.com.

Steiner tree predicts novel components of the chitin synthesis pathway

The Steiner tree network notably provides additional modules that capture biologically relevant information. No common regulator of *chsA* and *chsG* was identified when searching using the MERLIN module method. This can occur when genes are associated with independent modules without a common regulator. The Steiner tree method is useful for finding common regulators in these instances. After finding an approximate Steiner tree (red edges **Figure 7B**) between *chsA* and *chsG*, a common regulator AFUA_7G04300 was identified. AFUA_7G04300, an uncharacterized gene predicted to contain a RhoGAP and Fes/CIP4 domain, regulates not only *chsA* and *chsG* but is also predicted to regulate *gfa1*, a putative glutamine-fructose-6-phosphate transaminase. This was particularly interesting because this enzyme would theoretically catalyze the first reaction in the chitin synthesis process: the formation of glucosamine

6-phosphate (92). This predicted regulatory relationship was identified with the Steiner search algorithm.

AFUA_7G04300 was also implicated in broader cell wall activities, as it was predicted to regulate AFUA_5G13090, a putative alpha-1,2-mannosyltransferase and cell wall biosynthesis gene (95). AFUA_7G04300 is also connected to *rgd1,* a putative Rho-GTPase activating protein whose homolog in *Saccharomyces cerevisiae* has been implicated in cell wall integrity signaling (96). The modules containing the Steiner tree also connected *rfeF* to *chsA.* RfeF is a transcription factor regulated by CrzA, itself a transcription factor known to bind to promoters of both *chsA* and *chsG,* and thus is tied into chitin synthesis (97). The *chsC/chsG* Steiner tree presents a plausible connection between chitin regulatory pathways that can be further validated and explored.

DISCUSSION

In October 2022, the World Health Organization (WHO) published its first-ever report on priority fungal pathogens (98). *A. fumigatus* - along with *Cryptococcus neoformans, Candida albicans,* and *Candida auris* - was placed in the critical priority group (98). This placement was due to a substantial increase in severe aspergillosis cases, burgeoning mortality rates, co-infections with COVID-19 and other respiratory pathogens, and increasing antifungal resistance of this mold (98). Accordingly, and accompanying this recognition of *A. fumigatus* as a critical infectious agent, laboratories worldwide have focused on elucidating the genes and molecules that make *A. fumigatus* a successful pathogen (99, 100). Although a large number of RNA-seq experiments have been performed to understand the mode of virulence of *A. fumigatus* and, to ultimately

identify new targets for antifungal development (34, 35, 101, 102), these efforts alone have not fully revealed the regulatory networks and pathways required for the pathogenicity of this fungus. For example, although it has long been known that gliotoxin is a virulence determinant of invasive aspergillosis, a full understanding of the signaling networks promoting the synthesis of this toxin remains obscure. Our goal in this study was to leverage the wealth of existing RNA-seq datasets available for this fungus to construct a genome-scale GRN and make it easily accessible to the research community at large and, further, to integrate existing knowledge to predict regulators important in regulating fungal development and virulence factors.

By leveraging publicly available gene-expression data of multiple strains of *A. fumigatus*, MERLIN-P-TFA was able to reconstruct, to our knowledge, the first comprehensive gene regulatory network of the organism. We developed GRAsp, a user-friendly web portal, to query this inferred GRN with individual genes and gene sets to predict novel components of diverse biological pathways using one of three integrated features: Regulatory Modules, Steiner trees, or node diffusion. Here, we used regulatory modules to successfully recapitulate previously known pathways such as SrbA regulation of genes involved in ergosterol biosynthesis, nitrate assimilation, and heme biosynthesis during hypoxia; HapX regulation of genes involved in the synthesis and transport of siderophores; ZafA regulation of three zinc transporters *zrfA*, *zrfB*, and *zrfC* and FapR regulation of genes involved in the synthesis of the secondary metabolites, pseurotin and fumagillin.

The successful recovery of several known metabolic pathways using MERLIN-P-TFA and GRAsp led us to test the ability of GRAsp to identify unknown components regulating the modules. For our example, we choose to investigate gliotoxin regulation. Gliotoxin was isolated from several fungi in the 1940s, where it was quickly found to exhibit strong antifungal activity (103). Consideration of this metabolite for such use declined with the finding of its general eukaryotic toxicity. Identifying the *A. fumigatus* gliotoxin gene cluster allowed for molecular characterization and *gli* gene deletions, all leading to the conclusion that gliotoxin is an exacerbating factor in invasive aspergillosis (104, 105). Further, these studies showed how *A. fumigatus* protected itself from its toxin. It depended on several enzymes, including GliT and GtmA, that modified/prevented the toxic disulfide bridge in the gliotoxin molecule. Although the *gli* BGC regulator GliZ was characterized in 2006, it is unknown how *gliZ* is regulated (83). The input of *gliZ* into the GRAsp tool revealed a module predicted to be regulated by a gene coding for a putative transcription factor AFUA_3G11990, now named *rogA* (**Figure 5A**). This module contained all of the *gli* BGC genes and the trans-located *gtmA* gene involved in self-protection. Examination of *rogA* (AFUA_3G11990) mutants revealed that this putative transcription factor is a negative regulator of gliotoxin production (**Figure 5B**).

The accuracy of MERLIN-P-TFA and GRAsp predicted regulators was further supported by identifying *AfatfA* as a key regulator required for the developmental response of *A. fumigatus* to LCOs. These LCO signals are one of the two endogenous signals we identified to regulate lateral branching in *A. fumigatus (34, 35)*. Filamentous fungi such as *A. fumigatus* must balance hyphal extension with lateral branching for optimal colony

and invasive growth. Understanding the GRNs transmitting these signals has the potential for future therapies to control the growth of *A. fumigatus.* We used node diffusion to discover that *AfatfA* is required for *A. fumigatus* to respond to LCOs, thus uncovering a previously unknown mechanism of LCO signaling pathway (s) in fungi. Finally, we use Steiner trees to predict AFUA_7G04300 as a new regulator of two chitin synthases, *chsA* and *chsG*. While it needs to be validated experimentally, the prediction is further backed up by the other predicted targets of AFUA_7G04300, which are involved in cell wall integrity and possibly the synthesis of chitin precursors.

Our work shows the strength of our gene regulatory network as a powerful resource for generating new hypotheses. Still, at 80% confidence, the network only captures ~30% of all genes in the *A. fumigatus* genome, with 2,940 genes out of this fungus, a total of 9,859 genes into high confidence modules (**Figure 2**). One consequence is that some well-described pathways, like the BrlA-mediated conidiation pathway (106), are not represented in GRAsp. Furthermore, MERLIN-P-TFA and GRAsp did not always pick up every gene in the recovered pathways, which we postulate is due to the limitation of the number of RNA-seq datasets used in this study. However, as new expression datasets become publicly available, we can incorporate them into our framework to refine existing pathways and uncover new pathways. Beyond RNA-seq, other complementary omic data (e.g., ChiP-seq or ATAC-seq) can also be incorporated into the MERLIN-P-TFA framework, increasing our network's coverage and accuracy. Follow-up transcriptomic and epigenomic studies guided by the prioritized regulators using GRAsp could more efficiently improve the quality and coverage of our GRNs. To facilitate community access, GRAsp is available as a free online visualization tool that

can be used by individual researchers to examine this GRN and generate model-driven testable hypotheses. Such model-driven experiments provide a quantitative assessment of the network's quality and enable us to determine the most useful experiments for constructing a comprehensive GRN for *A. fumigatus*. Our inferred GRN and associated GRAsp tool will be useful for identifying the key genes and pathways underlying the pathogenic traits of *A. fumigatus*.

AVAILABILITY

Data preprocessing was performed utilizing Trimmomatic (v0.32), FastQC (v0.11.9), MultiQC, RSEM (v1.2.11), Bowtie2 (v2.2.0), and MATLAB (r2017b). Data preprocessing scripts and processed data can be found https://github.com/Roy-lab/merlin-preprocess.

Network inference was performed utilizing the MERLIN-P-TFA package (https://github.com/Roy-lab/MERLIN-P-TFA, Siahpirani *et al.* 2023 in preparation). MERLIN-P-TFA is dependent on the network component analysis package, EstimateNCA (https://github.com/Roy-lab/EstimateNCA), and the network inference algorithm, MERLIN-P (https://github.com/Roy-lab/merlin-p). After generating the network, analysis of the network structure was performed using the MERLIN-Auxiliary package (https://github.com/Roy-lab/merlin-auxillary).

The GRAsp RShiny app was constructed using the MERLIN-VIZ package (https://github.com/Roy-lab/MERLIN-VIZ). The GRAsp branch contains net_data.Rdata, which stores all network data. This paper also provides a wrapper function to make all

network figures. The GRAsp RShiny app is hosted at https://grasp.wid.wisc.edu/ and is a publicly available resource for hypothesis generation. GRAsp was constructed using the tidyverse package suite (v2.0.0), tidygraph (v1.2.3), pracma (v2.4.2) and igraph (v1.4.1). Network visualization in GRAsp utilizes networkD3 (v0.4), ggraph (v2.1.0), and RColorBrewer (v1.1-3). Tables in GRAsp utilize the DT package (v0.27).

ACCESSION NUMBERS

The RNA-seq dataset generated in-house for this study has been deposited with GEO under accession number GSE231238. It can be accessed with the reviewer's token wxoziaowndsbdwr. The remaining accession numbers for the publically available RNA-seq datasets utilized in this study are contained in supplementary **Table S1**.

FUNDING

Funding for open access charge: National Institutes of Health (NIH). This work was supported by the United States Department of Agriculture Hatch grant [WIS03041] to J.M.A. and N.P.K, and in part by NIH 5 R01 [AI 150669 – 02, GM 112739 – 06] and Department of Energy grant [DE-SC0021052] to N.P.K. This work is also supported in part by the National Science Foundation grant [2010789] and NIH 1 R01 [GM 144708] (S.H. and S.R.). The NIH training grant [5T32GM007133-46] supported C.C.C., also supported by the Advanced Opportunity Fellowship through SciMed Graduate Research Scholars at the University of Wisconsin–Madison. Support for this fellowship is provided by the Graduate School, part of the Office of the Vice Chancellor for Research and

Graduate Education at the University of Wisconsin–Madison, with funding from the Wisconsin Alumni Research Foundation.

CONFLICT OF INTEREST

Author N.P.K. declares potential conflicts of interest as co-founder of company Terra Bioforge and Scientific Advisory Board member for Clue Genetics, Inc.

Supplementary Text

A network-based model of *Aspergillus fumigatus* elucidates regulators of development and defensive natural products of an opportunistic pathogen

Cristobal Carrera Carriel, Saptarshi Pyne, Spencer A. Halberg-Spencer, Sung Chul Park, Hye-won Seo, Aidan Schmidt, Dante G. Calise, Jean-Michel Ané, Nancy P. Keller, Sushmita Roy

Table of Contents

Supplementary Tables

Supplementary Table S1. RNAseq datasets used to create GRAsp. Dataset ID refers to Bioproject Accession. Sample No. refers to the number of samples from the dataset used to create GRAsp. S.I No., Serial Number.

Sl. No.	Dataset ID	Year	WIldtype Strain	Description	Sample No.	Reference
1	PRJEB3185	2012	CEA17	WT and Δ*mpkA*	6	(21)
2	PRJEB2987	2014	Af293	WT and Δ*gliT*	15	(22)
3	PRJNA390719	2017	Af293	WT, Δ*rax1*, Δ*rgsD*	6	(23, 24)
4	PRJNA508764	2018	Af293	WT, Δ*atrR, atrR*-3X HA ,hspA-*atrR*	8	(25)
5	PRJNA554811	2019	ATCC 46645	WT and cytomegalovirus coinfection of human dendritic cells	16	(26)
6	PRJNA558954	2019	ATCC 46645	WT exposure to human dendritic cells (2,4,6 h). MOI of 1,0,5	9	(26)
7	PRJNA144647	2011	CEA10	Treatment of hypoxia or normoxia (12,24,36 h)	4	(27)
8	PRJNA240324	2014	CEA17	WT and Δ*akuB* exposure to humidimycin	12	(28)
9	PRJNA240892	2014	A1163	Caspofungin exposure of WT and Δ*akuB* (0,0.5,1,4,8 h); Δ*mpkA* and Δ*sakA* (0,1,4 h)	53	(15)
10	PRJNA241401	2014	CEA10	WT exposure to hypoxic or normoxic conditions (0,15,30 min)	12	(29)
11	PRJNA376829	2017	Af293	WT grown on sugarcane bagasse or fructose	6	(30)
12	PRJNA399754	2017	CEA10/Af293	WT infection of A549 type II pneumocyte cell line (6,16 h)	24	(31)

13	PRJNA408076	2017	AFIR964/AFIR974	WT germination (0,2,4,6,8 h)	20	(7)
14	PRJNA482512	2018	Af155-40 Af130–14 Af147–03	WT exposure to itraconazole (30,60,120,240 min)	30	(32)
15	PRJNA622251	2020	CEA17	WT and Δ*fhdA* exposure to caspofungin (48 h)	24	(33)
16	PRJNA642658	2020	Af293	WT exposure to LCO-IV (30 min and 2 h)	16	(34)
17	PRJNA658306	2020	Af293	WT and Δ*ppoA* exposure to 5,8-diHODE (30 min and 2 h)	16	(35)
18	GSE231238	2023	Af293	WT, OE::*zfpA*, and Δ*zfpA* at 0 hours and after 16 hours of shaking incubation	24	This study

Supplementary Table S2. Fungal strains used in this study

Name	Genotype	Reference
CEA17 KU80	pyrG1, ΔakuB::pyrG, pyrG1	(59)
TAJS1.7	pyrG1, ΔakuB::pyrG, pyrG1, ΔAFUB_037850::pyrG	(60)
TAJS2.2	pyrG1, ΔakuB::pyrG, pyrG1, ΔAFUB_064280::pyrG, gpdA(p)::AFUB_037850::argB	(60)
TFYL80.1	*A.fumigatus fumiargB; ΔnkuA::mluc; pyrG1; argB1*	(61)
TSCP2.1	*A.fumigatus fumiargB; ΔnkuA::mluc; pyrG1; argB1; ΔrogA::para_pyrG*	This study
THWS25.1	*A.fumigatus fumiargB; ΔnkuA::mluc;pyrG1;argB1;argB1;para_pyrG::gpdA(P)::rogA*	This study
TFYL81.5	*A. fumigatus pyrG1; argB1; ΔakuA::mluc; fumiargB; fumipyrG*	(Throckmorton et al. 2016)
TJW213.1	*A. fumigatus pyrG1; argB1; ΔakuA::mluc; fumiargB; ΔzfpA::parapyrG*	(Schoen et al. 2023)
TJW214.2	*A. fumigatus pyrG1; argB1; ΔakuA::mluc; fumiargB; parapyrG::gpdA(p)::zfpA*	(Schoen et al. 2023)

Supplementary Table S3. PCR primers for this study

Name	Sequence (5'-3')	Use
A. para pyrG For.	GTCGACGGTATCGATAAGCTTG	*ΔrogA*
A. para pyrG Rev	ATTCGACAATCGGAGAGGCTGC	*ΔrogA*
del_AFUA3G11990_3'F	CTGTCGCTGCAGCCTCTCCGATTGTCGAAT GTACGTTCCCAGTACAACTACTGAGCC	*ΔrogA*
del_AFUA3G11990_3'R	CATCCACTGAATCCAGTCGTCG	*ΔrogA*
del_AFUA3G11990_5'F	AGCAGCCGTTTGAGAGTCATGC	*ΔrogA*
del_AFUA3G11990_5'R	CGATATCAAGCTTATCGATACCGTCGACCGTT GGCGCAAAGGCTCATGCAAGG	*ΔrogA*
OE_AFUA_3G11990_5F	CGAGGCTTAGGCTTCTTCGAAC	OE::*rogA*
OE_AFUA3G11990_5R	CCTCTCGGGCCATCTGTTCGTATAAGCTTCTCGACG ATGACGTTGGCGCAAAGGC	OE::*rogA*
OE_AFUA_3G11990_3F	CTACCCCGCTTGAGCAGACATCACCATATGGCCGCC AATTCCAGTCCGTTC	OE::*rogA*
OE_AFUA_3G11990_3R	CCGGAGGGGTATCATAGATTCG	OE::*rogA*
PyrG+gpdA(P) F	CGTAATACGACTCACTATAGGGC	OE::*rogA*
PyrG+gpdA(P) R	GGTGATGTCTGCTCAAGCGGG	OE::*rogA*

Supplementary Figures

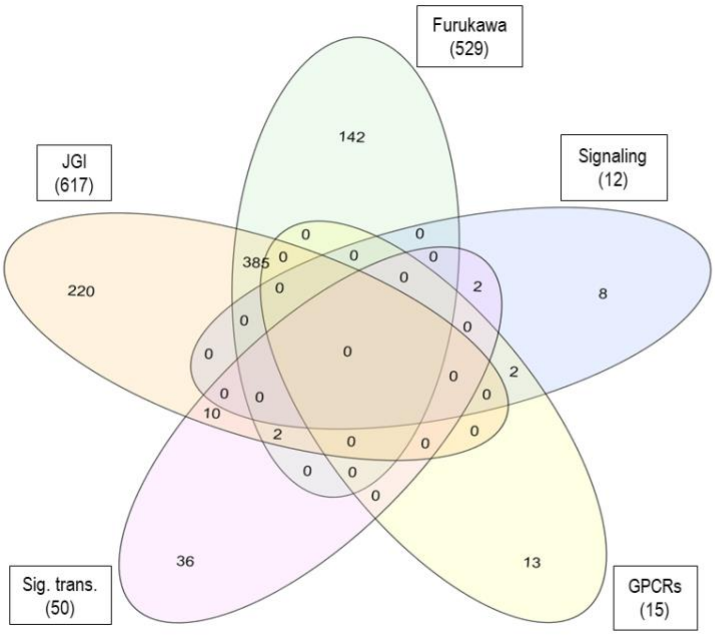

Source	No. of genes
JGI MyCoCosm	617
Furukawa et al.	529
Signaling genes	12
G-protein coupled receptors (GPCRs)	15
Signal transduction genes	50
All combined	*820*

Supplementary Figure S1. The number of regulator genes curated from five different sources. The Venn diagram presents the number of unique regulators contributed by each source. For example, we curated 617 regulators from the JGI MyCoCosm database (Grigoriev et al. 2014). However, only 220 of them are unique to this database i.e., they were not present in the sublists of regulators collected from other sources. Combining all the sources resulted in a list of 820 distinct regulators. Full list of regulators can be found in **Supplementary File S1_regulators.xlsx**.

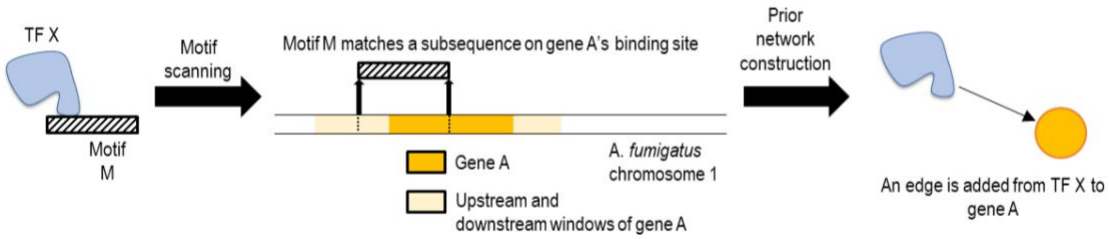

Supplementary Figure S2. The rationale behind the construction of the prior network based on sequence motifs. If transcription factor (TF) X can bind to DNA-sequence motif M, we scanned the A. *fumigatus* reference genome to find matches for motif M using the pwmmatch.exact.r of PIQ package from Sherwood et al. 2014. We defined the binding region of a gene to be 10 Kbp upstream of the gene through 1 Kbp downstream of the gene. If a match was found on the binding region (such as the promoter) of Gene A in chromosome 1, we added an edge from TF X to Gene A in the prior network.

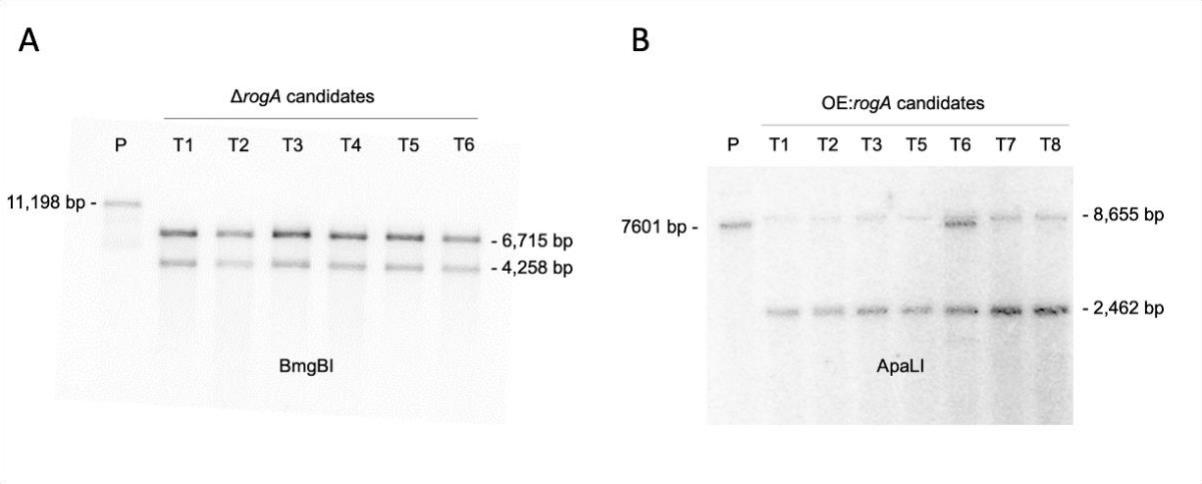

Supplementary Figure S3. Confirmation of *rogA* mutants. A) Southern confirmation of Δ*rogA* mutants. Genomic DNA was digested by BmgBI (Parent: P, 11198 bp; Transformants: T, 4258 and 6715 bp). B) Southern blot confirmation of OE::*rogA* mutants. Genomic DNA was digested by ApaLI (Parent: P, 7601 bp; Transformants: T, 2462 and 8655 bp).

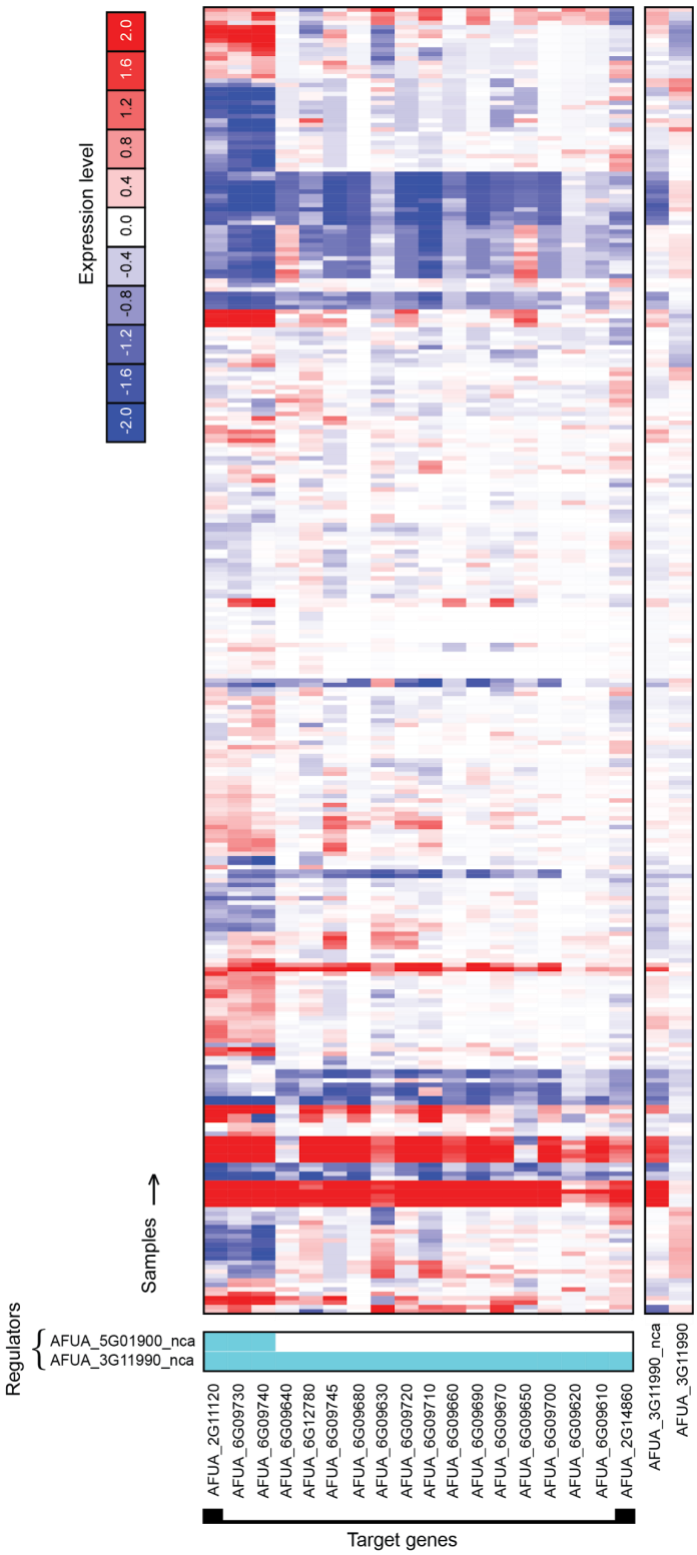

Supplementary Figure S4. A heatmap of the zero means quantile-normalized data of genes in module 5349. Systematic names for genes are on rows, and samples are on columns. The profiles of regulators are depicted below in the genes in the modules, in the last two rows. Regulator-target interactions are also labeled in the first two columns with light blue squares. AFUA_3G11990 is anti-correlated with many of the genes in the module, suggesting that it is a repressor of gliotoxin biosynthesis. The transcription factor activity of AFUA_3G11990, AFUA_3G11990_nca, is also depicted. The TFA profile is correlated with the gliotoxin genes within the module.

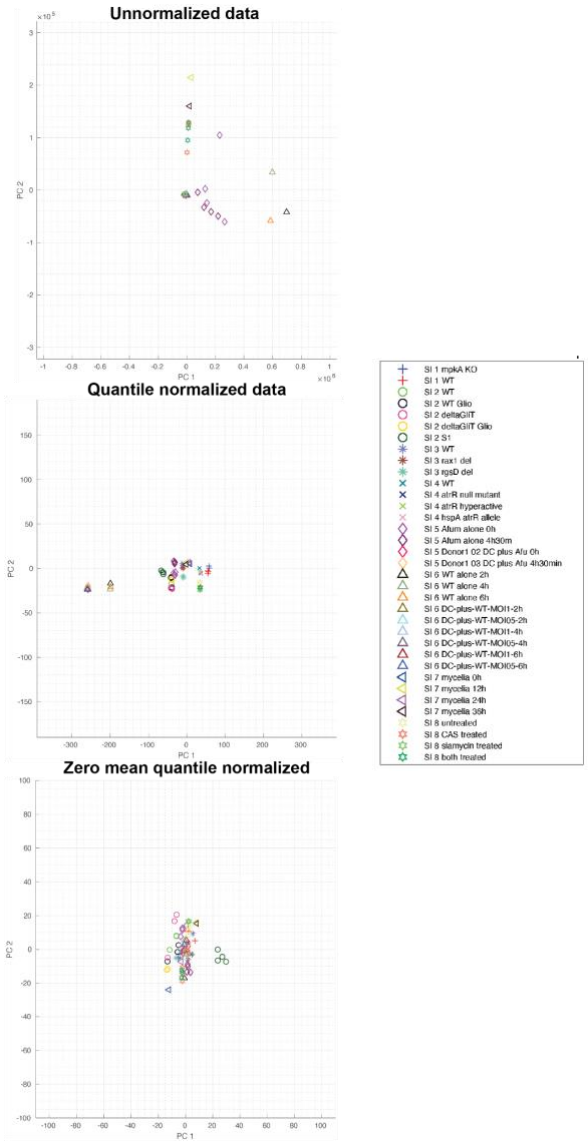

Supplementary figure S5. Principal components of samples SI 1-SI 8. Principal component scores of all samples were calculated simultaneously. Displayed are the PCA scores of samples from SI 1-SI 8. PCA of unnormalized and quantile normalized data demonstrates batch effects, that is, samples are clustered together by batch (shape) regardless of the experimental condition (color). After zero mean normalization, the batch effect is largely removed. Samples are clustered by similar experimental conditions, regardless of batch.

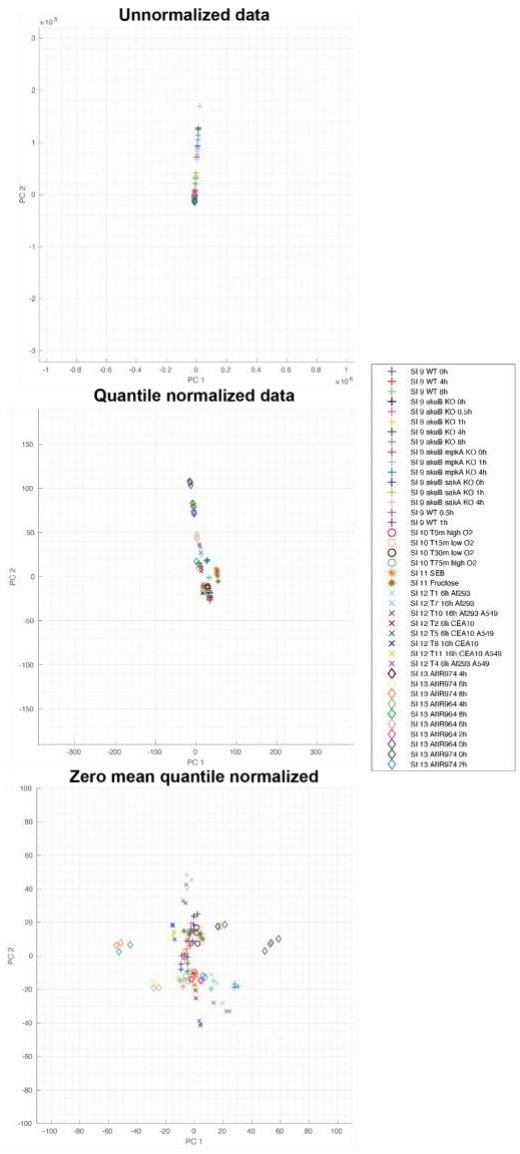

Supplementary figure S6. Principal components of samples SI 9-SI 13. Principal component scores of all samples were calculated simultaneously. Displayed are the PCA scores of samples from SI 9-SI 13. PCA of unnormalized and quantile normalized data demonstrates batch effects. Samples are clustered by batch (shape) regardless of the experimental condition (color). After zero mean normalization, the batch effect is largely removed. Samples are clustered by similar experimental conditions, regardless of batch.

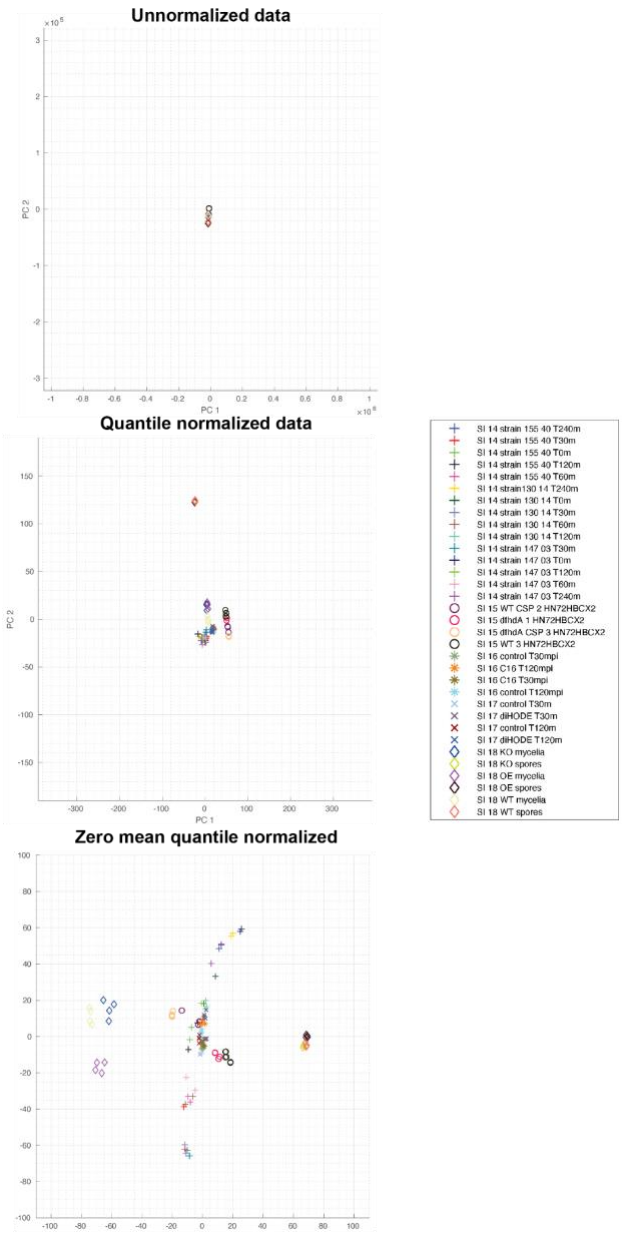

Supplementary figure S7. Principal components of samples SI 14-SI 18. Principal component scores of all samples were calculated simultaneously. Displayed are the PCA scores of samples from SI 14-SI 18. PCA of unnormalized and quantile normalized data demonstrates batch effects. Samples are clustered by batch (shape) regardless of the experimental condition (color). After zero mean normalization, the batch effect is largely removed. Samples are clustered by similar experimental conditions, regardless of batch.

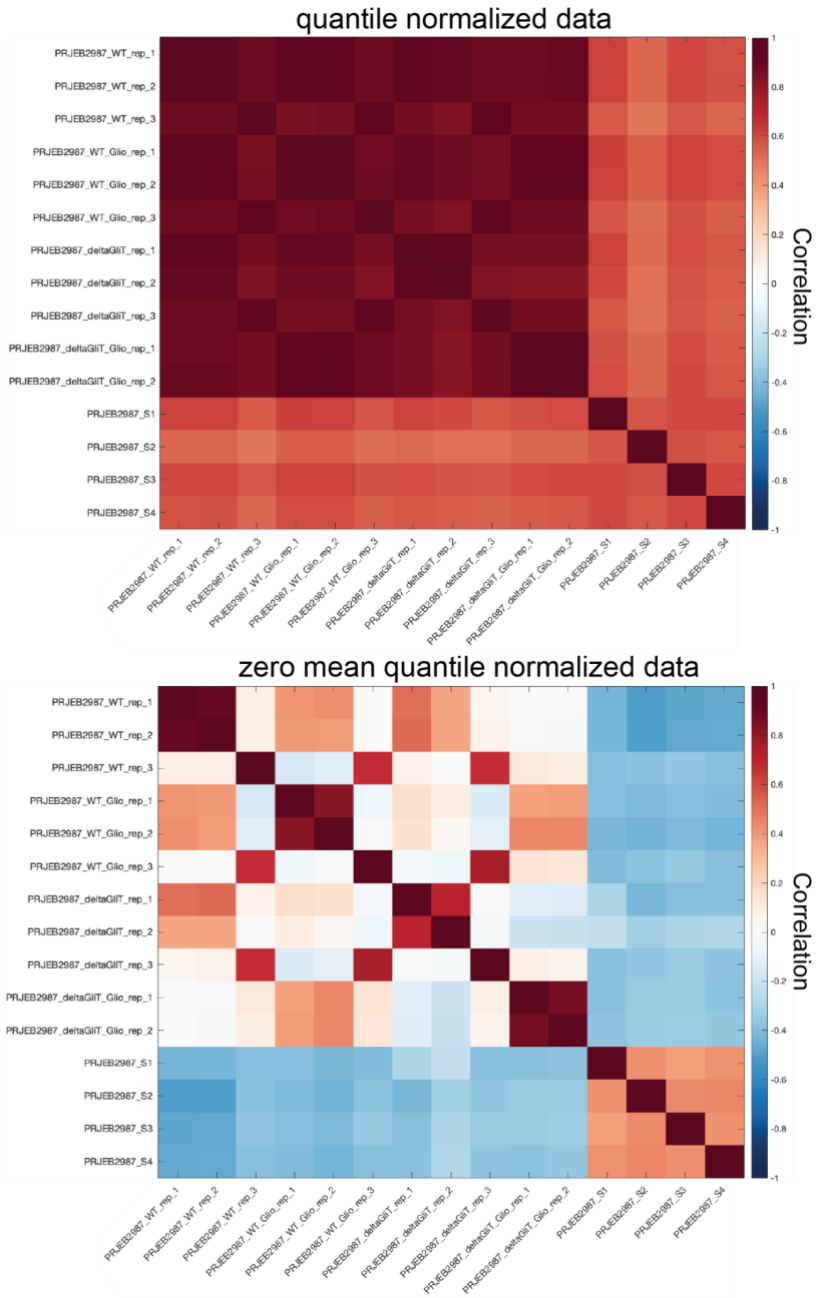

Supplementary Figure S8: Reference SI 2 (PRJEB2987) sample correlation: Samples of SI 2 are all strongly correlated before batch correction by zero-mean normalization. After zero-mean correction, replicates 1 and 2 of each condition are strongly correlated, e.g., WT rep1 and 2. Rep 3 samples are strongly correlated regardless of condition and were removed before network inference.

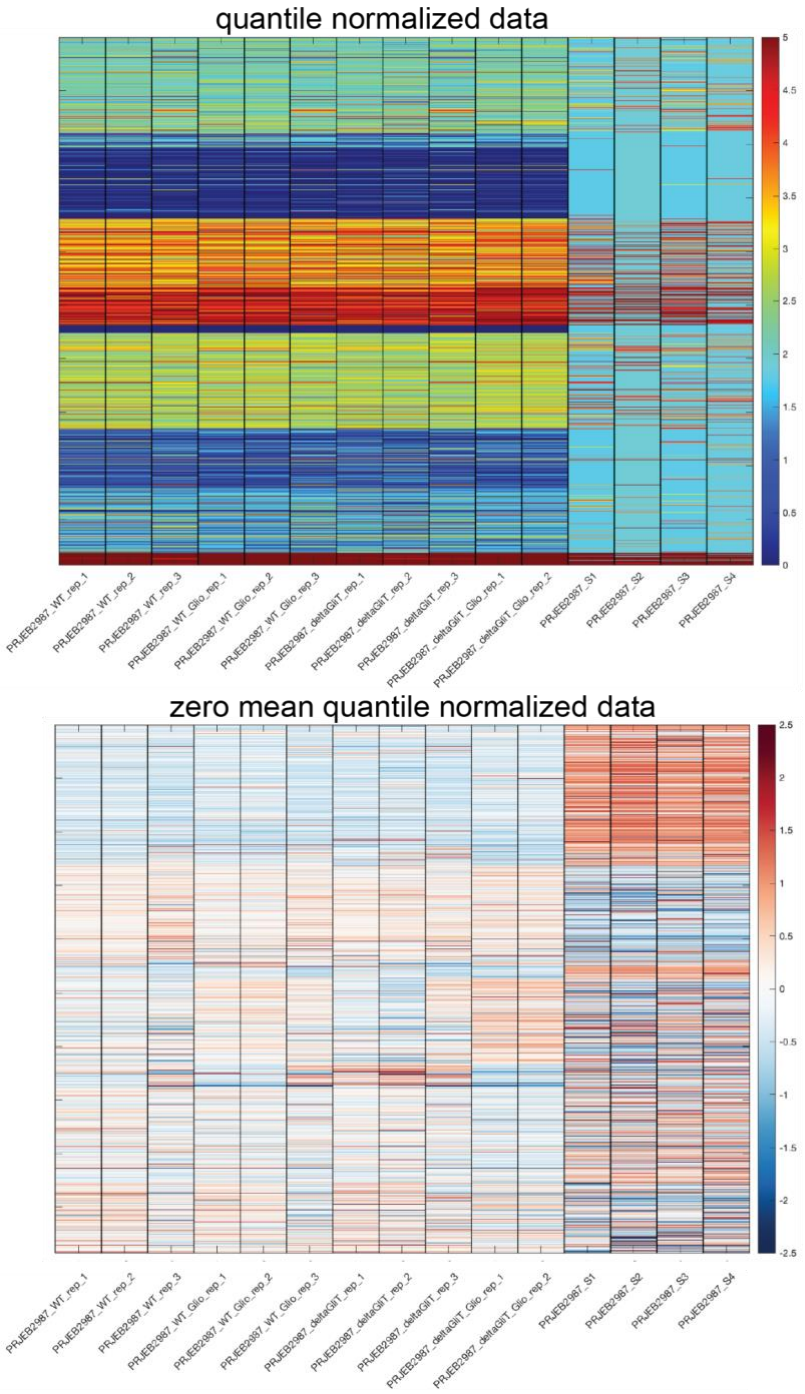

Supplementary Figure S9: Reference SI 2 (PRJEB2987) expression heatmaps: Expression of genes per sample before and after zero-mean normalization. Expression of SI 2 genes in quantile normalized data is increased relative to other samples (~1.75). These samples were removed before network inference because of this inconsistency.

Supplementary Methods

Supplementary Method S1. Descriptions of the previously characterized TF binding site sequence motifs

This section describes the previously characterized TF binding site sequence motifs used in this study. There are a total of four such motifs corresponding to two TFs – somA and xanC – as described below.

TF name: somA

Protein: Transcriptional activator somA

(ORF) GENEID: AFUA_7G02260 (source: https://www.uniprot.org/uniprot/Q4WAR8)

The following motif preferences were recently characterized by Chen et al. [DOI: https://doi.org/10.1128/mBio.02329-20].

Motif 1: GTACTCCGTAC

Motif 2: RTGGBMTGATS

Motif 3: CCTMCAGAGCAG

Note 1: IUPAC symbols for bases are used

(Reference for the IUPAC symbols: https://www.bioinformatics.org/sms/iupac.html).

R = A/G

B = C/G/T

M = A/C

S = C/G

Note: We assumed that the probability of having a base other than the base(s) given for a particular base position is low.

TF name: xanC

Protein: Xanthocillin biosynthesis cluster transcription factor xanC

(ORF) GENEID: AFUA_5G02655 (source: https://www.uniprot.org/uniprot/A4DA05)

The following motif preference was recently characterized by Wang et al. [DOI: https://doi.org/10.1128/mBio.01399-21]

The motif is 5'-(A)GTCAGC(A)-3' (motif 4)

The parenthesized "(A)" implies that we are not certain whether the binding motif contains A's. All of the xan promoters had 5'-AGTCAGCA-3', but variations could exist. Hence, we decided to exclude the parenthesized parts and use 5'-GTCAGC-3' as the motif.

XanC is the bZip transcription factor of the xanthocillin biosynthetic gene cluster. We conjectured that XanC might be a regulator of the copper homeostasis genes. That motivated us to include XanC's binding motifs in this study.

Converting sequence motifs into position weight matrices (PWMs)

We produced a position weight matrix (PWM) for each of the four motifs by using 0.9 to indicate a high probability. Let us illustrate with an example. Suppose a particular base position in a given motif has a high probability for G and very low probability for the remaining letters. Then, G will be assigned a probability value of 0.9, and 0.1 will be equally distributed between the remaining letters. Similarly, if more than one letter has a high probability for a particular position, then 0.9 will be equally distributed among them. Again, 0.1 will be equally distributed between the remaining letters. Thus, we produced the PWMs of the previously characterized motifs; the PWMs are presented below.

The position weight matrix of motif 1 (GTACTCCGTAC):

Position	A	C	G	T
1	0.1	0.1	0.9	0.1
2	0.1	0.1	0.1	0.9
3	0.9	0.1	0.1	0.1
4	0.1	0.9	0.1	0.1
5	0.1	0.1	0.1	0.9
6	0.1	0.9	0.1	0.1
7	0.1	0.9	0.1	0.1
8	0.1	0.1	0.9	0.1
9	0.1	0.1	0.1	0.9
10	0.9	0.1	0.1	0.1
11	0.1	0.9	0.1	0.1

The position weight matrix of motif 2 (RTGGBMTGATS):
R = A/G; B = C/G/T; M = A/C; S = C/G.

Position	A	C	G	T
1	0.45	0.05	0.45	0.05
2	0.1	0.1	0.1	0.9
3	0.1	0.1	0.9	0.1
4	0.1	0.1	0.9	0.1
5	0.1	0.3	0.3	0.3
6	0.45	0.45	0.05	0.05
7	0.1	0.1	0.1	0.9
8	0.1	0.1	0.9	0.1
9	0.9	0.1	0.1	0.1
10	0.1	0.1	0.1	0.9
11	0.05	0.45	0.45	0.05

The position weight matrix of motif 3 (CCTMCAGAGCAG):
R = A/G; B = C/G/T; M = A/C; S = C/G.

Position	A	C	G	T
1	0.1	0.9	0.1	0.1
2	0.1	0.9	0.1	0.1
3	0.1	0.1	0.1	0.9
4	0.45	0.45	0.05	0.05
5	0.1	0.9	0.1	0.1
6	0.9	0.1	0.1	0.1

7	0.1	0.1	0.9	0.1
8	0.9	0.1	0.1	0.1
9	0.1	0.1	0.9	0.1
10	0.1	0.9	0.1	0.1
11	0.9	0.1	0.1	0.1
12	0.1	0.1	0.9	0.1

The position weight matrix of motif 4 (GTCAGC):

Position	**A**	**C**	**G**	**T**
1	0.1	0.1	0.9	0.1
2	0.1	0.1	0.1	0.9
3	0.1	0.9	0.1	0.1
4	0.9	0.1	0.1	0.1
5	0.1	0.1	0.9	0.1
6	0.1	0.9	0.1	0.1

REFERENCES

1. Levdansky,E., Romano,J., Shadkchan,Y., Sharon,H., Verstrepen,K.J., Fink,G.R. and Osherov,N. (2007) Coding tandem repeats generate diversity in Aspergillus fumigatus genes. *Eukaryot. Cell*, **6**, 1380–1391.

2. Latgé,J.P. (2001) The pathobiology of Aspergillus fumigatus. *Trends Microbiol.*, **9**, 382–389.

3. Tekaia,F. and Latgé,J.-P. (2005) Aspergillus fumigatus: saprophyte or pathogen? *Curr. Opin. Microbiol.*, **8**, 385–392.

4. Balloy,V. and Chignard,M. (2009) The innate immune response to Aspergillus fumigatus. *Microbes Infect.*, **11**, 919–927.

5. del Palacio,A., Cuétara,M.S. and Pontón,J. (2003) Invasive aspergillosis. *Rev. Iberoam. Micol.*, **20**, 77–78.

6. Desoubeaux,G. and Cray,C. (2017) Rodent Models of Invasive Aspergillosis due to Aspergillus fumigatus: Still a Long Path toward Standardization. *Front. Microbiol.*, **8**, 841.

7. Baltussen,T.J.H., Coolen,J.P.M., Zoll,J., Verweij,P.E. and Melchers,W.J.G. (2018) Gene co-expression analysis identifies gene clusters associated with isotropic and polarized growth in Aspergillus fumigatus conidia. *Fungal Genet. Biol.*, **116**, 62–72.

8. Lai,C.-C. and Yu,W.-L. (2021) COVID-19 associated with pulmonary aspergillosis: A literature review. *J. Microbiol. Immunol. Infect.*, **54**, 46–53.

9. Guthke,R., Kniemeyer,O., Albrecht,D., Brakhage,A.A. and Möller,U. (2007) Discovery of Gene Regulatory Networks in Aspergillus fumigatus. In *Knowledge Discovery and Emergent Complexity in Bioinformatics*. Springer Berlin Heidelberg, pp. 22–41.

10. Guthke,R., Gerber,S., Conrad,T., Vlaic,S., Durmuş,S., Çakır,T., Sevilgen,F.E., Shelest,E. and Linde,J. (2016) Data-based Reconstruction of Gene Regulatory Networks of Fungal Pathogens. *Front. Microbiol.*, **7**, 570.

11. Acerbi,E., Hortova-Kohoutkova,M., Choera,T., Keller,N., Fric,J., Stella,F., Romani,L. and Zelante,T. (2020) Modeling Approaches Reveal New Regulatory Networks in Aspergillus fumigatus Metabolism. *J Fungi (Basel)*, **6**.

12. Brandon,M.G. (2013) A mathematical model of the iron regulatory network in aspergilus fumigatus.

13. Conrad,T., Kniemeyer,O., Henkel,S.G., Krüger,T., Mattern,D.J., Valiante,V., Guthke,R., Jacobsen,I.D., Brakhage,A.A., Vlaic,S., *et al.* (2018) Module-detection approaches for the integration of multilevel omics data highlight the comprehensive response of Aspergillus fumigatus to caspofungin. *BMC Syst. Biol.*, **12**, 88.

14. Do,J.H., Yamaguchi,R. and Miyano,S. (2009) Exploring temporal transcription regulation structure of Aspergillus fumigatus in heat shock by state space model. *BMC Genomics*, **10**, 306.

15. Altwasser,R., Baldin,C., Weber,J., Guthke,R., Kniemeyer,O., Brakhage,A.A., Linde,J. and Valiante,V. (2015) Network Modeling Reveals Cross Talk of MAP Kinases during Adaptation to Caspofungin Stress in Aspergillus fumigatus. *PLoS One*, **10**, e0136932.

16. Linde,J., Hortschansky,P., Fazius,E., Brakhage,A.A., Guthke,R. and Haas,H. (2012) Regulatory interactions for iron homeostasis in Aspergillus fumigatus inferred by a Systems Biology approach. *BMC Syst. Biol.*, **6**, 6.

17. Barber,A.E., Sae-Ong,T., Kang,K., Seelbinder,B., Li,J., Walther,G., Panagiotou,G. and Kurzai,O. (2021) Aspergillus fumigatus pan-genome analysis identifies genetic variants associated with human infection. *Nat Microbiol*, **6**, 1526–1536.

18. Roy,S., Lagree,S., Hou,Z., Thomson,J.A., Stewart,R. and Gasch,A.P. (2013) Integrated module and gene-specific regulatory inference implicates upstream signaling networks. *PLoS Comput. Biol.*, **9**, e1003252.

19. Schäpe,P., Kwon,M.J., Baumann,B., Gutschmann,B., Jung,S., Lenz,S., Nitsche,B., Paege,N., Schütze,T., Cairns,T.C., *et al.* (2019) Updating genome annotation for the microbial cell factory Aspergillus niger using gene co-expression networks. *Nucleic Acids Res.*, **47**, 559–569.

20. Koller,D. and Friedman,N. (2009) Probabilistic Graphical Models: Principles and Techniques MIT Press.

21. Müller,S., Baldin,C., Groth,M., Guthke,R., Kniemeyer,O., Brakhage,A.A. and Valiante,V. (2012) Comparison of transcriptome technologies in the pathogenic fungus Aspergillus fumigatus reveals novel insights into the genome and MpkA dependent gene expression. *BMC Genomics*, **13**, 519.

22. O'Keeffe,G., Hammel,S., Owens,R.A., Keane,T.M., Fitzpatrick,D.A., Jones,G.W. and Doyle,S. (2014) RNA-seq reveals the pan-transcriptomic impact of attenuating the gliotoxin self-protection mechanism in Aspergillus fumigatus. *BMC Genomics*, **15**, 894.

23. Choi,Y.-H., Lee,M.-W., Igbalajobi,O.A., Yu,J.-H. and Shin,K.-S. (2019) Transcriptomic and Functional Studies of the RGS Protein Rax1 in Aspergillus fumigatus. *Pathogens*, **9**.

24. Kim,Y., Lee,M.-W., Jun,S.-C., Choi,Y.-H., Yu,J.-H. and Shin,K.-S. (2019) RgsD negatively controls development, toxigenesis, stress response, and virulence in Aspergillus fumigatus. *Sci. Rep.*, **9**, 811.

25. Paul,S., Stamnes,M., Thomas,G.H., Liu,H., Hagiwara,D., Gomi,K., Filler,S.G. and Moye-Rowley,W.S. (2019) AtrR Is an Essential Determinant of Azole Resistance in Aspergillus fumigatus. *MBio*, **10**.

26. Seelbinder,B., Wallstabe,J., Marischen,L., Weiss,E., Wurster,S., Page,L., Löffler,C., Bussemer,L., Schmitt,A.-L., Wolf,T., *et al.* (2020) Triple RNA-Seq Reveals Synergy in a Human Virus-Fungus Co-infection Model. *Cell Rep.*, **33**, 108389.

27. Losada,L., Barker,B.M., Pakala,S., Pakala,S., Joardar,V., Zafar,N., Mounaud,S., Fedorova,N., Nierman,W.C. and Cramer,R.A. (2014) Large-scale transcriptional response to hypoxia in Aspergillus fumigatus observed using RNAseq identifies a novel hypoxia regulated ncRNA. *Mycopathologia*, **178**, 331–339.

28. Valiante,V., Monteiro,M.C., Martín,J., Altwasser,R., El Aouad,N., González,I., Kniemeyer,O., Mellado,E., Palomo,S., de Pedro,N., *et al.* (2015) Hitting the caspofungin salvage pathway of human-pathogenic fungi with the novel lasso peptide humidimycin (MDN-0010). *Antimicrob. Agents Chemother.*, **59**, 5145–5153.

29. Hillmann,F., Linde,J., Beckmann,N., Cyrulies,M., Strassburger,M., Heinekamp,T., Haas,H., Guthke,R., Kniemeyer,O. and Brakhage,A.A. (2014) The novel globin protein fungoglobin is involved in low oxygen adaptation of Aspergillus fumigatus. *Mol. Microbiol.*, **93**, 539–553.

30. de Gouvêa,P.F., Bernardi,A.V., Gerolamo,L.E., de Souza Santos,E., Riaño-Pachón,D.M., Uyemura,S.A. and Dinamarco,T.M. (2018) Transcriptome and secretome analysis of Aspergillus fumigatus in the presence of sugarcane bagasse. *BMC Genomics*, **19**, 232.

31. Watkins,T.N., Liu,H., Chung,M., Hazen,T.H., Dunning Hotopp,J.C., Filler,S.G. and Bruno,V.M. (2018) Comparative transcriptomics of Aspergillus fumigatus strains upon exposure to human airway epithelial cells. *Microb Genom*, **4**.

32. Hokken,M.W.J., Zoll,J., Coolen,J.P.M., Zwaan,B.J., Verweij,P.E. and Melchers,W.J.G. (2019) Phenotypic plasticity and the evolution of azole resistance in Aspergillus fumigatus; an expression profile of clinical isolates upon exposure to itraconazole. *BMC Genomics*, **20**, 28.

33. Valero,C., Colabardini,A.C., Chiaratto,J., Pardeshi,L., de Castro,P.A., Ferreira Filho,J.A., Silva,L.P., Rocha,M.C., Malavazi,I., Costa,J.H., *et al.* (2020) Aspergillus fumigatus Transcription Factors Involved in the Caspofungin Paradoxical Effect. *MBio*, **11**.

34. Rush,T.A., Puech-Pagès,V., Bascaules,A., Jargeat,P., Maillet,F., Haouy,A., Maës,A.Q., Carriel,C.C., Khokhani,D., Keller-Pearson,M., *et al.* (2020) Lipo-chitooligosaccharides as regulatory signals of fungal growth and development. *Nat. Commun.*, **11**, 3897.

35. Niu,M., Steffan,B.N., Fischer,G.J., Venkatesh,N., Raffa,N.L., Wettstein,M.A., Bok,J.W., Greco,C., Zhao,C., Berthier,E., *et al.* (2020) Fungal oxylipins direct programmed developmental switches in filamentous fungi. *Nat. Commun.*, **11**, 5158.

36. Bolger,A.M., Lohse,M. and Usadel,B. (2014) Trimmomatic: a flexible trimmer for Illumina sequence data. *Bioinformatics*, **30**, 2114–2120.

37. Li,B. and Dewey,C.N. (2011) RSEM: accurate transcript quantification from RNA-Seq data with or without a reference genome. *BMC Bioinformatics*, **12**, 1–16.

38. Siahpirani,A.F. and Roy,S. (2017) A prior-based integrative framework for functional transcriptional regulatory network inference. *Nucleic Acids Res.*, **45**, 2221.

39. Lafon,A., Han,K.-H., Seo,J.-A., Yu,J.-H. and d'Enfert,C. (2006) G-protein and cAMP-mediated signaling in aspergilli: a genomic perspective. *Fungal Genet. Biol.*, **43**, 490–502.

40. Furukawa,T., van Rhijn,N., Fraczek,M., Gsaller,F., Davies,E., Carr,P., Gago,S., Fortune-Grant,R., Rahman,S., Gilsenan,J.M., *et al.* (2020) The negative cofactor 2 complex is a key regulator of drug resistance in Aspergillus fumigatus. *Nature Communications*, **11**.

41. Grigoriev,I.V., Nikitin,R., Haridas,S., Kuo,A., Ohm,R., Otillar,R., Riley,R., Salamov,A., Zhao,X., Korzeniewski,F., *et al.* (2014) MycoCosm portal: gearing up for 1000 fungal genomes. *Nucleic Acids Res.*, **42**, D699–704.

42. Arnaud,M.B., Chibucos,M.C., Costanzo,M.C., Crabtree,J., Inglis,D.O., Lotia,A., Orvis,J., Shah,P., Skrzypek,M.S., Binkley,G., *et al.* (2010) The Aspergillus Genome Database, a curated comparative genomics resource for gene, protein and sequence information for the Aspergillus research community. *Nucleic Acids Res.*, **38**, D420–7.

43. Emms,D.M. and Kelly,S. (2015) OrthoFinder: solving fundamental biases in whole genome comparisons dramatically improves orthogroup inference accuracy. *Genome Biol.*, **16**, 157.

44. Emms,D.M. and Kelly,S. (2019) OrthoFinder: phylogenetic orthology inference for comparative genomics. *Genome Biology*, **20**.

45. Weirauch,M.T., Yang,A., Albu,M., Cote,A.G., Montenegro-Montero,A., Drewe,P., Najafabadi,H.S., Lambert,S.A., Mann,I., Cook,K., *et al.* (2014) Determination and inference of eukaryotic transcription factor sequence specificity. *Cell*, **158**, 1431–1443.

46. Chen,Y., Le Mauff,F., Wang,Y., Lu,R., Sheppard,D.C., Lu,L. and Zhang,S. (2020) The Transcription Factor SomA Synchronously Regulates Biofilm Formation and Cell Wall Homeostasis in Aspergillus fumigatus. *MBio*, **11**.

47. Wang,W., Drott,M., Greco,C., Luciano-Rosario,D., Wang,P. and Keller,N.P. (2021) Transcription Factor Repurposing Offers Insights into Evolution of Biosynthetic Gene Cluster Regulation. *MBio*, **12**, e0139921.

48. Sherwood,R.I., Hashimoto,T., O'Donnell,C.W., Lewis,S., Barkal,A.A., van Hoff,J.P., Karun,V., Jaakkola,T. and Gifford,D.K. (2014) Discovery of directional and nondirectional pioneer transcription factors by modeling DNase profile magnitude and shape. *Nat. Biotechnol.*, **32**, 171–178.

49. Yoro,E., Suzaki,T., Toyokura,K., Miyazawa,H., Fukaki,H. and Kawaguchi,M. (2014) A Positive Regulator of Nodule Organogenesis, NODULE INCEPTION, Acts as a Negative Regulator of Rhizobial Infection in Lotus japonicus. *Plant Physiol.*, **165**, 747–758.

50. Liu,J., Rutten,L., Limpens,E., van der Molen,T., van Velzen,R., Chen,R., Chen,Y., Geurts,R., Kohlen,W., Kulikova,O., *et al.* (2019) A Remote cis-Regulatory Region Is Required for NIN Expression in the Pericycle to Initiate Nodule Primordium Formation in Medicago truncatula. *Plant Cell*, **31**, 68–83.

51. Wasserman,W.W. and Sandelin,A. (2004) Applied bioinformatics for the identification of regulatory elements. *Nat. Rev. Genet.*, **5**, 276–287.

52. Pagès,H., Aboyoun,P., Gentleman,R. and DebRoy,S. Biostrings: Efficient Manipulation of Biological Strings; R Package Version 2.56. 0; 2020.

53. Liao,J.C., Boscolo,R., Yang,Y.-L., Tran,L.M., Sabatti,C. and Roychowdhury,V.P. (2003) Network component analysis: Reconstruction of regulatory signals in biological systems. *Proceedings of the National Academy of Sciences*, **100**, 15522–15527.

54. Ma,C.Z. and Brent,M.R. (2021) Inferring TF activities and activity regulators from gene expression data with constraints from TF perturbation data. *Bioinformatics*, **37**, 1234–1245.

55. Miraldi,E.R., Pokrovskii,M., Watters,A., Castro,D.M., De Veaux,N., Hall,J.A., Lee,J.-Y., Ciofani,M., Madar,A., Carriero,N., *et al.* (2019) Leveraging chromatin accessibility for transcriptional regulatory network inference in T Helper 17 Cells. *Genome Res.*, **29**, 449–463.

56. Amos,B., Aurrecoechea,C., Barba,M., Barreto,A., Basenko,E.Y., Bażant,W., Belnap,R., Blevins,A.S., Böhme,U., Brestelli,J., *et al.* (2022) VEuPathDB: the eukaryotic pathogen, vector and host bioinformatics resource center. *Nucleic Acids Res.*, **50**, D898–D911.

57. Kou,L., Markowsky,G. and Berman,L. (1981) A fast algorithm for Steiner trees. *Acta Inform.*, **15**, 141–145.

58. Köhler,S., Bauer,S., Horn,D. and Robinson,P.N. (2008) Walking the interactome for prioritization of candidate disease genes. *Am. J. Hum. Genet.*, **82**.

59. da Silva Ferreira,M.E., Kress,M.R.V.Z., Savoldi,M., Goldman,M.H.S., Härtl,A., Heinekamp,T., Brakhage,A.A. and Goldman,G.H. (2006) The akuB KU80 mutant deficient for nonhomologous end joining is a powerful tool for analyzing pathogenicity in Aspergillus fumigatus. *Eukaryot. Cell*, **5**, 207–211.

60. Wiemann,P., Perevitsky,A., Lim,F.Y., Shadkchan,Y., Knox,B.P., Landero Figueora,J.A., Choera,T., Niu,M., Steinberger,A.J., Wüthrich,M., *et al.* (2017) Aspergillus fumigatus Copper Export Machinery and Reactive Oxygen Intermediate Defense Counter Host Copper-Mediated Oxidative Antimicrobial Offense. *Cell Rep.*, **19**, 1008–1021.

61. Lim,F.Y., Won,T.H., Raffa,N., Baccile,J.A., Wisecaver,J., Rokas,A., Schroeder,F.C. and Keller,N.P. (2018) Fungal Isocyanide Synthases and Xanthocillin Biosynthesis in Aspergillus fumigatus. *MBio*, **9**.

62. Throckmorton,K., Lim,F.Y., Kontoyiannis,D.P., Zheng,W. and Keller,N.P. (2016) Redundant synthesis of a conidial polyketide by two distinct secondary metabolite clusters in Aspergillus fumigatus. *Environ. Microbiol.*, **18**, 246–259.

63. Schoen,T.J., Calise,D.G., Bok,J.W., Giese,M.A., Nwagwu,C.D., Zarnowski,R., Andes,D., Huttenlocher,A. and Keller,N.P. (2023) Aspergillus fumigatus transcription factor ZfpA regulates hyphal development and alters susceptibility to antifungals and neutrophil killing during infection. *PLoS Pathog.*, **19**, e1011152.

64. Shimizu,K. and Keller,N.P. (2001) Genetic involvement of a cAMP-dependent protein kinase in a G protein signaling pathway regulating morphological and chemical transitions in Aspergillus nidulans. *Genetics*, **157**, 591–600.

65. Shaaban,M.I., Bok,J.W., Lauer,C. and Keller,N.P. (2010) Suppressor mutagenesis identifies a velvet complex remediator of Aspergillus nidulans secondary metabolism. *Eukaryot. Cell*, **9**, 1816–1824.

66. Soukup,A.A., Farnoodian,M., Berthier,E. and Keller,N.P. (2012) NosA, a transcription factor important in Aspergillus fumigatus stress and developmental response, rescues the germination defect of a laeA deletion. *Fungal Genet. Biol.*, **49**, 857–865.

67. Bok,J.W., Soukup,A.A., Chadwick,E., Chiang,Y.-M., Wang,C.C.C. and Keller,N.P. (2013) VeA and MvlA repression of the cryptic orsellinic acid gene cluster in Aspergillus nidulans involves histone 3 acetylation. *Mol. Microbiol.*, **89**, 963–974.

68. Shannon,P., Markiel,A., Ozier,O., Baliga,N.S., Wang,J.T., Ramage,D., Amin,N., Schwikowski,B. and Ideker,T. (2003) Cytoscape: a software environment for integrated models of biomolecular interaction networks. *Genome Res.*, **13**, 2498–2504.

69. Chung,D., Barker,B.M., Carey,C.C., Merriman,B., Werner,E.R., Lechner,B.E., Dhingra,S., Cheng,C., Xu,W., Blosser,S.J., *et al.* (2014) ChIP-seq and in vivo transcriptome analyses of the Aspergillus fumigatus SREBP SrbA reveals a new regulator of the fungal hypoxia response and virulence. *PLoS Pathog.*, **10**, e1004487.

70. Kroll,K., Pähtz,V., Hillmann,F., Vaknin,Y., Schmidt-Heck,W., Roth,M., Jacobsen,I.D., Osherov,N., Brakhage,A.A. and Kniemeyer,O. (2014) Identification of hypoxia-inducible target genes of Aspergillus fumigatus by transcriptome analysis reveals cellular respiration as an important contributor to hypoxic survival. *Eukaryot. Cell*, **13**, 1241–1253.

71. Vicentefranqueira,R., Amich,J., Marín,L., Sánchez,C.I., Leal,F. and Calera,J.A. (2018) The Transcription Factor ZafA Regulates the Homeostatic and Adaptive Response to Zinc Starvation in Aspergillus fumigatus. *Genes* , **9**.

72. Abad,A., Fernández-Molina,J.V., Bikandi,J., Ramírez,A., Margareto,J., Sendino,J., Hernando,F.L., Pontón,J., Garaizar,J. and Rementeria,A. (2010) What makes Aspergillus fumigatus a successful pathogen? Genes and molecules involved in invasive aspergillosis. *Rev. Iberoam. Micol.*, **27**, 155–182.

73. Haas,H. (2014) Fungal siderophore metabolism with a focus on Aspergillus fumigatus. *Nat. Prod. Rep.*, **31**, 1266–1276.

74. Raffa,N. and Keller,N.P. (2019) A call to arms: Mustering secondary metabolites for success and survival of an opportunistic pathogen. *PLoS Pathog.*, **15**, e1007606.

75. Keller,N.P. (2019) Fungal secondary metabolism: regulation, function and drug discovery. *Nat. Rev. Microbiol.*, **17**, 167–180.

76. Guruceaga,X., Perez-Cuesta,U., Pellon,A., Cendon-Sanchez,S., Pelegri-Martinez,E., Gonzalez,O., Hernando,F.L., Mayayo,E., Anguita,J., Alonso,R.M., *et al.* (2021) Aspergillus fumigatus Fumagillin Contributes to Host Cell Damage. *J Fungi (Basel)*, **7**.

77. Guruceaga,X., Perez-Cuesta,U., Abad-Diaz de Cerio,A., Gonzalez,O., Alonso,R.M., Hernando,F.L., Ramirez-Garcia,A. and Rementeria,A. (2019) Fumagillin, a Mycotoxin of Aspergillus fumigatus: Biosynthesis, Biological Activities, Detection, and Applications. *Toxins* , **12**.

78. Wiemann,P., Guo,C.-J., Palmer,J.M., Sekonyela,R., Wang,C.C.C. and Keller,N.P. (2013) Prototype of an intertwined secondary-metabolite supercluster. *Proc. Natl. Acad. Sci. U. S. A.*, **110**, 17065–17070.

79. Pinheiro,E.A.A., Carvalho,J.M., dos Santos,D.C.P., Feitosa,A. de O., Marinho,P.S.B., Guilhon,G.M.S.P., de Souza,A.D.L., da Silva,F.M.A. and Marinho,A.M. do R. (2013) Antibacterial activity of alkaloids produced by endophytic fungus

Aspergillus sp. EJC08 isolated from medical plant Bauhinia guianensis. *Nat. Prod. Res.*, **27**, 1633–1638.

80. Baccile,J.A., Spraker,J.E., Le,H.H., Brandenburger,E., Gomez,C., Bok,J.W., Macheleidt,J., Brakhage,A.A., Hoffmeister,D., Keller,N.P., *et al.* (2016) Plant-like biosynthesis of isoquinoline alkaloids in Aspergillus fumigatus. *Nat. Chem. Biol.*, **12**, 419–424.

81. Carberry,S., Molloy,E., Hammel,S., O'Keeffe,G., Jones,G.W., Kavanagh,K. and Doyle,S. (2012) Gliotoxin effects on fungal growth: mechanisms and exploitation. *Fungal Genet. Biol.*, **49**, 302–312.

82. Sugui,J.A., Pardo,J., Chang,Y.C., Zarember,K.A., Nardone,G., Galvez,E.M., Müllbacher,A., Gallin,J.I., Simon,M.M. and Kwon-Chung,K.J. (2007) Gliotoxin is a virulence factor of Aspergillus fumigatus: gliP deletion attenuates virulence in mice immunosuppressed with hydrocortisone. *Eukaryot. Cell*, **6**, 1562–1569.

83. Bok,J.W., Chung,D., Balajee,S.A., Marr,K.A., Andes,D., Nielsen,K.F., Frisvad,J.C., Kirby,K.A. and Keller,N.P. (2006) GliZ, a transcriptional regulator of gliotoxin biosynthesis, contributes to Aspergillus fumigatus virulence. *Infect. Immun.*, **74**, 6761–6768.

84. Domingo,M.P., Colmenarejo,C., Martínez-Lostao,L., Müllbacher,A., Jarne,C., Revillo,M.J., Delgado,P., Roc,L., Meis,J.F., Rezusta,A., *et al.* (2012) Bis(methyl)gliotoxin proves to be a more stable and reliable marker for invasive aspergillosis than gliotoxin and suitable for use in diagnosis. *Diagn. Microbiol. Infect. Dis.*, **73**, 57–64.

85. Gao,J., Xu,X., Huang,K. and Liang,Z. (2021) Fungal G-Protein-Coupled Receptors: A Promising Mediator of the Impact of Extracellular Signals on Biosynthesis of Ochratoxin A. *Front. Microbiol.*, **0**.

86. Maillet,F., Poinsot,V., André,O., Puech-Pagès,V., Haouy,A., Gueunier,M., Cromer,L., Giraudet,D., Formey,D., Niebel,A., *et al.* (2011) Fungal lipochitooligosaccharide symbiotic signals in arbuscular mycorrhiza. *Nature*, **469**, 58–63.

87. Feng,F., Sun,J., Radhakrishnan,G.V., Lee,T., Bozsóki,Z., Fort,S., Gavrin,A., Gysel,K., Thygesen,M.B., Andersen,K.R., *et al.* (2019) A combination of chitooligosaccharide and lipochitooligosaccharide recognition promotes arbuscular mycorrhizal associations in Medicago truncatula. *Nat. Commun.*, **10**, 5047.

88. Cope,K.R., Bascaules,A., Irving,T.B., Venkateshwaran,M., Maeda,J., Garcia,K., Rush,T.A., Ma,C., Labbé,J., Jawdy,S., *et al.* (2019) The Ectomycorrhizal Fungus Laccaria bicolor Produces Lipochitooligosaccharides and Uses the Common Symbiosis Pathway to Colonize Populus Roots. *Plant Cell*, **31**, 2386–2410.

89. Khokhani,D., Carrera Carriel,C., Vayla,S., Irving,T.B., Stonoha-Arther,C., Keller,N.P. and Ané,J.-M. (2021) Deciphering the Chitin Code in Plant Symbiosis, Defense, and Microbial Networks. *Annu. Rev. Microbiol.*, **75**, 583–607.

90. Hagiwara,D., Suzuki,S., Kamei,K., Gonoi,T. and Kawamoto,S. (2014) The role of AtfA and HOG MAPK pathway in stress tolerance in conidia of Aspergillus fumigatus. *Fungal Genet. Biol.*, **73**, 138–149.

91. Sakamoto,K., Iwashita,K., Yamada,O., Kobayashi,K., Mizuno,A., Akita,O., Mikami,S., Shimoi,H. and Gomi,K. (2009) Aspergillus oryzae atfA controls conidial germination and stress tolerance. *Fungal Genet. Biol.*, **46**, 887–897.

92. Brauer,V.S., Pessoni,A.M., Freitas,M.S., Cavalcanti-Neto,M.P., Ries,L.N.A. and Almeida,F. (2023) Chitin Biosynthesis in Aspergillus Species. *Journal of Fungi*, **9**, 89.

93. Poinsot,V., Crook,M.B., Erdn,S., Maillet,F., Bascaules,A. and Ané,J.-M. (2016) New insights into Nod factor biosynthesis: Analyses of chitooligomers and lipo-chitooligomers of Rhizobium sp. IRBG74 mutants. *Carbohydr. Res.*, **434**, 83.

94. Muszkieta,L., Aimanianda,V., Mellado,E., Gribaldo,S., Alcàzar-Fuoli,L., Szewczyk,E., Prevost,M.-C. and Latgé,J.-P. (2014) Deciphering the role of the chitin synthase families 1 and 2 in the in vivo and in vitro growth of Aspergillus fumigatus by multiple gene targeting deletion. *Cell. Microbiol.*, **16**, 1784–1805.

95. Valsecchi,I., Sarikaya-Bayram,Ö., Wong Sak Hoi,J., Muszkieta,L., Gibbons,J., Prevost,M.-C., Mallet,A., Krijnse-Locker,J., Ibrahim-Granet,O., Mouyna,I., *et al.* (2017) MybA, a transcription factor involved in conidiation and conidial viability of the human pathogen Aspergillus fumigatus. *Mol. Microbiol.*, **105**, 880–900.

96. de Bettignies,G., Barthe,C., Morel,C., Peypouquet,M.F., Doignon,F. and Crouzet,M. (1999) RGD1 genetically interacts with MID2 and SLG1, encoding two putative sensors for cell integrity signalling in Saccharomyces cerevisiae. *Yeast*, **15**, 1719–1731.

97. Ries,L.N.A., Rocha,M.C., de Castro,P.A., Silva-Rocha,R., Silva,R.N., Freitas,F.Z., de Assis,L.J., Bertolini,M.C., Malavazi,I. and Goldman,G.H. (2017) The CrzA Transcription Factor Activates Chitin Synthase Gene Expression during the Caspofungin Paradoxical Effect. *MBio*, **8**.

98. Parums,D.V. (2022) Editorial: The World Health Organization (WHO) Fungal Priority Pathogens List in Response to Emerging Fungal Pathogens During the COVID-19 Pandemic. *Med. Sci. Monit.*, **28**, e939088.

99. Gao,L., Ouyang,H., Pei,C., Zhou,H., Yang,J. and Jin,C. (2022) Emp47 and Vip36 are required for polarized growth and protein trafficking between ER and Golgi apparatus in opportunistic fungal pathogen Aspergillus fumigatus. *Fungal Genet. Biol.*, **158**, 103638.

100. He,C., Wei,Q., Xu,J., Cai,R., Kong,Q., Chen,P., Lu,L. and Sang,H. (2022) bHLH transcription factor EcdR controls conidia production, pigmentation and virulence in Aspergillus fumigatus. *Fungal Genet. Biol.*, **164**, 103751.

101. Zhai,P., Du,W., Long,N. and Lu,L. (2022) A GATA-type transcription factor SreA affects manganese susceptibility by regulating the expression of iron uptake-related genes. *Fungal Genet. Biol.*, **163**, 103731.

102. Lofgren,L.A., Ross,B.S., Cramer,R.A. and Stajich,J.E. (2022) The pan-genome of Aspergillus fumigatus provides a high-resolution view of its population structure revealing high levels of lineage-specific diversity driven by recombination. *PLoS Biol.*, **20**, e3001890.

103. Brian,P.W. (1946) Production of gliotoxin by penicillium terlikowskii Zal. *Trans. Br. Mycol. Soc.*, **29**, 211–218.

104. Kwon-Chung,K.J. and Sugui,J.A. (2009) What do we know about the role of gliotoxin in the pathobiology of Aspergillus fumigatus? *Med. Mycol.*, **47 Suppl 1**, S97–103.

105. de Castro,P.A., Colabardini,A.C., Moraes,M., Horta,M.A.C., Knowles,S.L., Raja,H.A., Oberlies,N.H., Koyama,Y., Ogawa,M., Gomi,K., *et al.* (2022) Regulation of gliotoxin biosynthesis and protection in Aspergillus species. *PLoS Genet.*, **18**, e1009965.

106. Yu,J.-H., Baldin,C., Kühbacher,A., Merschak,P. and Gsaller,F. (2010) Central regulatory pathway in Aspergillus fumigatus conidiation. BrlA,. *ResearchGate*.

Chapter 3

Expanding the Role of LysM Effectors in Fungi: *AfldpA* from the human pathogen *Aspergillus fumigatus* is required for responses to Lipochitooligosaccharides

Cristobal Carrera Carriel[1], Aidan Schmidt[2], Grant Nickles[3], Tomás A. Rush[6], Nancy P. Keller[5,6], Jean-Michel Ané[2,4*]

[1] Department of Genetics
[2] Departments of Bacteriology
[3] Department of Cellular and Molecular Biology,
[4] Department of Agronomy
[5] Department of Medical Microbiology and Immunology
[6] Department of Plant Pathology
[7] Biosciences Division, Oak Ridge National Laboratory, Oak Ridge, Tennessee, US

University of Wisconsin-Madison, Madison, Wisconsin, USA 53715

* To whom correspondence should be addressed. Email: jeanmichel.ane@wisc.edu.
The authors wish it to be known that, in their opinion, the first two authors should be regarded as joint First Authors.

Cristobal Carrera Carriel's Contribution to Chapter 3

CCC wrote Introduction, Methods for work regarding *A. fumigatus*, and Conclusion. CCC illustrated all figures except. CCC performed RNAseq and physiological assays of *AfldpA* mutants. CCC also performed computational expression analysis of *A. fumigatus* datasets. GN illustrated Figure 4 and AS performed replicate branching analysis of mutants. J.-M.A, N.P.K, and SW provided input on writing.

Abstract

Lipochitooligosaccharides (LCOs) are chitin-based signaling molecules that influence the growth and development of fungi. While it is widely believed that these molecules act as autocrine and paracrine agents, the genetic processes involved in how fungi perceive these signals are not yet fully understood. Our research aimed to analyze the expression of *Aspergillus fumigatus* genes when exposed to different chitin-based molecules. We observed significant changes in the expression of genes encoding secreted LysM effectors. LysM domains, which are known to bind chitin molecules and function as LCO receptors in plants, led us to investigate whether LysM effectors also play a role in responses to LCOs in fungi. Our findings indicate that LysM effector *Af*LdpA in the human pathogen *A. fumigatus* is absolutely required for fungal developmental responses to LCOs. Strikingly, we found that, unlike the *A. fumigatus* wild-type strain, the transcriptome of the Δ*AfldpA* mutant remains unchanged in response to LCOs. Our ongoing goal is to confirm that LysM effectors act as receptors and are capable of binding these chitin-based molecules. This significant discovery expands our understanding of the LCO-signaling pathway in fungi and new functions of fungal LysM effectors.

Introduction

Lipo-chitooligosaccharides (LCOs) are a class of signaling molecules found throughout the fungal kingdom (1, 2). These chitin-based molecules comprise short chitin oligomers, an attached lipid chain, and various functional groups (1–4). LCOs were initially found to be involved in plant-microbe interactions, where nitrogen-fixing

bacteria collectively called rhizobia would synthesize and secrete these molecules to initiate symbioses with their plant hosts (5, 6). While initially thought to be exclusive to rhizobia, these molecules would eventually be found in arbuscular mycorrhizal fungi in 2011 (7) and in ectomycorrhizal fungi in 2019 (8). Like in rhizobia, LCOs from mycorrhizal fungi also serve to initiate plant-microbe symbioses (8, 9).

In 2020, researchers discovered that most fungi, regardless of lifestyle, synthesize LCOs, expanding the role of these molecules (1). Furthermore, fungi treated with exogenous LCOs exhibit a variety of regulatory responses. For example, treatment of *Aspergillus fumigatus* with C:16 sulfated LCOs (sLCOs) leads to an increase in the germination of conidia and a decrease in the number of secondary branches coming off the primary hypha (1). In the ectomycorrhizal fungus, *Laccaria bicolor,* treatment with a variety of LCOs and short chitin oligomers (COs) generally reduced both radial growth and hyphal branching while increasing hyphal clamp connections (10). Thus, LCOs could function as autocrine and paracrine signals within the fungal kingdom (1).

While we do not yet know the receptors necessary for LCO perception in fungi, the receptors in plants are well-studied. In plant-microbe interactions, plants utilize transmembrane receptors containing LysM domains to bind chitin molecules (2, 11). These receptors are, therefore, instrumental in initiating a signaling cascade that activates the Common Signaling Pathway, a conserved genetic mechanism crucial for most plant-microbe symbiotic interactions (12, 13). Regarding defense, plants also use LysM-domain-containing receptors to recognize pathogenic fungi (14). Whether the scenario is mutualism or pathogenicity, the LysM domain in plant chitin receptors binds LCOs and COs (14). While LysM transmembrane receptors are well characterized in

plants, recent findings suggest that plant LysM effectors, proteins containing one or more LysM domains and a signal peptide, can bind LCOs and COs to enhance symbiosis (15, 16).

LysM effectors are also found throughout the fungal kingdom (17, 18). These effectors have been implicated in two major functions: disrupting the host immune response by sequestering chitin fragments and protecting the cell wall from host chitinases (19–31). The fact that these effectors are present in fungi that aren't associated with plants could mean that LysM effectors have broader functions.

Interestingly, Zeng *et al.* found that RiSLM, the LysM effector of the arbuscular mycorrhizal fungus *Rhizophagus irregularis,* can physically bind COs and LCOs, facilitating symbiosis by sequestering chitin molecules and disrupting plant immune response (32). We suggest that fungal proteins with LysM domains, found throughout the fungal kingdom, act as chitin receptors that allow fungi to respond to LCOs and COs.

A. fumigatus has two LysM effectors, *Af*LdpA and *Af*LdpB (33). However, Muraosa et al. 2019 found that deleting these genes did not affect radial growth or pathogenicity in murine models. Interestingly, *Af*LdpA localized to the cell wall and extracellular matrix, while *Af*LdpB localized to the septa. If one of these molecules plays a role in LCO binding, it could be *Af*LdpA as it is localized to areas where it is most likely to encounter exogenous LCOs.

Thus, we hypothesize that *Af*LdpA acts as a receptor for chitin molecules and is necessary for the observable phenotypes that *A. fumigatus* exhibits in response to LCO

treatment. While past research surrounding these proteins focuses on fungi-plant interactions, our study highlights their potential functions beyond this context.

Materials and Methods

Fungal Strains and Cultural Conditions

Table S1 lists the strains we used in this study**.** For three days, *A. fumigatus* strains were grown on glucose minimal media (GMM) agar plates. We collected conidia using sterile water containing Tween 80 (0.01%). GMM was prepared as described in Shimizu and Keller, 2001 (34). Strains were maintained in 50% glycerol at −80 °C for long-term storage.

Analysis of secondary branching in *A. fumigatus* strains

To quantify secondary branches in *A. fumigatus*, we inoculated $1x10^6$ conidia per mL of *A. fumigatus* strains in GMM containing either 10^{-8} M sulfated LCOs purified from *Sinorhizobium meliloti* or 0.005% ethanol/water (v/v) negative control (1, 10, 34). 100 µL of inoculated and treated broth was dispensed into a well in a 96-well flat bottom plate in triplicate. The plate was incubated at 37 °C for 11 hours, followed by imaging every 15 minutes over 3 hours using a Nikon TI inverted microscope with a 40X objective. Each frame captures the growth of one hypha, and ten frames were taken per well. We counted the number of secondary branches per apical hyphae using NIS-Elements AR Analysis Version 4.30.

RNAseq extraction from *A. fumigatus AfldpA* mutant

We inoculated 10^6 spores per mL of *A. fumigatus* strains in liquid glucose minimal media and incubated for 48 hours at 37˚C shaking at 250 RPM overnight (35).

For our expression analysis of Δ*AfldpA* in response to LCOs, we treated the AFS35 wildtype and Δ*AfldpA* strains with a two-hour treatment of 10^{-8} M of sulfated LCOs purified from *Sinorhizobium meliloti* or 0.005% ethanol/water (v/v) negative control (10, 34). RNA was extracted using QIAzol Lysis Reagent (Qiagen) according to the manufacturer's instructions with an additional phenol:chloroform:isoamyl alcohol (24:1:1) extraction step before RNA precipitation.

For our expression analysis of *A. fumigatus* treated with various LCOs and COs, we treated the AF293 wildtype for two hours with 10^{-8} M sLCOs purified from *Sinorhizobium meliloti*, nsLCOs purified from Rhizobium sp. IRBG74, chitotetraose (CO4), chitooctaose (CO8), or 0.005% ethanol/water (v/v) negative control. COs were acquired from IsoSep, Tullinge, Sweden. RNA was extracted using a Sigma Aldrich Spectrum Plant Total RNA kit.

RNA integrity was tested via nanodrop, gel electrophoresis, and the Agilent 2100 Bioanalyzer. Library preparation and RNA sequencing were performed by Novogene, Inc. using the TruSeq Stranded mRNA Library Prep Kit and Illumina Novaseq 6000 Platform.

Quality filtering of RNA-Seq single-end reads was done using fastp v0.20.1 (36). Paired-end reads were aligned using HISAT2 v2.2.1 (37) with the reference transcriptome of A. fumigatus Af293 (ASM265v1) downloaded from NCBI. Conversion of SAM files into BAM files, sorting, and indexing using Samtools v1.19.2 (38). Reads were further counted FeatureCounts v2.0.1 (39). Count normalization and differential expression analysis were done using DESeq2 v1.42.1 (40). We defined transcripts as differentially expressed if they had an adjusted p-value < 0.05 and log2 Fold Change

values < −1 or >1. GRAsp module tables were created by uploading a loading list of DEGs to GRAsp.WID.WISC.edu. Tables were subsequently trimmed by only taking the top-scoring regulators and GO-enrichment terms.

Reconstruction of the fungal kingdom's species tree

We ran the coalescent model, ASTRAL v5.7.8(41, 42), on a set of 290 BUSCO(43) gene trees. We utilized the same pipeline to create all gene trees. First the sequences were aligned with MAFFT v7.475(44) with the '-auto' parameter. All alignments were then trimmed using trimAl v1.2(45) with the '-gappyout' parameter. Lastly, the gene trees were generated using the maximum likelihood software IQTree v2.0.3(46) with 1000 ultrafast bootstrap replicates. The most suitable model of sequence evolution for each gene tree was determined using ModelFinder(47). We forced multiple isolates within the same species (as determined from NCBI taxonomic metadata) to be monophyletic by passing a species map file. The tree was rooted using the most recent common ancestor of Cryptomycota and Microsporidia, which are the earliest diverging lineages within the Kingdom Fungi(48). All visualizations and phylogenetic plots were made with the ape v5.7-1(49), ggtree v3.11.0(50) and ggplot2 v3.4.4(51).

Analysis of LysM domain-containing proteins across the fungal kingdom

Publicly available annotated and assembled fungal genomes (*n* = 3077) were downloaded from the NCBI database on 12/1/2023 using the NCBI's Dataset tool, version 11.32.1. Protein domain predictions were obtained for every protein using HMMER v3.1b2(52) (e-value <= 1e-5) with the Pfam database v34(53). To identify putative proteins with LysM domains, we searched for the Lysin motif PF01476. Lastly, all extracted proteins containing LysM domains were analyzed using DeepTMHMM

(Deep Learning Model for Transmembrane Topology Prediction and Classification) v1.0.24(54) to identify potential signal peptides and transmembrane domains.

Results

Chitin oligomers alter the expression of *AfldpA* and *AfldpB* genes in *A. fumigatus*

While only sLCO induced changes to secondary branching in *A. fumigatus* and was further shown to alter the fungus' transcriptome, treatment with non-sulfated LCOs (nsLCO), chitin oligomers CO4 and CO8, interestingly, also induced unique transcriptomic profiles depicted by separate clustering in principal component analysis **Figure S1.A**. sLCO treatment differentially regulated the most amount of genes (835 genes total), followed by CO4 (94 genes total), nsLCO (92 genes total) and CO8 (30 genes total) **Figure S2**. There were also shared genes among treatments where the highest overall amount occurs between sLCO and nsLCO treatments (68 overlapping genes). The four treatments have 48 genes in common **Figure S1.B**.

The treatments also differentially express genes that fall into various GRAsp modules, small groups of inferred regulatory gene networks **Figure S3**. GO-term enrichment suggests that all modules are involved in processes such as secondary metabolite synthesis (helvolic acid biosynthesis, gliotoxin biosynthesis, etc.) and cell-wall modification (galactoaminogalactan biosynthesis, polysaccharide catabolic process).

We found that treating *A. fumigatus* with chitin oligomers altered the expression of *AfldpA* and *AfldpB*. The molecules sLCO, nsLCO, and CO4 downregulated *AfldpA.*

Both sLCO and nsLCO caused differential expression (Adjusted P-Value: < 0.0001)

Figure 1.

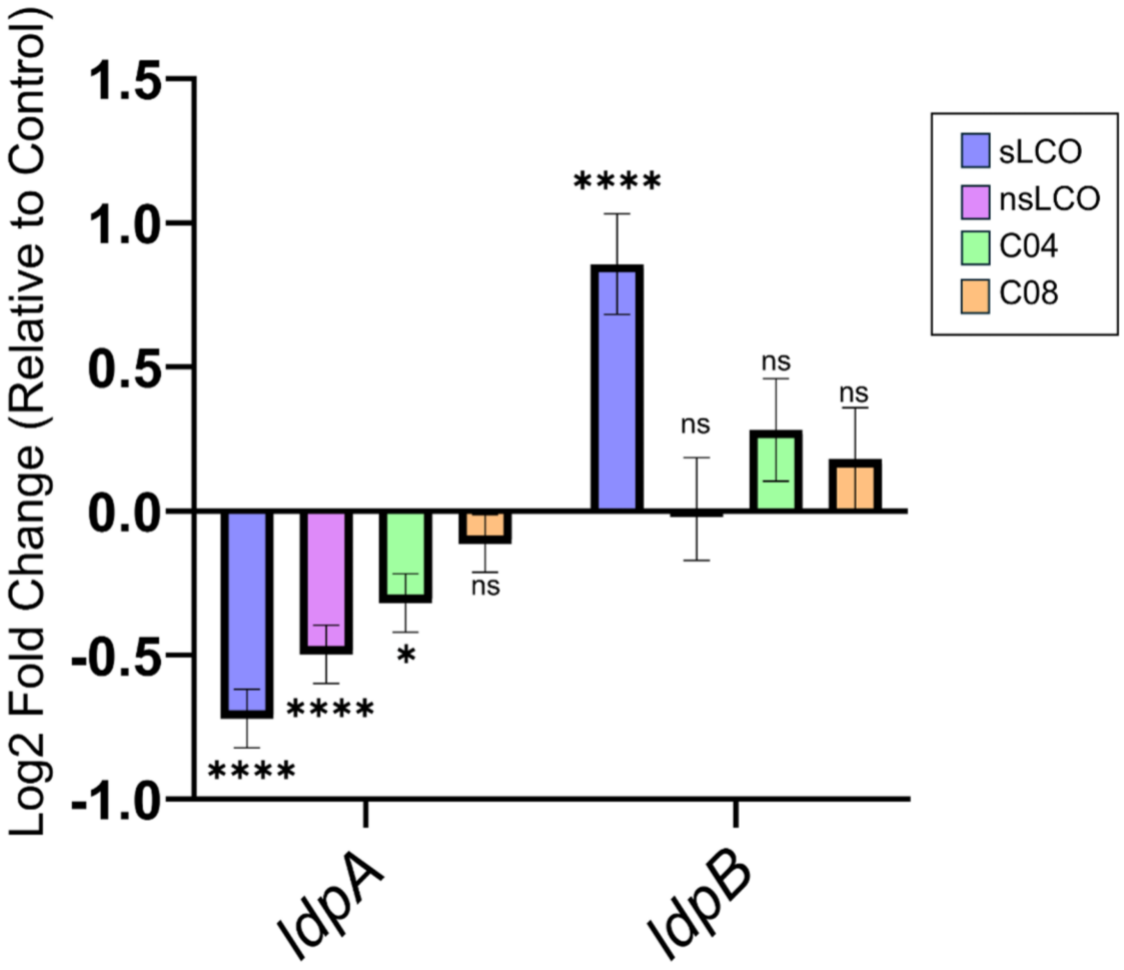

Figure 1. Expression *AfldpA* and *AfldpB* Expression in response to chitin molecules. Log2 fold-change of *AfldpA* and *AfldpB* in the Wild-type *A. fumigatus* strain treated with various chitin molecules (Relative to negative control). Significance refers to gene's adjusted p-value (*, p<0.0332; **, p<0.0021; ***, p<0.0002; ****, p<0.0001; NS, not significant).

sLCO induced the highest log-fold change out of the molecules, causing a downregulation of -0.72 Log2 fold-change, followed by nsLCO with a downregulation of -0.50 Log2 fold-change. CO4 also downregulated *AfldpA*, but with lower significance (Adjusted P-Value: = 0.0056) and Log fold-change (-0.28 Log2 fold-change) compared to LCOs. CO8 treatment did not differentially alter the expression of *AfldpA.* Furthermore, sLCO also led to the differential expression of *AfldpB* (Adjusted P-Value: = 0.006), upregulating expression by 0.90 Log2 fold-change.

***AfldpA* is required for LCO-induced hypobranching in *Aspergillus fumigatus*.**

To test the importance of LysM effectors in *A. fumigatus* response to LCOs, we examined secondary branching in *⊿AfldpA* and *⊿AfldpB* single and double deletion strains after treatment with LCO-IV (C:16, S), referred to as sLCO **Figure 2.A**. While the wild-type AFS35 strain and *⊿AfldpB* still exhibited a reduction in the secondary branches, this reduction did not occur in *⊿AfldpA* and the double deletion mutant *⊿AfldpA⊿AfldpB.* Previous studies found that sLCO increased germination in the AF293 and CEA10 wild-type strains, but this phenotype was not observed in AFS35 (Data not shown). This is likely due to AFS35's reduced response to sLCOs.

The single and double mutants had altered branching phenotypes even without treatment. The *⊿AfldpA* strain had a reduction in secondary branches, while *⊿AfldpB* had an increase. Interestingly, *⊿AfldpA⊿AfldpB* had a level of secondary branching similar to that of the wild-type strain, which could signify that the branching of both mutants balanced each other out.

These findings implicate *AfldpA* as necessary for proper response to sLCOs and part of the LCO signaling pathway. Since *AfldpA* codes for a chitin effector protein and

localizes to the cell wall, we suggest this protein acts as an LCO receptor. Specifically, *Af*LdpA binds exogenous LCOs at the cell wall, activating a signaling cascade that leads to LCO-induced phenotypes regulated by *AfatfA*. Furthermore, we propose a genetic model: LCO-binding inhibits the expression of *AfldpA*, which inhibits the expression of *AfatfA* and results in the inhibition of hyphal branching in *A. fumigatus* **Figure 2.B**.

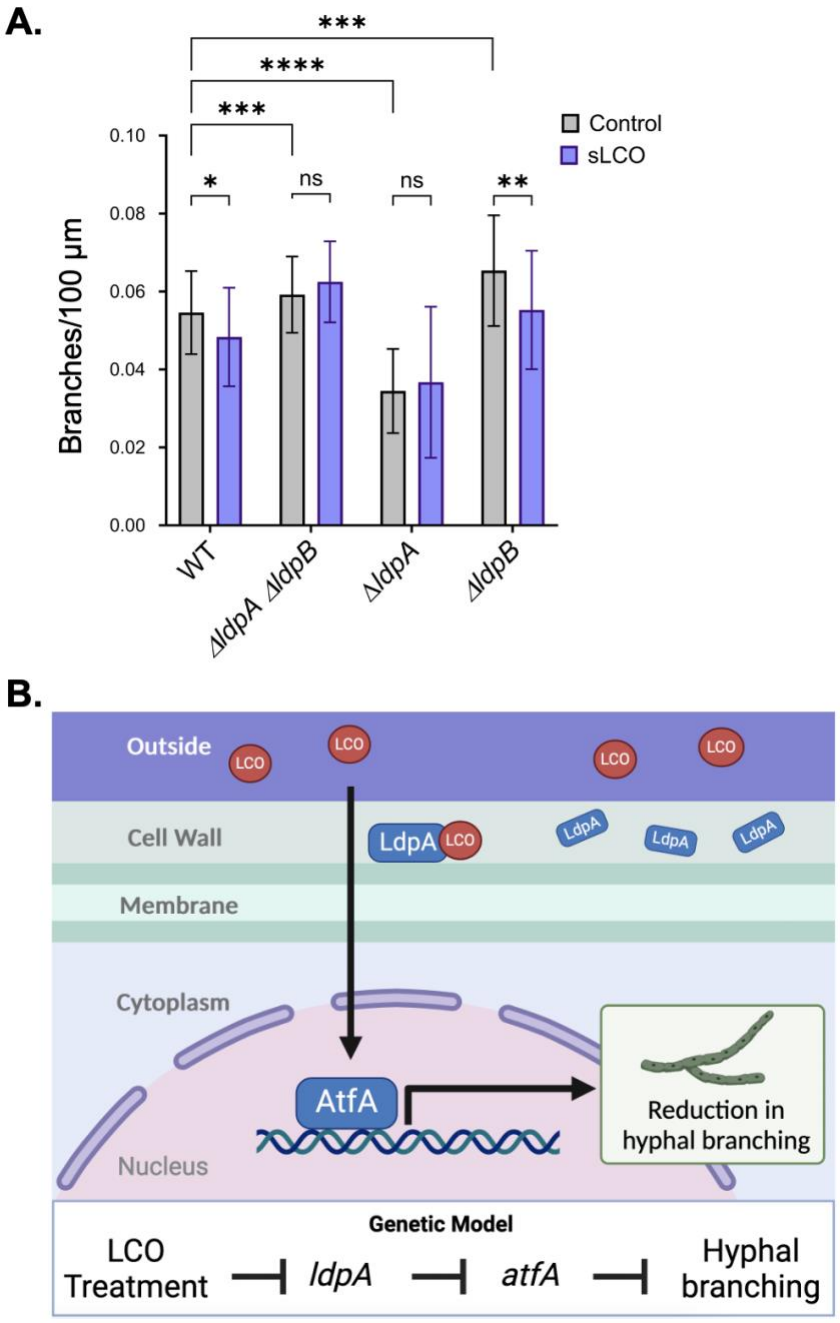

Figure 2. *AfldpA* is necessary for branching response to sLCO. A) Secondary branching per micrometer of hyphae, 12 hours after treatment with sLCO, LCO-IV (C:16, S) or Control, 0.005% EtOH. B) Hypothetical LCO-response pathway where 1, *Af*LdpA (referred to as Ldap), localized to the cell wall, binds an exogenous LCO molecule. 2, Through an unknown mechanism, *Af*LdpA activates a signaling cascade that activates transcription factor *Af*AtfA (referred to as AtfA). 3, Pathways downstream of *Af*AtfA are activated and results in a reduction in hyphal branching. The lower panel depicts the proposed genetic model; the Blunt arrows depict inhibition. Multiple two-sided *t*-tests were used to compare LCO and negative control treatments within each strain. ANOVA test, followed by Dunnett's multiple comparison test, was performed to compare strains of the negative control group. Error bars represent mean ± Standard Error (*, $p<0.0332$; **, $p<0.0021$; ***, $p<0.0002$; ****, $p<0.0001$; NS, not significant).

Deletion of *AfldpA* alters the transcriptome of *Aspergillus fumigatus* but is non-responsive to LCOs

Deletion of *AfldpA* differentially regulated 328 genes in *A. fumigatus* **Figure S4.A**. and DEGs belonged to several GRAsp modules. Module 5491 had the highest enrichment of DEGs, and the top predicted regulator of this module is *AfatfA*, which we previously found was involved in LCO response **Figure S4.B**. Other modules suggest, via GO-term enrichment, that disrupting *AfldpA* affects various processes: mRNA modification, protein refolding, secondary metabolite synthesis, long-chain fatty acid synthesis, membrane lipid metabolism, and reactive nitrogen species metabolism.

Considering that *⊿AfldpA* does not respond to LCOs, we further hypothesized that the transcription profile of *AfldpA* would not be affected by sLCO treatment. The

Principal Component Analysis reveals little to no clustering among wild-type and ⊿*AfldpA* strains treated with LCO or negative control **Figure S4**.

However, volcano plots reveal that while the *A. fumigatus* wild-type strain treated with sLCOs led to 48 DEGs, the ⊿*AfldpA* strain treated with sLCOs had only one DEG: AFUA_8G06980, a putative GH25 lysozyme **Figure 3.A**. We further showed that ⊿*AfldpA* strains did not respond to LCOs by demonstrating that the top ten DEGs from LCO-treated wild-type did not change expression in sLCO-treated ⊿*AfldpA* strains **Figure 3.B**.

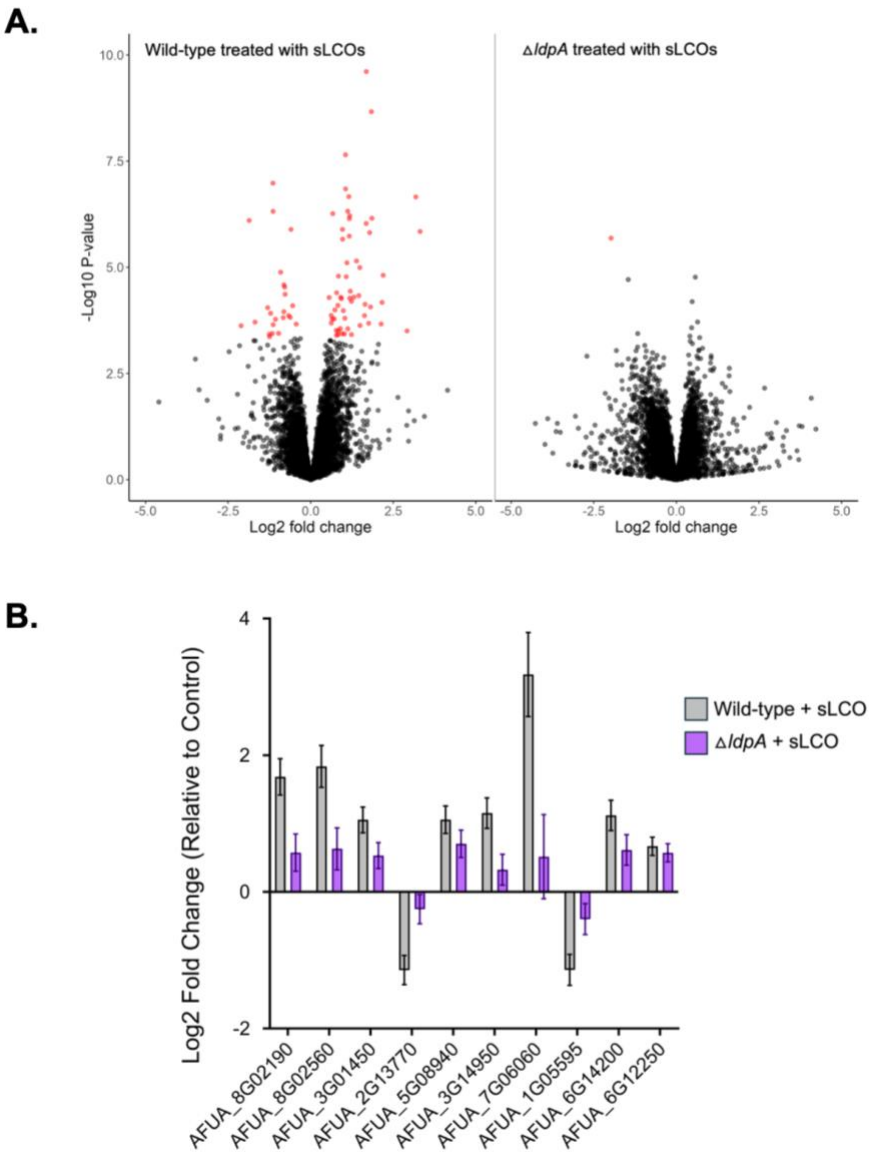

Figure 3. Transcriptomic analysis of *⊿AfldpA* mutant treated with LCOs. A) Volcano plots of wild-type *A. fumigatus* (left) or *⊿AfldpA (*right*)* treated with LCOs. The Y-axis represents -Log10 P-value, and the X-axis represents the Log2 fold change. Red dots represent differentially expressed genes, while black dots are not significant. B) Expression levels of the top 10 differentially expressed genes after we treated Wild-type *A. fumigatus* strain with LCOs (relative to negative control). Grey bars (left) represent the log2 fold change of the gene in the wild-type strain, and the purple (right) represents

the log2 fold change of the gene in ⊿*AfldpA* treated with LCOs; All are non-significant. Significant genes have an adjusted p-value < 0.05 and abs(log2 Fold Change) >= 1.

LysM effectors are found throughout the fungal kingdom

While previous studies have looked at the presence of LysM domain-containing proteins across fungi, we sought to expand upon this work by looking at a larger set of fungi and focusing on LysM effectors. We searched 3077 publicly available fungal genomes, which span different phyla, for the presence of LysM effectors.

We find that these effectors are present in most fungi. Generally, LysM effectors comprise half of the fungal proteins containing LysM domains, with the other half containing either catalytic domains and/or lacking signal peptides. Interestingly, there are some fungi where the LysM effectors tend to make up most of LysM-containing proteins and seem to be common in Mucoromycota. This could perhaps be due to the phylum containing arbuscular mycorrhizal fungi like *Rhizophagus irregularis*, whose LysM effector can bind LCOs (32, 55).

The number of predicted LysM effectors in a fungus ranges from 1 effector up to 29 effectors, as seen in the ascomycete *Drepanopeziza brunnea* from the class Leotiomycetes. *D. brunnea* is a plant pathogen causing leaf spot disease in poplar trees (56). There are, however, fungi throughout the fungal kingdom that have low numbers of LysM-containing proteins and no predicted LysM effectors. A strain of *Candida albicans* and *Ustilago maydis,* seven strains of *Cryptococcus neoformans*, and, surprisingly, five strains of *Rhizophagus irregularis* lack LysM effectors.

While these predictions must be characterized and verified, it provides evidence that LysM effectors are found throughout the fungal kingdom and could, therefore, feasibly act as LCO receptors in fungi.

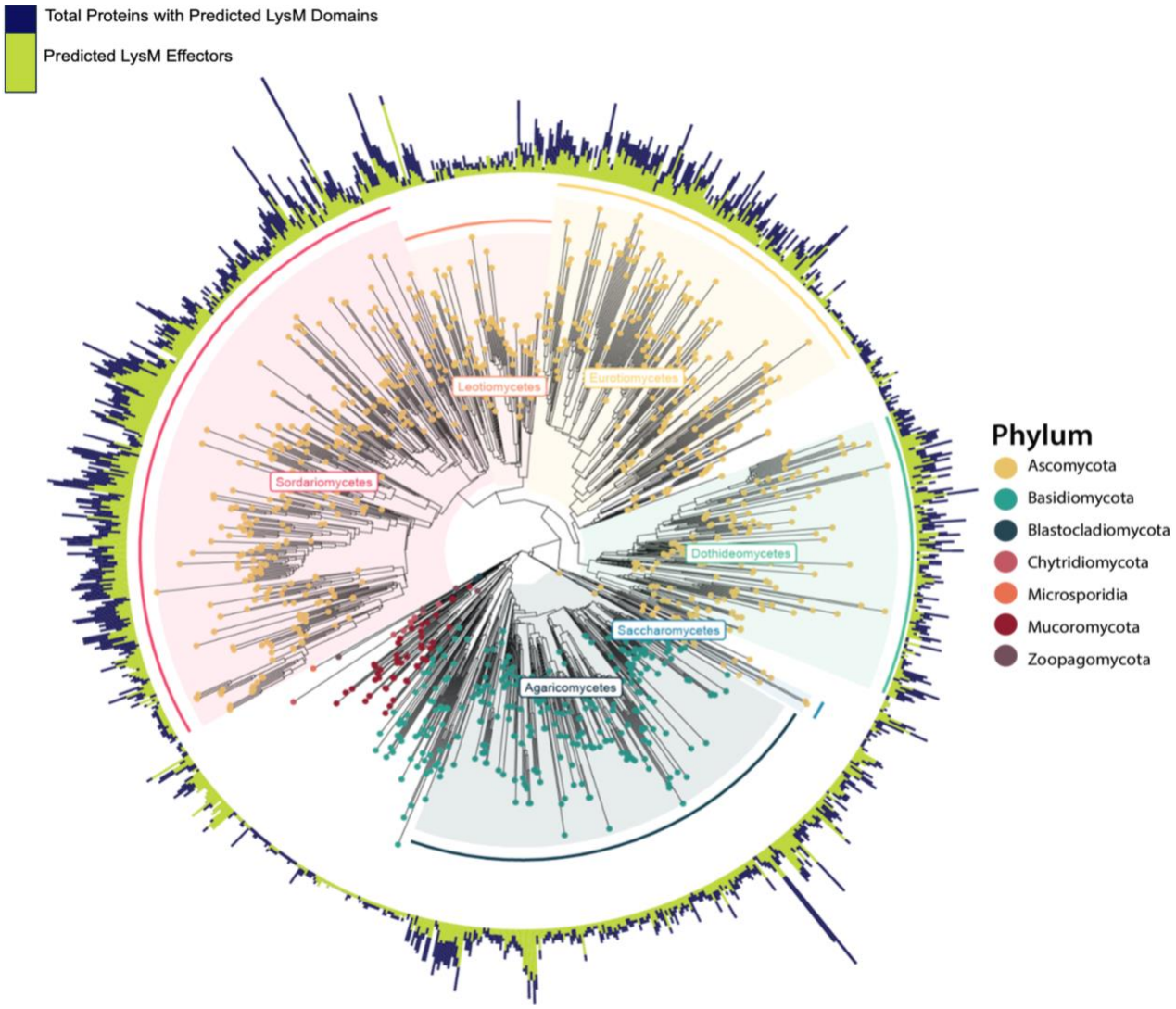

Figure 4. Distribution of LysM effectors in fungi. Bars in the outer ring depicts the # of LysM effectors (Green) versus the total # of proteins with predicted LysM domains (Purple) in a species. Tree nodes are colored according to phyla. Tree is also labeled in the inner ring by the major class and colored accordingly.

Discussion

Research surrounding LysM effectors has primarily focused on its roles in the fungus' interactions with plants (25). Here, we demonstrated that fungal responses to LCOs require LysM effectors. Specifically, deletion of the LysM effector *AfldpA* in the human pathogen *A. fumigatus* no longer exhibited a reduction in secondary branching or change in transcription when treated with sLCOs.

The importance of LysM effectors was alluded to by expression analysis of *A. fumigatus* treated with various chitin molecules: sLCO, nsLCO, CO4, and CO8. sLCO, nsLCO, and CO4 downregulated the expression of *AfldpA*. Interestingly, sLCO also upregulated the expression of *AfldpB*, possibly signifying that it could also be necessary for chitin signaling, but our branching assay didn't capture it. This expression analysis also implies that *A. fumigatus* responds to other chitin molecules besides sLCOs. Still, we have not found the appropriate phenotypes to measure the fungus'' response to these molecules accurately (1).

Furthermore, deleting *AfldpA* resulted in a sizeable transcriptional shift, affecting a wide range of regulatory processes from secondary metabolite synthesis to protein refolding. Previous work characterized LysM effectors but found no effects on radial growth, chitin content, and pathogenicity. While we also saw no noticeable changes to radial morphology, our findings expand on this work to show that there are consequences to deleting these effectors: a shift in the level of secondary branching, response to LCOs, and alteration of the transcriptome (33). This provides compelling evidence that *AfldpA* alters the development of *A. fumigatus*, thus implying that LysM

effectors play roles beyond interactions with plants, as previous studies with other fungi have shown (25).

While our work adds the LysM effector *AfldpA* to the LCO response pathway, it does not yet prove that this effector acts as an LCO receptor. Our next step is to conduct structure characterization and binding assays between *AfldpA* and chitin oligomers. Future directions will focus on how effectors relay information back into the cell; GRAsp previously implicated the two-component system and the MAP kinase pathway as part of the LCO response pathway. These pathways are upstream of *Af*AtfA, so *Af*LdpA could interact with members of the two-component pathway, like histidine kinases, located on the cell membrane to activate LCO signaling (57).

Supplementary Data

Chapter 3: Expanding the Role of LysM Effectors in Fungi: AfldpA from the human pathogen Aspergillus fumigatus is required for responses to Lipochitooligosaccharides

Table of Contents

Supplementary Table S1. Fungal strains used in this study

Organism	Strain Name	Background	Genotype	Reference
A. fumigatus	WT AF293	AF293	Clinical Isolate	Brookman & Denning 2000 (58)
A. fumigatus	WT AFS35	AFS35	ΔakuA::loxP	Wagener et al. 2008 (59)
A. fumigatus	Δ*AfldpA*	AFS35	Δ*AfldpA*::*hph*, Δ*aku*::*loxP*	Muraosa et al. 2019 (33)
A. fumigatus	Δ*AfldpB*	AFS35	Δ*AfldpB*::*hph*, Δ*aku*::*loxP*	Muraosa et al. 2019 (33)
A. fumigatus	Δ*AfldpA/B*	AFS35	Δ*AfldpA*::*ptrA*, Δ*AfldpB*::*hph*, Δ*aku*::*loxP*	Muraosa et al. 2019 (33)

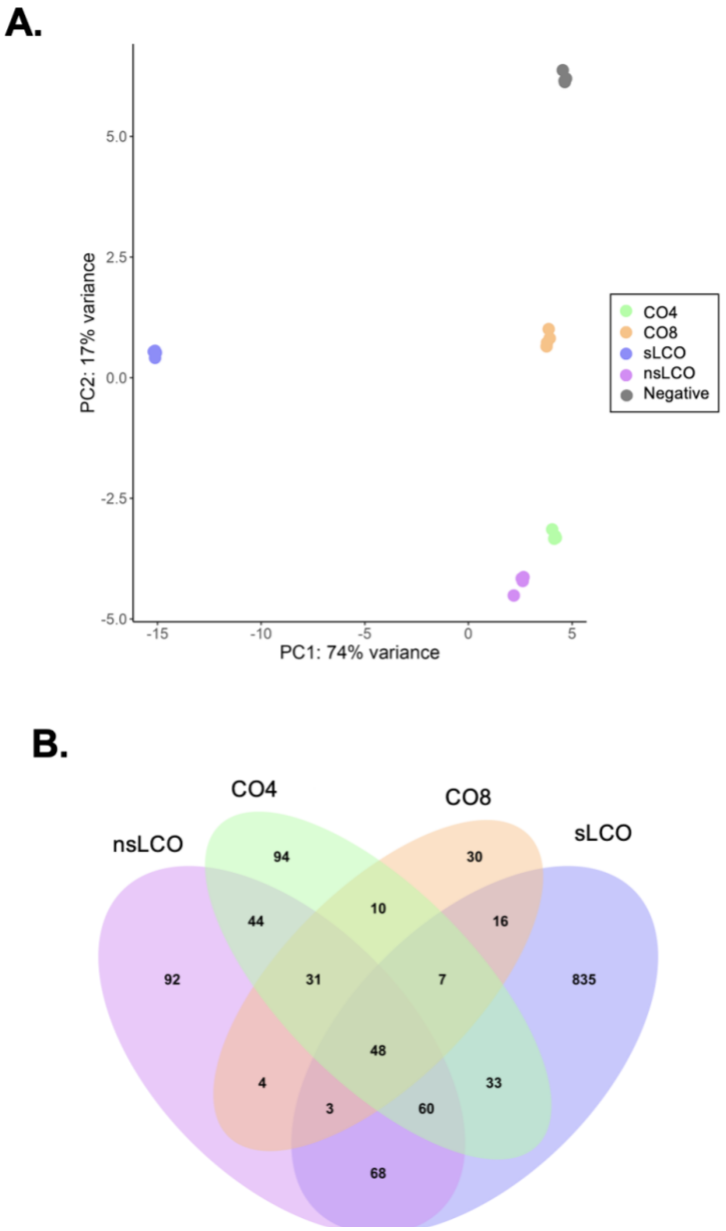

Supplementary figure S1. Transcriptomic analysis of *A. fumigatus* treated with chitin molecules. Principal Component Analysis (PCA) plot visualizes normalized expression variance of the four biological replicates of the *A. fumigatus* AF293 wild-type strain treated with sulfated LCOs (sLCO), non-sulfated LCOs, CO4, CO8, and negative control. Percentages correspond to the amount of variance that each of the two components contributes to. B) Venn diagram depicting the number of shared and unique genes across conditions.

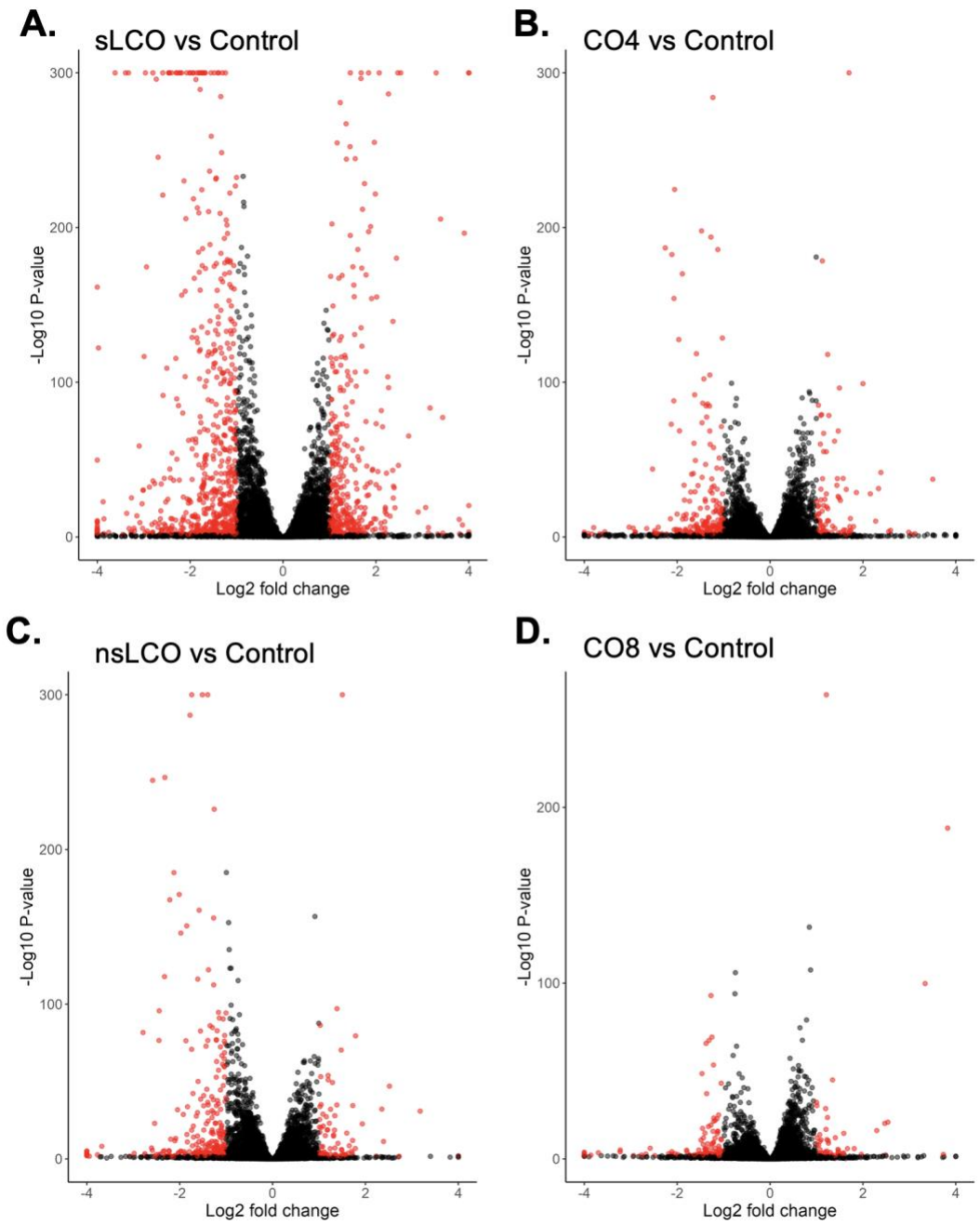

Supplementary figure S2. Volcano plots of *A. fumigatus* treated with chitin-derived molecules. Volcano plot of gene expression in the *A. fumigatus* AF293 wild-type strain treated with A) sulfated LCOs, B) CO4, C) non-sulfated LCOs, or D) CO8. The Y-axis represents -Log10 P-value and the X-axis represents the Log2 fold change. Red dots represent differentially expressed genes (DEGs), while black dots are not significant.

A. sLCO

Module	Gene List Enrichment P-value	Top Module GO term	Top Module Regulator
4569	0	sulfate assimilation	AFUA_5G14390
5396	4.6805944697878E-10	pseurotin A biosynthetic process	lreA_nca
5058	0.000456818470782355	NA	AFUA_8G05460
4698	0.0014429122403663 4	secondary metabolite biosynthetic process	
5379	0.00477698632032952	nitrogen utilization	AFUA_3G08050
4952	0.0079560394747021	secondary metabolite biosynthetic process	
5063	0.011384636262617	protein refolding	Gem1
4901	0.0126883405896611	siderophore-dependent iron import into cell	sidG
5349	0.0236122974918253	gliotoxin biosynthetic process	AFUA_3G11990_nca
5120	0.0255955360764857	NA	AFUA_6G12130

B. CO4

Module	Gene List Enrichment P-value	Top Module GO term	Top Module Regulator
4645	0.0000092197960038322	helvolic acid biosynthetic process	skn7_nca
5116	0.00446567258555199	reactive oxygen species metabolic process	rosA
5414	0.0128049588119416	secondary metabolite biosynthetic process	AFUA_5G09740_nca
5195	0.0187499492902501	NA	AFUA_2G17895
5150	0.0466668133334087	anatomical structure formation involved in morphogenesis	AFUA_4G12410_nca
5224	0.0508016107455682	transmembrane transport	AFUA_5G00290
4900	0.0508016107455682	NA	AFUA_1G00630
5059	0.0898044813080208	galactosaminogalactan biosynthetic process	medA
5494	0.0991932582008427	NA	
4803	0.1743827207573	terpenoid biosynthetic process	AFUA_7G04340_nca

C. nsLCO

Module	Gene List Enrichment P-value	Top Module GO term	Top Module Regulator
4645	1.408410877415 31E-11	helvolic acid biosynthetic process	skn7_nca
5124	0.00138111895607652	NA	atfA_nca
5367	0.0016273366544132	NA	AFUA_4G05980
5116	0.00646978808387783	reactive oxygen species metabolic process	rosA
5349	0.0441171030118655	gliotoxin biosynthetic process	AFUA_3G11990_nca
5059	0.121146294567071	galactosaminogalactan biosynthetic process	medA
5380	0.184849379452452	secondary metabolite biosynthetic process	nsdD_nca
4937	0.205169969558668	NA	nopA
5208	0.467871884021473	tyrosine catabolic process	AFUA_2G04262
4800	0.467871884021473	NA	AFUA_6G07010

D. CO8

Module	Gene List Enrichment P-value	Top Module GO term	Top Module Regulator
4645	9.81336951273906E-07	helvolic acid biosynthetic process	skn7_nca
4803	0.000294365786719906	terpenoid biosynthetic process	AFUA_7G04340_nca
4826	0.0101751749321633	NA	AFUA_6G11930
5354	0.279943761622421	isoprenoid biosynthetic process	AFUA_4G06880
5224	0.348554447820499	transmembrane transport	AFUA_5G00290
5349	0.364206228253147	gliotoxin biosynthetic process	AFUA_3G11990_nca
5408	0.497888128842018	polysaccharide catabolic process	AFUA_5G02800_nca
5494	0.517744084264667	NA	NA
5059	0.658158602087937	galactosaminogalactan biosynthetic process	medA
5380	0.846479725231926	secondary metabolite biosynthetic process	nsdD_nca

Supplementary figure S3. GRAsp modules enriched in DEGs of *A. fumigatus* AF293 wild-type strain treated with chitin molecules. Treatments are A) sulfated LCOs, B) CO4, C) non-sulfated LCOs, or D) CO8. Gene List Enrichment P-Value refers to the probability that the DEGs found in the corresponding module rather than anywhere else in the network. Top regulators ending in "_NCA" are predicted regulators inferred GRAsp's Transcription factor activity feature that takes into transcription factor-target gene binding motifs. DEGs have an adjusted p-value < 0.05 and abs(log2 Fold Change) >= 1.

A.

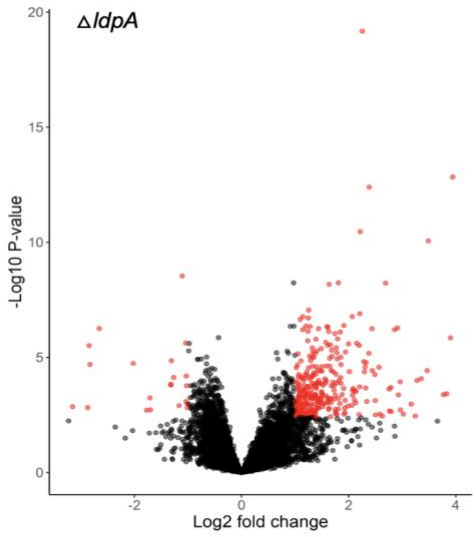

B.

Module	Gene List Enrichment P-value	Top Module GO term	Top Module Regulator
5465	1.27087707830825E-14	NA	atfA_nca
5461	8.46646274155449E-13	mRNA modification	noc4
5063	8.28481037605338E-09	protein refolding	Gem1
5380	0.0141442280262642	secondary metabolite biosynthetic process	nsdD_nca
5520	0.0308128895292237	long-chain fatty acid biosynthetic process	AFUA_2G13380
5080	0.113283052622132	NA	AFUA_4G00660
5120	0.170941886420156	NA	AFUA_6G12130
4954	0.267020854365615	NA	zfpA
5353	0.953358844568378	membrane lipid metabolic process	AFUA_3G05760
5395	0.97812894379196	reactive nitrogen species metabolic proces	AFUA_6G02180

Supplementary figure S4. Transcriptomic analysis of *⊿AfldpA* mutant compared to the wild-type strain. A) Volcano plot of gene expression in the *⊿AfldpA* strain compared to *A. fumigatus* AFS35 wild-type strain. The Y-axis represents -Log10 P-value, and X- axis represents the Log2 fold change. Red dots represent differentially expressed genes (DEGs), while black dots are not significant. B) Table of GRAsp modules enriched in DEGs of *⊿AfldpA* strain compared to AFS35 wild-type. Gene List Enrichment P-Value refers to the probability that the DEGs are found in the corresponding module rather than anywhere else in the network. Top regulators ending in "_NCA" are predicted regulators inferred GRAsp's Transcription factor activity feature that takes into transcription factor-target gene binding motifs. DEGs have an adjusted p-value < 0.05 and abs(log2 Fold Change) >= 1.

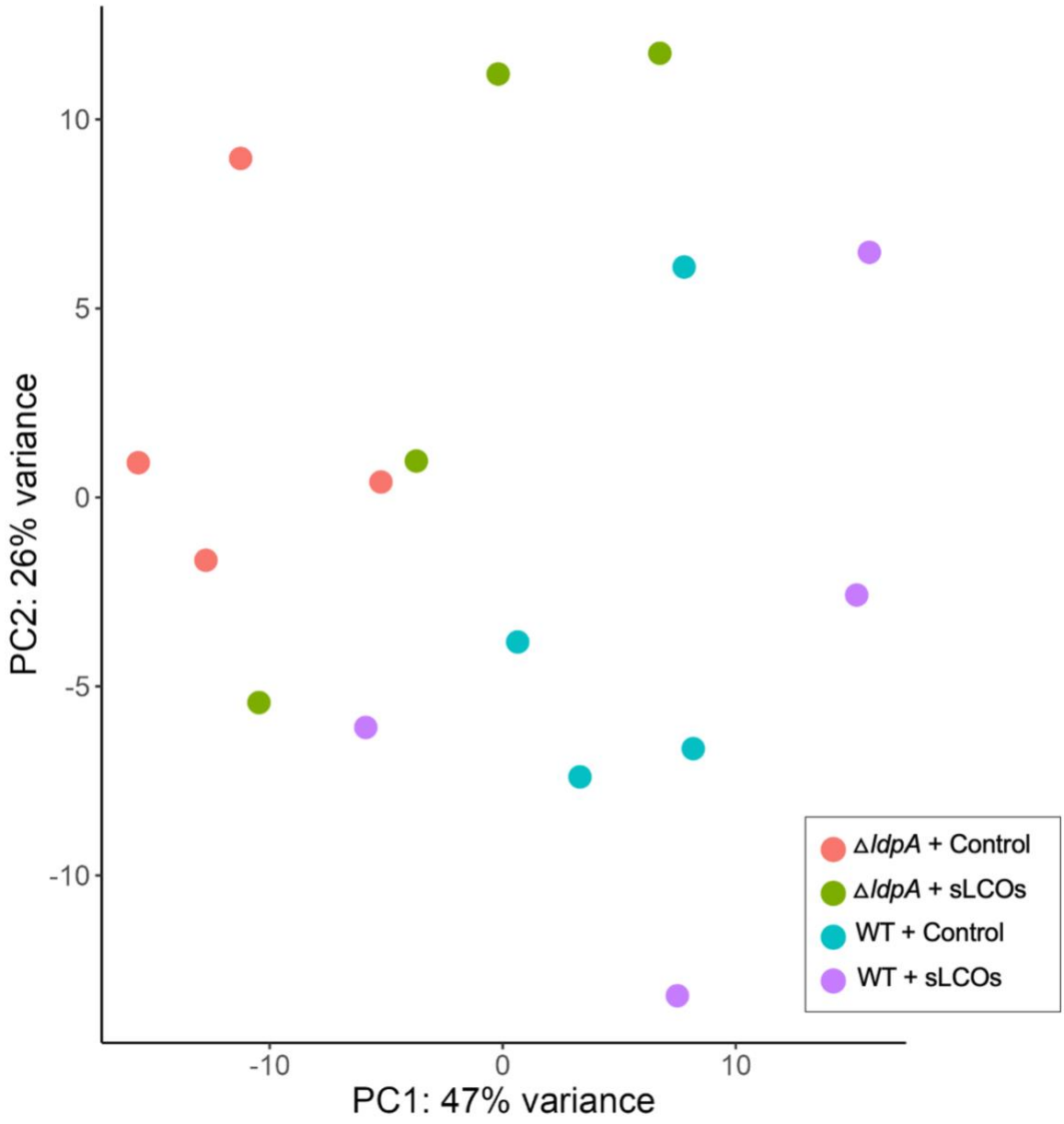

Supplementary figure S5. PCA of *A. fumigatus* wild-type and *⊿AfldpA* treated with sLCOs or negative control. Principal Component Analysis (PCA) plot visualizes normalized expression variance of the four biological replicates of two strains, *A. fumigatus* AFS35 wild-type strain (WT) or *⊿AfldpA* (referred to as *⊿ldpA*) treated with sulfated LCO (sLCOs) or negative control. Percentages correspond to the amount of variance contributed by each of the two components.

References

1. Rush,T.A., Puech-Pagès,V., Bascaules,A., Jargeat,P., Maillet,F., Haouy,A., Maës,A.Q., Carriel,C.C., Khokhani,D., Keller-Pearson,M., *et al.* (2020) Lipo-chitooligosaccharides as regulatory signals of fungal growth and development. *Nat. Commun.*, **11**, 3897.

2. Khokhani,D., Carrera Carriel,C., Vayla,S., Irving,T.B., Stonoha-Arther,C., Keller,N.P. and Ané,J.-M. (2021) Deciphering the Chitin Code in Plant Symbiosis, Defense, and Microbial Networks. *Annu. Rev. Microbiol.*, **75**, 583–607.

3. Poinsot,V., Crook,M.B., Erdn,S., Maillet,F., Bascaules,A. and Ané,J.-M. (2016) New insights into Nod factor biosynthesis: Analyses of chitooligomers and lipo-chitooligomers of Rhizobium sp. IRBG74 mutants. *Carbohydr. Res.*, **434**, 83–93.

4. Gough,C. and Cullimore,J. (2011) Lipo-chitooligosaccharide signaling in endosymbiotic plant-microbe interactions. *Mol. Plant. Microbe. Interact.*, **24**, 867–878.

5. Lerouge,P., Roche,P., Faucher,C., Maillet,F., Truchet,G., Promé,J.C. and Dénarié,J. (1990) Symbiotic host-specificity of Rhizobium meliloti is determined by a sulphated and acylated glucosamine oligosaccharide signal. *Nature*, **344**, 781–784.

6. Krönauer,C. and Radutoiu,S. (2021) Understanding Nod factor signalling paves the way for targeted engineering in legumes and non-legumes. *Curr. Opin. Plant Biol.*, **62**, 102026.

7. Maillet,F., Poinsot,V., André,O., Puech-Pagès,V., Haouy,A., Gueunier,M., Cromer,L., Giraudet,D., Formey,D., Niebel,A., *et al.* (2011) Fungal lipochitooligosaccharide symbiotic signals in arbuscular mycorrhiza. *Nature*, **469**, 58–63.

8. Cope,K.R., Bascaules,A., Irving,T.B., Venkateshwaran,M., Maeda,J., Garcia,K., Rush,T.A., Ma,C., Labbé,J., Jawdy,S., *et al.* (2019) The Ectomycorrhizal Fungus Laccaria bicolor Produces Lipochitooligosaccharides and Uses the Common Symbiosis Pathway to Colonize Populus Roots. *Plant Cell*, **31**, 2386–2410.

9. Camps,C., Jardinaud,M.-F., Rengel,D., Carrère,S., Hervé,C., Debellé,F., Gamas,P., Bensmihen,S. and Gough,C. (2015) Combined genetic and transcriptomic analysis reveals three major signalling pathways activated by Myc-LCOs in Medicago truncatula. *New Phytol.*, **208**, 224–240.

10. Villalobos Solis,M.I., Engle,N.L., Spangler,M.K., Cottaz,S., Fort,S., Maeda,J., Ané,J.-M., Tschaplinski,T.J., Labbé,J.L., Hettich,R.L., *et al.* (2022) Expanding the

Biological Role of Lipo-Chitooligosaccharides and Chitooligosaccharides in Laccaria bicolor Growth and Development. *Front Fungal Biol*, **3**, 808578.

11. Bozsoki,Z., Gysel,K., Hansen,S.B., Lironi,D., Krönauer,C., Feng,F., de Jong,N., Vinther,M., Kamble,M., Thygesen,M.B., *et al.* (2020) Ligand-recognizing motifs in plant LysM receptors are major determinants of specificity. *Science*, **369**, 663–670.

12. Horváth,B., Yeun,L.H., Domonkos,A., Halász,G., Gobbato,E., Ayaydin,F., Miró,K., Hirsch,S., Sun,J., Tadege,M., *et al.* (2011) Medicago truncatula IPD3 is a member of the common symbiotic signaling pathway required for rhizobial and mycorrhizal symbioses. *Mol. Plant. Microbe. Interact.*, **24**, 1345–1358.

13. Oldroyd,G.E.D. (2013) Speak, friend, and enter: signalling systems that promote beneficial symbiotic associations in plants. *Nat. Rev. Microbiol.*, **11**, 252–263.

14. Hu,S.-P., Li,J.-J., Dhar,N., Li,J.-P., Chen,J.-Y., Jian,W., Dai,X.-F. and Yang,X.-Y. (2021) Lysin Motif (LysM) Proteins: Interlinking Manipulation of Plant Immunity and Fungi. *Int. J. Mol. Sci.*, **22**.

15. Yu,H., Bai,F., Ji,C., Fan,Z., Luo,J., Ouyang,B., Deng,X., Xiao,S., Bisseling,T., Limpens,E., *et al.* (2023) Plant lysin motif extracellular proteins are required for arbuscular mycorrhizal symbiosis. *Proc. Natl. Acad. Sci. U. S. A.*, **120**, e2301884120.

16. Tian,L., Hao,Y.-M., Guo,R., Guo,H.-R., Cheng,J.-F., Liu,T.-R., Liu,H., Lu,G. and Wang,B. (2024) Two lysin motif extracellular (LysMe) proteins are deployed in rice to facilitate arbuscular mycorrhizal symbiosis. *New Phytol.*, 10.1111/nph.19873.

17. Oguiza,J.A. (2022) LysM proteins in mammalian fungal pathogens. *Fungal Biol. Rev.*, **40**, 114–122.

18. Buist,G., Steen,A., Kok,J. and Kuipers,O.P. (2008) LysM, a widely distributed protein motif for binding to (peptido)glycans. *Mol. Microbiol.*, **68**, 838–847.

19. Sánchez-Vallet,A., Saleem-Batcha,R., Kombrink,A., Hansen,G., Valkenburg,D.-J., Thomma,B.P.H.J. and Mesters,J.R. (2013) Fungal effector Ecp6 outcompetes host immune receptor for chitin binding through intrachain LysM dimerization. *Elife*, **2**, e00790.

20. Sánchez-Vallet,A., Tian,H., Rodriguez-Moreno,L., Valkenburg,D.-J., Saleem-Batcha,R., Wawra,S., Kombrink,A., Verhage,L., de Jonge,R., van Esse,H.P., *et al.* (2020) A secreted LysM effector protects fungal hyphae through chitin-dependent homodimer polymerization. *PLoS Pathog.*, **16**, e1008652.

21. Tian,H., MacKenzie,C.I., Rodriguez-Moreno,L., van den Berg,G.C.M., Chen,H., Rudd,J.J., Mesters,J.R. and Thomma,B.P.H.J. (2021) Three LysM effectors of

Zymoseptoria tritici collectively disarm chitin-triggered plant immunity. *Mol. Plant Pathol.*, **22**, 683–693.

22. Mentlak,T.A., Kombrink,A., Shinya,T., Ryder,L.S., Otomo,I., Saitoh,H., Terauchi,R., Nishizawa,Y., Shibuya,N., Thomma,B.P.H.J., *et al.* (2012) Effector-mediated suppression of chitin-triggered immunity by magnaporthe oryzae is necessary for rice blast disease. *Plant Cell*, **24**, 322–335.

23. Kombrink,A., Rovenich,H., Shi-Kunne,X., Rojas-Padilla,E., van den Berg,G.C.M., Domazakis,E., de Jonge,R., Valkenburg,D.-J., Sánchez-Vallet,A., Seidl,M.F., *et al.* (2017) Verticillium dahliae LysM effectors differentially contribute to virulence on plant hosts. *Mol. Plant Pathol.*, **18**, 596–608.

24. Dölfors,F., Holmquist,L., Dixelius,C. and Tzelepis,G. (2019) A LysM effector protein from the basidiomycete Rhizoctonia solani contributes to virulence through suppression of chitin-triggered immunity. *Mol. Genet. Genomics*, **294**, 1211–1218.

25. de Jonge,R. and Thomma,B.P.H.J. (2009) Fungal LysM effectors: extinguishers of host immunity? *Trends Microbiol.*, **17**, 151–157.

26. de Jonge,R., van Esse,H.P., Kombrink,A., Shinya,T., Desaki,Y., Bours,R., van der Krol,S., Shibuya,N., Joosten,M.H.A.J. and Thomma,B.P.H.J. (2010) Conserved fungal LysM effector Ecp6 prevents chitin-triggered immunity in plants. *Science*, **329**, 953–955.

27. Kombrink,A. and Thomma,B.P.H.J. (2013) LysM effectors: secreted proteins supporting fungal life. *PLoS Pathog.*, **9**, e1003769.

28. Tian,H., MacKenzie,C.I., Rodriguez-Moreno,L., van den Berg,G.C.M., Chen,H., Rudd,J.J., Mesters,J.R. and Thomma,B.P.H.J. (2021) Three LysM effectors of Zymoseptoria tritici collectively disarm chitin-triggered plant immunity. *Mol. Plant Pathol.*, **22**, 683–693.

29. Dubey,M., Vélëz,H., Broberg,M., Jensen,D.F. and Karlsson,M. (2020) LysM Proteins Regulate Fungal Development and Contribute to Hyphal Protection and Biocontrol Traits in Clonostachys rosea. *Front. Microbiol.*, **11**, 679.

30. Romero-Contreras,Y.J., Ramírez-Valdespino,C.A., Guzmán-Guzmán,P., Macías-Segoviano,J.I., Villagómez-Castro,J.C. and Olmedo-Monfil,V. (2019) Tal6 From Trichoderma atroviride Is a LysM Effector Involved in Mycoparasitism and Plant Association. *Front. Microbiol.*, **10**, 2231.

31. Cen,K., Li,B., Lu,Y., Zhang,S. and Wang,C. (2017) Divergent LysM effectors contribute to the virulence of Beauveria bassiana by evasion of insect immune defenses. *PLoS Pathog.*, **13**, e1006604.

32. Zeng,T., Rodriguez-Moreno,L., Mansurkhodzaev,A., Wang,P., van den

Berg,W., Gasciolli,V., Cottaz,S., Fort,S., Thomma,B.P.H.J., Bono,J.-J., *et al.* (2020) A lysin motif effector subverts chitin-triggered immunity to facilitate arbuscular mycorrhizal symbiosis. *New Phytol.*, **225**, 448–460.

33. Muraosa,Y., Toyotome,T., Yahiro,M. and Kamei,K. (2019) Characterisation of novel-cell-wall LysM-domain proteins LdpA and LdpB from the human pathogenic fungus Aspergillus fumigatus. *Sci. Rep.*, **9**, 3345.

34. Shimizu,K. and Keller,N.P. (2001) Genetic involvement of a cAMP-dependent protein kinase in a G protein signaling pathway regulating morphological and chemical transitions in Aspergillus nidulans. *Genetics*, **157**, 591–600.

35. Schoen,T.J., Calise,D.G., Bok,J.W., Giese,M.A., Nwagwu,C.D., Zarnowski,R., Andes,D., Huttenlocher,A. and Keller,N.P. (2023) Aspergillus fumigatus transcription factor ZfpA regulates hyphal development and alters susceptibility to antifungals and neutrophil killing during infection. *PLoS Pathog.*, **19**, e1011152.

36. Chen,S. (2023) Ultrafast one-pass FASTQ data preprocessing, quality control, and deduplication using fastp. *Imeta*, **2**.

37. Kim,D., Paggi,J.M., Park,C., Bennett,C. and Salzberg,S.L. (2019) Graph-based genome alignment and genotyping with HISAT2 and HISAT-genotype. *Nat. Biotechnol.*, **37**, 907–915.

38. Danecek,P., Bonfield,J.K., Liddle,J., Marshall,J., Ohan,V., Pollard,M.O., Whitwham,A., Keane,T., McCarthy,S.A., Davies,R.M., *et al.* (2021) Twelve years of SAMtools and BCFtools. *Gigascience*, **10**.

39. Liao,Y., Smyth,G.K. and Shi,W. (2014) featureCounts: an efficient general purpose program for assigning sequence reads to genomic features. *Bioinformatics*, **30**, 923–930.

40. Love,M.I., Huber,W. and Anders,S. (2014) Moderated estimation of fold change and dispersion for RNA-seq data with DESeq2. *Genome Biol.*, **15**, 550.

41. Mirarab,S., Reaz,R., Bayzid,M.S., Zimmermann,T., Swenson,M.S. and Warnow,T. (2014) ASTRAL: genome-scale coalescent-based species tree estimation. *Bioinformatics*, **30**, i541–8.

42. Zhang,C., Rabiee,M., Sayyari,E. and Mirarab,S. (2018) ASTRAL-III: polynomial time species tree reconstruction from partially resolved gene trees. *BMC Bioinformatics*, **19**, 153.

43. Manni,M., Berkeley,M.R., Seppey,M., Simão,F.A. and Zdobnov,E.M. (2021) BUSCO Update: Novel and Streamlined Workflows along with Broader and Deeper Phylogenetic Coverage for Scoring of Eukaryotic, Prokaryotic, and Viral Genomes. *Mol. Biol. Evol.*, **38**, 4647–4654.

44. Katoh,K. and Standley,D.M. (2013) MAFFT multiple sequence alignment software version 7: improvements in performance and usability. *Mol. Biol. Evol.*, **30**, 772–780.

45. Capella-Gutiérrez,S., Silla-Martínez,J.M. and Gabaldón,T. (2009) trimAl: a tool for automated alignment trimming in large-scale phylogenetic analyses. *Bioinformatics*, **25**, 1972–1973.

46. Nguyen,L.-T., Schmidt,H.A., von Haeseler,A. and Minh,B.Q. (2015) IQ-TREE: a fast and effective stochastic algorithm for estimating maximum-likelihood phylogenies. *Mol. Biol. Evol.*, **32**, 268–274.

47. Kalyaanamoorthy,S., Minh,B.Q., Wong,T.K.F., von Haeseler,A. and Jermiin,L.S. (2017) ModelFinder: fast model selection for accurate phylogenetic estimates. *Nat. Methods*, **14**, 587–589.

48. Li,Y., Steenwyk,J.L., Chang,Y., Wang,Y., James,T.Y., Stajich,J.E., Spatafora,J.W., Groenewald,M., Dunn,C.W., Hittinger,C.T., *et al.* (2021) A genome-scale phylogeny of the kingdom Fungi. *Curr. Biol.*, **31**, 1653–1665.e5.

49. Paradis,E., Claude,J. and Strimmer,K. (2004) APE: Analyses of Phylogenetics and Evolution in R language. *Bioinformatics*, **20**, 289–290.

50. Yu,G., Smith,D.K., Zhu,H., Guan,Y. and Lam,T.T.-Y. (2017) Ggtree: An r package for visualization and annotation of phylogenetic trees with their covariates and other associated data. *Methods Ecol. Evol.*, **8**, 28–36.

51. Wickham,H. ggplot2 Springer New York.

52. Potter,S.C., Luciani,A., Eddy,S.R., Park,Y., Lopez,R. and Finn,R.D. (2018) HMMER web server: 2018 update. *Nucleic Acids Res.*, **46**, W200–W204.

53. El-Gebali,S., Mistry,J., Bateman,A., Eddy,S.R., Luciani,A., Potter,S.C., Qureshi,M., Richardson,L.J., Salazar,G.A., Smart,A., *et al.* (2019) The Pfam protein families database in 2019. *Nucleic Acids Res.*, **47**, D427–D432.

54. Hallgren,J., Tsirigos,K.D., Pedersen,M.D., Armenteros,J.J.A., Marcatili,P., Nielsen,H., Krogh,A. and Winther,O. (2022) DeepTMHMM predicts alpha and beta transmembrane proteins using deep neural networks. *bioRxiv*, 10.1101/2022.04.08.487609.

55. Howard,N., Pressel,S., Kaye,R.S., Daniell,T.J. and Field,K.J. (2022) The potential role of Mucoromycotina ‘fine root endophytes’ in plant nitrogen nutrition. *Physiol. Plant.*, **174**, e13715.

56. Spiers,A.G. and Hopcroft,D.H. (1998) Morphology of Drepanopeziza species pathogenic to poplars. *Mycol. Res.*, **102**, 1025–1037.

57. Hagiwara,D., Suzuki,S., Kamei,K., Gonoi,T. and Kawamoto,S. (2014) The role of AtfA and HOG MAPK pathway in stress tolerance in conidia of Aspergillus fumigatus. *Fungal Genet. Biol.*, **73**, 138–149.

58. Brookman,J.L. and Denning,D.W. (2000) Molecular genetics in Aspergillus fumigatus. *Curr. Opin. Microbiol.*, **3**, 468–474.

59. Wagener,J., Echtenacher,B., Rohde,M., Kotz,A., Krappmann,S., Heesemann,J. and Ebel,F. (2008) The putative alpha-1,2-mannosyltransferase AfMnt1 of the opportunistic fungal pathogen Aspergillus fumigatus is required for cell wall stability and full virulence. *Eukaryot. Cell*, **7**, 1661–1673.

Chapter 4: Discussion

Summary

The groundbreaking discovery that organisms throughout the fungal kingdom produce LCOs, which once were believed to be secreted solely by symbiotic microbes to initiate symbiosis with plant hosts, has caused a paradigm shift in our understanding of chitin signaling (1–3). This revelation unveils a new dimension of these molecules, demonstrating their potential to significantly alter the growth and development of fungi, from human pathogenic to ectomycorrhizal fungi.

The standing hypothesis states that LCOs function as autocrine and paracrine signaling molecules in fungi that can also modulate interspecies interactions (2). To implicate LCOs in these roles, we must first understand the genetic underpinnings of LCO signaling. Once we set this groundwork, we can use our knowledge to explore how LCOs affect the ecology of fungi (2, 4–6).

We set out to explore the genetics of how fungi respond to LCOs. While expression analysis of fungi responding to LCOs exists, the genetic determinants have not been characterized and validated (2). We used the ascomycete *A. fumigatus* as our primary model organism. While this fungus might not seem like an ideal model considering its status as a human pathogen, we chose this fungus for three primary reasons: 1) *A. fumigatus* can both synthesize and respond to LCOs, 2) physiological assays can determine if the fungus responds to LCOs and 3) the fungus is a genetically tractable organism with decades of research dedicated to it (2, 7, 8).

The first part of my thesis discusses how we found one of the genetic components required for *A. fumigatus* response to LCO: *Af*AtfA, a transcription factor involved in the stress tolerance of conidia. We found this component by predicting a genome-wide regulatory gene network and asking which regulators are most affected by *A. fumigatus* treated with LCOs.

Specifically, we used the MERLIN program to reconstruct a regulatory network (9). This program requires two main parameters: expression datasets of the organism of interest in various conditions and prior knowledge of regulators. We inferred a network using eighteen RNAseq datasets of *A. fumigatus* in multiple conditions and 820 regulators (9). Our network, called GRAsp (**G**ene **R**egulation of ***Asp****ergillus fumigatus),* contained 7,422 regulatory edges, or connections. Our network implicated *AfatfA* as a transcription factor-encoding gene predicted to regulate most differentially expressed genes when *A. fumigatus* received LCO treatment. We hypothesized that this regulator, previously implicated in conidial stress tolerance, was important for LCO response (10, 11). We supported this hypothesis by showing that a deletion mutant of *AfatfA* no longer exhibited a physiologic response to LCOs (2). Thus, we can claim that we found fungi's first regulator of LCO-response. However, our work in this chapter went beyond LCOs; we demonstrated the predictive power of GRAsp by showing that it could recapitulate known pathways in *A. fumigatus* and uncover a novel regulator of gliotoxin, a toxic metabolite (12, 13). This chapter ends with unveiling an online resource (grasp.wid.wisc.edu) allowing users to explore the network using their genes of interest.

Our next chapter focused on uncovering the LCO receptor in fungi. We concentrate on fungal proteins containing LysM domains since plants recognize LCOs

and COs using LysM-domain-containing receptors (14, 15). While *A. fumigatus* contained no transmembrane proteins with LysM domains, it did have these domains in effectors and chitinases (16). LysM effectors, secreted proteins with LysM domains and no catalytic activity, have acquired scientific interest in the last decade due to their role as virulence factors in host-fungi associations. Fungi employ these effectors to sequester their chitin molecules and avoid detection by host organisms (16–28). Without detection, the plant is less likely to initiate an immune response, increasing the likelihood of fungal colonization. Interestingly, these effectors also protect fungi from plant chitinases, though researchers have yet to describe this mechanism fully (14, 25–29).

Zeng et al. 2020 supported our hypothesis that the LysM effector can act as an LCO receptor (14). The group characterized RiSLM, a LysM effector from the mycorrhizal fungus, and asserted its role in promoting symbiosis by sequestering immunogenic long-chain COs. When testing the binding affinity of RiSLM to different chitin molecules, they found that the effector could bind sLCO and nsLCO molecules; this is, to our knowledge, the first reported instance of a LysM effector binding LCO molecule (14). Since this work was published before Rush *et al.,* 2020 discovered that LCOs were widespread among fungi, this work did not look further into RiSLM's role as a LysM receptor involved in LCO response (2).

We, thus, decided to pursue the two LysM effectors in *A. fumigatus, AfldpA, and AfldpB,* and ask if they're involved in LCO signaling (30). Muraosa et al. 2019 previously characterized the role of these proteins in *A. fumigatus* but found no changes to radial growth, chitin content, and pathogenicity (30). Interestingly, we found that sLCO,

nsLCO, and CO4 significantly reduced the expression of *AfldpA* and that sLCO upregulated the expression of *AfldpB*.

Excitingly, we found that the *AfldpA* deletion strain no longer exhibited a physiological response to LCOs, indicating the crucial role of *AfldpA* in a fungus' response to LCOs (30). This discovery, coupled with the fact that the transcriptome of a wild-type *A. fumigatus* undergoes global changes while the transcriptome of the *AfldpA* deletion mutant remains unchanged when challenged with LCOs, provides more compelling evidence of *AfldpA's* significance in LCO response. We are currently conducting binding assays between *Af*LdpA and chitin molecules to determine if this effector acts as an LCO receptor in *A. fumigatus.*

This work marks the initial strides in unraveling the genetic determinants that underlie the complex LCO signaling pathway in fungi. We have identified a transcription factor and a potential receptor crucial for LCO response. However, this is just the beginning. We have yet to fully explore this field's vast potential, and the following sections in this chapter will delve into the exciting future goals and perspectives.

Future directions

GRAsp and the potential to uncover components of the LCO response pathway

The comprehensive regulatory gene network we created helped us identify *AfatfA* as a potential regulator of LCO response, which we further verified in vivo. The diffusion analysis of *A. fumigatus* after treatment with LCOs identified *AfatfA* and nine other regulators that warrant further exploration.

One regulator of interest is the transcription factor ZfpA; previous work implicated this transcription factor in regulating hyphal morphology and the synthesis of 5,8-diHODE, referred to as oxylipins(31, 32). Oxylipins, like LCOs, are fungal signaling molecules altering hyphal branching; while LCOs reduce the number of secondary branches, oxylipins have the opposite effect, increasing the number of branches(31, 32). It would be interesting to see if *zfpA* also regulates LCO-response. One potential experiment would be similar to the one performed in Chapter 2, where we asked if the mutants of *zfpA* lose the ability to respond to LCOs by looking at changes to secondary branching.

Furthermore, GRAsp modules and previous literature provide insight into the direct regulators of *AfatfA*. GRAsp module enrichment of differentially expressed genes in *A. fumigatus* treated with LCOs implicated protein kinases of the high-osmolarity glycerol mitogen-activated protein kinase, HOG MAPK, a critical pathway cascade involved in the fungus' response to environmental cues (10). This prediction is reasonable, considering researchers already found that the HOG MAPK pathway regulates *Af*AtfA (10). While testing the deletion mutants for loss of hypobranching response to LCOs, we could also assay for phosphorylation of protein kinases in response to LCOs by western blotting using antibodies capable of detecting phosphorylated proteins, such as anti-phospho-p44/42 MAPK antibodies (33).

Aside from the HOG MAPK pathway, the MERLIN modules also implicate histidine kinases, members of the two-component system (TCS) (34, 35). This pathway, prevalent across bacteria and fungi, has roles in processing environmental signals through the HOG MAPK pathway (34, 36). Since histidine kinases in the TCS localize to

the cell membrane, their involvement in LCO response would likely make them early responders to exogenous LCOs (37). Similarly to MAP kinases, we can test their role in LCO response by testing phosphorylation with western blots and assaying for hypobranching response. Combining GRAsp's predictions with *in-vivo* validation can serve as a valuable tool for unraveling the LCO-response pathway.

GRAsp and the potential to uncover components of the LCO response pathway.

While we used *A. fumigatus,* a model organism in LCO-signaling research, the fungus has a robust research community dedicated to studying its role in human pathogenesis (8). As mentioned in **Chapter 2**, our regulatory gene network has helped the field uncover novel regulators in secondary metabolite synthesis. Specifically, collaborators discovered *rogA*, a novel negative regulator of the toxic metabolite gliotoxin (13). Knowing that the network can help other scientists, we were motivated to create GRAsp, an easy-to-use online resource. This tool allows researchers to look at their genes or pathways of interest and, ideally, uncover new regulators or targets. Still, GRAsp remains in its infancy, and we are now focusing on enhancing and expanding its capabilities.

While GRAsp could recapitulate known regulatory interaction pathways, we are also interested in quantifying global recapitulation with an unbiased metric. One potential way to confirm the network's reliability is to compare it to a "Gold Standard" network, a reference network that closely mirrors actual biology (9, 38). One major obstacle is that there currently needs to be a wide-scale standard. We seek to create our own Gold Standard using the available CHIP-seq dataset. In *A. fumigatus,* at least

15 publicly available CHiP-seq datasets of unique transcription factors (39–51). Our current objective is to see how well our network compares to this CHIP-seq standard.

As early as next year, we can immediately advance our network by updating it with new expression datasets, which we believe will increase GRAsp's predictive power. While we added most of the publicly available RNAseq datasets as of 2023, many more have been released since then. We are also interested in integrating DNA microarray datasets into GRAsp, having initially focused solely on RNAseq datasets for the practical purpose of only working with one dataset type.

Furthermore, our goal for the online resource was to make it user-friendly. Since its inception, we have continuously made updates that enhance user experience (addition of tooltips, streamlined data entry, visual customization of the output network, etc.). We've recently added an online feedback form to our resource that should allow user feedback. As the resource gains more popularity, we expect new ideas for improved accessibility and new features to make it truly user-friendly.

Finally, we must consider the longevity of GRAsp and our need to "future-proof." The resource is currently hosted through the University of Wisconsin-Madison, which provides a stable hosting environment. Ideally, we'd like to see GRAsp hosted by platforms that keep the resource updated years from now. One potential platform is FungiDB, an online resource for bioinformatic analysis of fungal genes and genomes, which curates data from a wide range of resources. One resource it offers is transcriptomic analysis of expression datasets in various fungi, including *A. fumigatus*. We could, thus, envision platforms like FungiDB hosting our network and enhancing it

with new transcriptomic data. It also allows for inferring regulatory gene networks in other model fungi.

GRAsp and the inference algorithm that created it, MERLIN+P+TFA, are powerful tools in system biology, and we believe that they'll help make future groundbreaking discoveries.

LysM effectors and upstream LCO-signaling

Chapter 3 revealed that LysM effectors were critical for LCO response in *A. fumigatus.* We hypothesize that these proteins have a role as LCO/CO receptors. The immediate next steps are to show that *Af*LdpA *A. fumigatus* can bind chitin molecules.

Muraosa *et al.* 2024 created the *Pichia pastoris* strain that heterologously and reliably expresses *Af*LdpA (30, 52). We aim to purify tagged *Af*LdpA from these strains and conduct binding assays with LCOs and COs via Microscale thermophoresis. This assay, which measures binding affinity by detecting changes in the movement of labeled proteins in response to a temperature gradient, was previously used to demonstrate the binding of LCOs/COs in RiSLM, the LysM effector from *Rhizophagus irregularis (14, 53).*

Follow-up experiments should focus on elucidating the binding structure of LysM effectors and LCOs, possibly using techniques like X-ray crystallography. Since *Af*LdpA has multiple LysM domains, it would be interesting to determine which domains bind LCOs.

Structural analysis could also provide insight into which of the two strategies *Af*LdpA uses for LCO/CO binding: intermolecular dimerization, where two LysM

domains from different LysM effectors bind an LCO molecule, or intramolecular dimerization, where two LysM domains within the same effector bind LCOs (54).

The other LysM effector in *A. fumigatus, AfldpB,* did not seem necessary for sLCO response since the *AfldpB* deletion strain still exhibited hypobranching. However, we noted that sLCOs upregulated the expression *AfldpB*; perhaps this gene still plays a role in LCO response, but branching assays do not capture it. If we observe binding, it would be worth performing binding assays and subsequent structural elucidation. If it does bind, it could further implicate *Af*LdpB in having a role in chitin signaling, and structural analysis could further identify important motifs for LCO binding.

Suppose the binding assays support our hypothesis that LysM effectors are chitin signaling receptors. In that case, it raises a new question: How does a LysM effector relate information to the cell? Most of the research involved in LysM effectors focuses on its role as an extracellular, or cell wall-localized, component that can sequester chitin to prevent host immune signaling; a role as a fungal autocrine and paracrine receptor would be groundbreaking.

Future work should uncover how a LysM effector *Af*LdpA signals information back into the cell. One potential experiment to test if *Af*LdpA interacts with a cell membrane receptor is proximity labeling with TurboID assays (55, 56). With TurboID, we can fuse *Af*LdpA to a biotin ligase, which results in the tagging of interacting proteins with biotin; these biotinylated proteins can then be isolated and identified with mass spectrometry (55, 56). However, if evidence suggests that LCO response requires membrane-localized histidine kinases from the two-component system, it could imply that *Af*LdpA interacts with this kinase. We could take a more direct approach and test

the interaction between the two proteins with a yeast two-hybrid technique (57). This finding would be the first reported fungal effector capable of signaling information back into the organism's cell that synthesized it.

Develop a reporter system to monitor LCO response in A. fumigatus

Our current method of detecting LCO response in *A. fumigatus* relies on physiological assays that are not high-throughput and can only respond to sulfated LCOs. Future work could leverage our RNAseq dataset of *A. fumigatus* treated with LCO and COs to create a fast, high-throughput assay. Specifically, we envision tagging genes upregulated explicitly in response to LCOs and COs with a reporter marker like Enhanced Green-Fluorescent Protein (EGFP). Researchers previously used this reporter marker to visualize the differential expression of a virulence-associated gene under various conditions (58).

A similar strategy for detecting responsiveness to LCOs has been implemented in the legume *Medicago truncatula* using β-glucuronidase (GUS) reporter assay (2, 59). However, we will likely need to make some optimizations: a suitable reporter gene would have little to no expression in untreated samples and visually distinguishable fluorescence in LCO/CO treatments.

If successful, Instead of conducting branching experiments, we could test the fungus' response to LCOs by observing whether or not it fluoresces. Since these LCO/CO RNAseq experiments occur two hours after treatments, the incubation time between treatments and analysis would be much shorter than hyphal branching experiments. Furthermore, since our RNAseq analysis in **Chapter 3** demonstrated that

sulfated LCOs, non-sulfated LCOs, CO4, and CO8 differently expressed their own unique set of differentially expressed genes, there is also a possibility that we can create reporters specific to each molecule.

We could also leverage this reporter strain and forward screens to uncover genes in the LCO-response pathway. Conducting mutagenesis studies of this proposed GFP strain, followed by LCO/CO-induced fluorescent screening, would allow us to find genes required for chitin signaling if this gene is downstream of the GFP-tagged reporter.

Uncovering the genes involved in fungal LCO synthesis

Research into rhizobia, like *Rhizobium* strain IRBG74, reveals three genes required to synthesize an LCO: chitin synthesis, chitin deacetylation, and *N*-acylation. Nitrogen-fixing bacteria largely conserve the genes responsible for these processes (60); *nodC* encodes a chitin synthase that creates a chitin backbone, *nodB* encodes a chitin deacetylase that deacetylates the backbone, and *nodA* encodes an *N*-acyltransferase that attaches the lipid chain to the backbone (4, 59).

A. fumigatus has multiple genes capable of performing these functions; researchers have previously deleted and characterized seven chitin deacetylase genes and eight chitin synthases (5, 61, 62). To uncover genes responsible for the fungal synthesis of LCOs, we could screen these deletion mutants for loss of LCOs. While a hyphal branching assay in *A. fumigatus* or GUS assay in *M. truncatula* can help us detect the presence or absence of LCOs, a GFP-reporter strain in *A. fumigatus* could make this screen efficient and high-throughput (59).

We can further validate the fungal genes involved in LCO synthesis with complementation assays using *nod* genes from *Rhizobium* IRBG74. For example, we provide more evidence that a candidate chitin deacetylase from *A. fumigatus* is involved in LCO synthesis by asking if the gene can rescue LCO synthesis in *nodC* deletion strain from *Rhizobium* IRBG74.

From foundational genetics to fungal behavior

Our discovery of the genetic determinants underlying LCO-signaling opens up new avenues for studying LCO-mediated fungal interactions using our mutants. Exploring LCOs' role in these interactions can provide insight into LCO's role in fungal behavior and potential biotechnological applications.

Our current hypothesis states that LCOs serve as autocrine and paracrine molecules and modulate fungal behavior with other fungi and bacteria. Rush *et al.* 2022 found that treatment of *A. fumigatus* with LCOs altered the fungus' metabolome and, subsequently, its interaction with bacteria (5). We can expand on this work by asking how LCO treatment affects fungal-fungal interactions. These interactions could take the form of cooperative or competitive behaviors. We could examine these interactions by examining the growth of *A. fumigatus* after treatment with the exudates of LCO-treated fungi, similar to the experiment in Rush *et al.* 2022 (5).

We could also leverage our understanding of genes required for LCO response. Considering that the *AfldpA* deletion strain in *A. fumigatus* is non-responsive to LCOs and is, thus, practically "blind" to these molecules, we propose using these strains as a negative control when studying how LCOs modulate fungal behavior and interactions.

Considering that LCOs are secreted molecules, we could also explore LCOs' potential role as a quorum-sensing molecule in *A. fumigatus*. Like quorum sensing in bacteria, fungal quorum sensing modulates fungal behavior in response to population density. Specifically, fungi secrete quorum-sensing molecules until the amount of molecule reaches a certain threshold. Density-dependent processes are activated once the threshold is surpassed (63, 64). We could test if disruption of LCO signaling alters known quorum-sensing phenotypes. A notable density-dependent process in fungi is the conidia-sclerotia shift in the plant pathogen *Aspergillus flavus*; when population density is low, the production of conidia is low, while the production of sclerotia, a mass of vegetative spore, is high. However, conidia development is high at high population densities and low sclerotia development. If we can dissect LCO synthesis and response response pathways in *A. flavus,* we could see if LCO signaling plays a role in these processes. For example, we could ask if these high-density phenotypes are still observed in LCO receptor or synthesis mutants.

The information gained from these studies will advance our understanding of chitin-signaling in fungi and pave the way for biotechnological applications in the medical and agricultural sectors. For the future of our field, we envision pioneering new strategies to manipulate microbial communities, which can help enhance beneficial symbiotic interactions between fungi and their plant hosts while effectively mitigating the growth of dangerous pathogens.

References

1. Feng,F., Sun,J., Radhakrishnan,G.V., Lee,T., Bozsóki,Z., Fort,S., Gavrin,A., Gysel,K., Thygesen,M.B., Andersen,K.R., *et al.* (2019) A combination of chitooligosaccharide and lipochitooligosaccharide recognition promotes arbuscular mycorrhizal associations in Medicago truncatula. *Nat. Commun.*, **10**, 5047.

2. Rush,T.A., Puech-Pagès,V., Bascaules,A., Jargeat,P., Maillet,F., Haouy,A., Maës,A.Q., Carriel,C.C., Khokhani,D., Keller-Pearson,M., *et al.* (2020) Lipo-chitooligosaccharides as regulatory signals of fungal growth and development. *Nat. Commun.*, **11**, 3897.

3. Lerouge,P., Roche,P., Faucher,C., Maillet,F., Truchet,G., Promé,J.C. and Dénarié,J. (1990) Symbiotic host-specificity of Rhizobium meliloti is determined by a sulphated and acylated glucosamine oligosaccharide signal. *Nature*, **344**, 781–784.

4. Khokhani,D., Carrera Carriel,C., Vayla,S., Irving,T.B., Stonoha-Arther,C., Keller,N.P. and Ané,J.-M. (2021) Deciphering the Chitin Code in Plant Symbiosis, Defense, and Microbial Networks. *Annu. Rev. Microbiol.*, **75**, 583–607.

5. Rush,T.A., Tannous,J., Lane,M.J., Gopalakrishnan Meena,M., Carrell,A.A., Golan,J.J., Drott,M.T., Cottaz,S., Fort,S., Ané,J.-M., *et al.* (2022) Lipo-Chitooligosaccharides Induce Specialized Fungal Metabolite Profiles That Modulate Bacterial Growth. *mSystems*, **7**, e0105222.

6. Villalobos Solis,M.I., Engle,N.L., Spangler,M.K., Cottaz,S., Fort,S., Maeda,J., Ané,J.-M., Tschaplinski,T.J., Labbé,J.L., Hettich,R.L., *et al.* (2022) Expanding the Biological Role of Lipo-Chitooligosaccharides and Chitooligosaccharides in Laccaria bicolor Growth and Development. *Front Fungal Biol*, **3**, 808578.

7. Rhodes,J.C. and Askew,D.S. (2014) Aspergillus fumigatus. In *Cellular and Molecular Biology of Filamentous Fungi*. ASM Press, Washington, DC, USA, pp. 695–716.

8. Brakhage,A.A. and Langfelder,K. (2002) Menacing mold: the molecular biology of Aspergillus fumigatus. *Annu. Rev. Microbiol.*, **56**, 433–455.

9. Roy,S., Lagree,S., Hou,Z., Thomson,J.A., Stewart,R. and Gasch,A.P. (2013) Integrated module and gene-specific regulatory inference implicates upstream signaling networks. *PLoS Comput. Biol.*, **9**, e1003252.

10. Hagiwara,D., Suzuki,S., Kamei,K., Gonoi,T. and Kawamoto,S. (2014) The role of AtfA and HOG MAPK pathway in stress tolerance in conidia of Aspergillus fumigatus. *Fungal Genet. Biol.*, **73**, 138–149.

11. Hagiwara,D., Asano,Y., Yamashino,T. and Mizuno,T. (2008) Characterization of bZip-type transcription factor AtfA with reference to stress responses of conidia of Aspergillus nidulans. *Biosci. Biotechnol. Biochem.*, **72**, 2756–2760.

12. Kwon-Chung,K.J. and Sugui,J.A. (2009) What do we know about the role of gliotoxin in the pathobiology of Aspergillus fumigatus? *Med. Mycol.*, **47 Suppl 1**, S97–103.

13. Bok,J.W., Chung,D., Balajee,S.A., Marr,K.A., Andes,D., Nielsen,K.F., Frisvad,J.C., Kirby,K.A. and Keller,N.P. (2006) GliZ, a transcriptional regulator of gliotoxin biosynthesis, contributes to Aspergillus fumigatus virulence. *Infect. Immun.*, **74**, 6761–6768.

14. Zeng,T., Rodriguez-Moreno,L., Mansurkhodzaev,A., Wang,P., van den Berg,W., Gasciolli,V., Cottaz,S., Fort,S., Thomma,B.P.H.J., Bono,J.-J., *et al.* (2020) A lysin motif effector subverts chitin-triggered immunity to facilitate arbuscular mycorrhizal symbiosis. *New Phytol.*, **225**, 448–460.

15. Bozsoki,Z., Cheng,J., Feng,F., Gysel,K., Vinther,M., Andersen,K.R., Oldroyd,G., Blaise,M., Radutoiu,S. and Stougaard,J. (2017) Receptor-mediated chitin perception in legume roots is functionally separable from Nod factor perception. *Proc. Natl. Acad. Sci. U. S. A.*, **114**, E8118–E8127.

16. Kombrink,A. and Thomma,B.P.H.J. (2013) LysM effectors: secreted proteins supporting fungal life. *PLoS Pathog.*, **9**, e1003769.

17. Sánchez-Vallet,A., Saleem-Batcha,R., Kombrink,A., Hansen,G., Valkenburg,D.-J., Thomma,B.P.H.J. and Mesters,J.R. (2013) Fungal effector Ecp6 outcompetes host immune receptor for chitin binding through intrachain LysM dimerization. *Elife*, **2**, e00790.

18. Sánchez-Vallet,A., Tian,H., Rodriguez-Moreno,L., Valkenburg,D.-J., Saleem-Batcha,R., Wawra,S., Kombrink,A., Verhage,L., de Jonge,R., van Esse,H.P., *et al.* (2020) A secreted LysM effector protects fungal hyphae through chitin-dependent homodimer polymerization. *PLoS Pathog.*, **16**, e1008652.

19. Tian,H., MacKenzie,C.I., Rodriguez-Moreno,L., van den Berg,G.C.M., Chen,H., Rudd,J.J., Mesters,J.R. and Thomma,B.P.H.J. (2021) Three LysM effectors of Zymoseptoria tritici collectively disarm chitin-triggered plant immunity. *Mol. Plant Pathol.*, **22**, 683–693.

20. Mentlak,T.A., Kombrink,A., Shinya,T., Ryder,L.S., Otomo,I., Saitoh,H., Terauchi,R., Nishizawa,Y., Shibuya,N., Thomma,B.P.H.J., *et al.* (2012) Effector-mediated suppression of chitin-triggered immunity by magnaporthe oryzae is necessary for rice blast disease. *Plant Cell*, **24**, 322–335.

21. Kombrink,A., Rovenich,H., Shi-Kunne,X., Rojas-Padilla,E., van den

Berg,G.C.M., Domazakis,E., de Jonge,R., Valkenburg,D.-J., Sánchez-Vallet,A., Seidl,M.F., *et al.* (2017) Verticillium dahliae LysM effectors differentially contribute to virulence on plant hosts. *Mol. Plant Pathol.*, **18**, 596–608.

22. Dölfors,F., Holmquist,L., Dixelius,C. and Tzelepis,G. (2019) A LysM effector protein from the basidiomycete Rhizoctonia solani contributes to virulence through suppression of chitin-triggered immunity. *Mol. Genet. Genomics*, **294**, 1211–1218.

23. de Jonge,R. and Thomma,B.P.H.J. (2009) Fungal LysM effectors: extinguishers of host immunity? *Trends Microbiol.*, **17**, 151–157.

24. de Jonge,R., van Esse,H.P., Kombrink,A., Shinya,T., Desaki,Y., Bours,R., van der Krol,S., Shibuya,N., Joosten,M.H.A.J. and Thomma,B.P.H.J. (2010) Conserved fungal LysM effector Ecp6 prevents chitin-triggered immunity in plants. *Science*, **329**, 953–955.

25. Tian,H., MacKenzie,C.I., Rodriguez-Moreno,L., van den Berg,G.C.M., Chen,H., Rudd,J.J., Mesters,J.R. and Thomma,B.P.H.J. (2021) Three LysM effectors of Zymoseptoria tritici collectively disarm chitin-triggered plant immunity. *Mol. Plant Pathol.*, **22**, 683–693.

26. Dubey,M., Vélëz,H., Broberg,M., Jensen,D.F. and Karlsson,M. (2020) LysM Proteins Regulate Fungal Development and Contribute to Hyphal Protection and Biocontrol Traits in Clonostachys rosea. *Front. Microbiol.*, **11**, 679.

27. Romero-Contreras,Y.J., Ramírez-Valdespino,C.A., Guzmán-Guzmán,P., Macías-Segoviano,J.I., Villagómez-Castro,J.C. and Olmedo-Monfil,V. (2019) Tal6 From Trichoderma atroviride Is a LysM Effector Involved in Mycoparasitism and Plant Association. *Front. Microbiol.*, **10**, 2231.

28. Cen,K., Li,B., Lu,Y., Zhang,S. and Wang,C. (2017) Divergent LysM effectors contribute to the virulence of Beauveria bassiana by evasion of insect immune defenses. *PLoS Pathog.*, **13**, e1006604.

29. Kombrink,A., Rovenich,H., Shi-Kunne,X., Rojas-Padilla,E., van den Berg,G.C.M., Domazakis,E., de Jonge,R., Valkenburg,D.-J., Sánchez-Vallet,A., Seidl,M.F., *et al.* (2017) Verticillium dahliae LysM effectors differentially contribute to virulence on plant hosts. *Mol. Plant Pathol.*, **18**, 596–608.

30. Muraosa,Y., Toyotome,T., Yahiro,M. and Kamei,K. (2019) Characterisation of novel-cell-wall LysM-domain proteins LdpA and LdpB from the human pathogenic fungus Aspergillus fumigatus. *Sci. Rep.*, **9**, 3345.

31. Schoen,T.J., Calise,D.G., Bok,J.W., Giese,M.A., Nwagwu,C.D., Zarnowski,R., Andes,D., Huttenlocher,A. and Keller,N.P. (2023) Aspergillus fumigatus transcription factor ZfpA regulates hyphal development and alters susceptibility to antifungals and neutrophil killing during infection. *PLoS Pathog.*, **19**, e1011152.

32. Niu,M., Steffan,B.N., Fischer,G.J., Venkatesh,N., Raffa,N.L., Wettstein,M.A., Bok,J.W., Greco,C., Zhao,C., Berthier,E., *et al.* (2020) Fungal oxylipins direct programmed developmental switches in filamentous fungi. *Nat. Commun.*, **11**, 5158.

33. Valiante,V., Jain,R., Heinekamp,T. and Brakhage,A.A. (2009) The MpkA MAP kinase module regulates cell wall integrity signaling and pyomelanin formation in Aspergillus fumigatus. *Fungal Genet. Biol.*, **46**, 909–918.

34. McCormick,A., Jacobsen,I.D., Broniszewska,M., Beck,J., Heesemann,J. and Ebel,F. (2012) The two-component sensor kinase TcsC and its role in stress resistance of the human-pathogenic mold Aspergillus fumigatus. *PLoS One*, **7**, e38262.

35. Kruppa,M. and Calderone,R. (2006) Two-component signal transduction in human fungal pathogens. *FEMS Yeast Res.*, **6**, 149–159.

36. Baltussen,T.J.H., Zoll,J., Verweij,P.E. and Melchers,W.J.G. (2020) Molecular Mechanisms of Conidial Germination in Aspergillus spp. *Microbiol. Mol. Biol. Rev.*, **84**.

37. Chapeland-Leclerc,F., Dilmaghani,A., Ez-Zaki,L., Boisnard,S., Da Silva,B., Gaslonde,T., Porée,F.H. and Ruprich-Robert,G. (2015) Systematic gene deletion and functional characterization of histidine kinase phosphorelay receptors (HKRs) in the human pathogenic fungus Aspergillus fumigatus. *Fungal Genet. Biol.*, **84**, 1–11.

38. Jansen,R. and Gerstein,M. (2004) Analyzing protein function on a genomic scale: the importance of gold-standard positives and negatives for network prediction. *Curr. Opin. Microbiol.*, **7**, 535–545.

39. Chung,D., Barker,B.M., Carey,C.C., Merriman,B., Werner,E.R., Lechner,B.E., Dhingra,S., Cheng,C., Xu,W., Blosser,S.J., *et al.* (2014) ChIP-seq and in vivo transcriptome analyses of the Aspergillus fumigatus SREBP SrbA reveals a new regulator of the fungal hypoxia response and virulence. *PLoS Pathog.*, **10**, e1004487.

40. Paul,S., Stamnes,M., Thomas,G.H., Liu,H., Hagiwara,D., Gomi,K., Filler,S.G. and Moye-Rowley,W.S. (2019) AtrR Is an Essential Determinant of Azole Resistance in Aspergillus fumigatus. *MBio*, **10**.

41. Colabardini,A.C., Van Rhijn,N., LaBella,A.L., Valero,C., Dineen,L., Rokas,A. and Goldman,G.H. (2022) Aspergillus fumigatus FhdA Transcription Factor Is Important for Mitochondrial Activity and Codon Usage Regulation during the Caspofungin Paradoxical Effect. *Antimicrob. Agents Chemother.*, **66**, e0070122.

42. Alves de Castro,P., Valero,C., Chiaratto,J., Colabardini,A.C., Pardeshi,L.,

Pereira Silva,L., Almeida,F., Campos Rocha,M., Nascimento Silva,R., Malavazi,I., *et al.* (2021) Novel Biological Functions of the NsdC Transcription Factor in Aspergillus fumigatus. *MBio*, **12**.

43. Ries,L.N.A., Pardeshi,L., Dong,Z., Tan,K., Steenwyk,J.L., Colabardini,A.C., Ferreira Filho,J.A., de Castro,P.A., Silva,L.P., Preite,N.W., *et al.* (2020) The Aspergillus fumigatus transcription factor RglT is important for gliotoxin biosynthesis and self-protection, and virulence. *PLoS Pathog.*, **16**, e1008645.

44. Chen,Y., Le Mauff,F., Wang,Y., Lu,R., Sheppard,D.C., Lu,L. and Zhang,S. (2020) The Transcription Factor SomA Synchronously Regulates Biofilm Formation and Cell Wall Homeostasis in Aspergillus fumigatus. *MBio*, **11**.

45. Paul,S., Stamnes,M.A. and Moye-Rowley,W.S. (2023) Transcription factor FfmA interacts both physically and genetically with AtrR to properly regulate gene expression in the fungus Aspergillus fumigatus. *bioRxiv*, 10.1101/2023.06.06.543935.

46. Park,Y.-S., Kang,S., Seo,H. and Yun,C.-W. (2018) A copper transcription factor, AfMac1, regulates both iron and copper homeostasis in the opportunistic fungal pathogen Aspergillus fumigatus. *Biochem. J*, **475**, 2831–2845.

47. Furukawa,T., Scheven,M.T., Misslinger,M., Zhao,C., Hoefgen,S., Gsaller,F., Lau,J., Jöchl,C., Donaldson,I., Valiante,V., *et al.* (2020) The fungal CCAAT-binding complex and HapX display highly variable but evolutionary conserved synergetic promoter-specific DNA recognition. *Nucleic Acids Res.*, **48**, 3567–3590.

48. Colabardini,A.C., Wang,F., Dong,Z., Pardeshi,L., Rocha,M.C., Costa,J.H., Dos Reis,T.F., Brown,A., Jaber,Q.Z., Fridman,M., *et al.* (2022) Heterogeneity in the transcriptional response of the human pathogen Aspergillus fumigatus to the antifungal agent caspofungin. *Genetics*, **220**.

49. Long,N., Orasch,T., Zhang,S., Gao,L., Xu,X., Hortschansky,P., Ye,J., Zhang,F., Xu,K., Gsaller,F., *et al.* (2018) The Zn2Cys6-type transcription factor LeuB cross-links regulation of leucine biosynthesis and iron acquisition in Aspergillus fumigatus. *PLoS Genet.*, **14**, e1007762.

50. Dos Reis,T.F., Horta,M.A.C., Colabardini,A.C., Fernandes,C.M., Silva,L.P., Bastos,R.W., Fonseca,M.V. de L., Wang,F., Martins,C., Rodrigues,M.L., *et al.* (2021) Screening of Chemical Libraries for New Antifungal Drugs against Aspergillus fumigatus Reveals Sphingolipids Are Involved in the Mechanism of Action of Miltefosine. *MBio*, **12**, e0145821.

51. Valero,C., Colabardini,A.C., de Castro,P.A., Silva,L.P., Ries,L.N.A., Pardeshi,L., Wang,F., Rocha,M.C., Malavazi,I., Silva,R.N., *et al.* (2021) Aspergillus Fumigatus ZnfA, a Novel Zinc Finger Transcription Factor Involved in Calcium Metabolism and Caspofungin Tolerance. *Front Fungal Biol*, **2**, 689900.

52. Muraosa,Y., Hino,Y., Takatsuka,S., Watanabe,A., Sakaida,E., Saijo,S., Miyazaki,Y., Yamasaki,S. and Kamei,K. (2024) Fungal chitin-binding glycoprotein induces Dectin-2-mediated allergic airway inflammation synergistically with chitin. *PLoS Pathog.*, **20**, e1011878.

53. Wienken,C.J., Baaske,P., Rothbauer,U., Braun,D. and Duhr,S. (2010) Protein-binding assays in biological liquids using microscale thermophoresis. *Nat. Commun.*, **1**, 100.

54. Tian,H., Fiorin,G.L., Kombrink,A., Mesters,J.R. and Thomma,B.P.H.J. (2022) Fungal dual-domain LysM effectors undergo chitin-induced intermolecular, and not intramolecular, dimerization. *Plant Physiol.*, **190**, 2033–2044.

55. Sunbul,M. and Jäschke,A. (2019) Proximity Labeling: Methods and Protocols Springer Nature.

56. Branon,T.C., Bosch,J.A., Sanchez,A.D., Udeshi,N.D., Svinkina,T., Carr,S.A., Feldman,J.L., Perrimon,N. and Ting,A.Y. (2018) Efficient proximity labeling in living cells and organisms with TurboID. *Nat. Biotechnol.*, **36**, 880–887.

57. Miller,J. and Stagljar,I. (2004) Using the yeast two-hybrid system to identify interacting proteins. *Methods Mol. Biol.*, **261**, 247–262.

58. Langfelder,K., Philippe,B., Jahn,B., Latgé,J.P. and Brakhage,A.A. (2001) Differential expression of the Aspergillus fumigatus pksP gene detected in vitro and in vivo with green fluorescent protein. *Infect. Immun.*, **69**, 6411–6418.

59. Journet,E.P., El-Gachtouli,N., Vernoud,V., de Billy,F., Pichon,M., Dedieu,A., Arnould,C., Morandi,D., Barker,D.G. and Gianinazzi-Pearson,V. (2001) Medicago truncatula ENOD11: a novel RPRP-encoding early nodulin gene expressed during mycorrhization in arbuscule-containing cells. *Mol. Plant. Microbe. Interact.*, **14**, 737–748.

60. Poinsot,V., Crook,M.B., Erdn,S., Maillet,F., Bascaules,A. and Ané,J.-M. (2016) New insights into Nod factor biosynthesis: Analyses of chitooligomers and lipo-chitooligomers of Rhizobium sp. IRBG74 mutants. *Carbohydr. Res.*, **434**, 83–93.

61. Mouyna,I., Dellière,S., Beauvais,A., Gravelat,F., Snarr,B., Lehoux,M., Zacharias,C., Sun,Y., de Jesus Carrion,S., Pearlman,E., *et al.* (2020) What Are the Functions of Chitin Deacetylases in Aspergillus fumigatus? *Front. Cell. Infect. Microbiol.*, **10**, 28.

62. Muszkieta,L., Aimanianda,V., Mellado,E., Gribaldo,S., Alcàzar-Fuoli,L., Szewczyk,E., Prevost,M.-C. and Latgé,J.-P. (2014) Deciphering the role of the chitin synthase families 1 and 2 in the in vivo and in vitro growth of Aspergillus fumigatus by multiple gene targeting deletion. *Cell. Microbiol.*, **16**, 1784–1805.

63. Affeldt,K.J., Brodhagen,M. and Keller,N.P. (2012) Aspergillus oxylipin signaling and quorum sensing pathways depend on g protein-coupled receptors. *Toxins* , **4**, 695–717.

64. Horowitz Brown,S., Zarnowski,R., Sharpee,W.C. and Keller,N.P. (2008) Morphological transitions governed by density dependence and lipoxygenase activity in Aspergillus flavus. *Appl. Environ. Microbiol.*, **74**, 5674–5685.